2001

Center Vortices in Confinement.

Viorel-andrei Alexandru
Louisiana State University and Agricultural & Mechanical College

INFORMATION TO USERS

This manuscript has been reproduced from the microfilm master. UMI films the text directly from the original or copy submitted. Thus, some thesis and dissertation copies are in typewriter face, while others may be from any type of computer printer.

The quality of this reproduction is dependent upon the quality of the copy submitted. Broken or indistinct print, colored or poor quality illustrations and photographs, print bleedthrough, substandard margins, and improper alignment can adversely affect reproduction.

In the unlikely event that the author did not send UMI a complete manuscript and there are missing pages, these will be noted. Also, if unauthorized copyright material had to be removed, a note will indicate the deletion.

Oversize materials (e.g., maps, drawings, charts) are reproduced by sectioning the original, beginning at the upper left-hand corner and continuing from left to right in equal sections with small overlaps.

Photographs included in the original manuscript have been reproduced xerographically in this copy. Higher quality 6" x 9" black and white photographic prints are available for any photographs or illustrations appearing in this copy for an additional charge. Contact UMI directly to order.

ProQuest Information and Learning
300 North Zeeb Road, Ann Arbor, MI 48106-1346 USA
800-521-0600

CENTER VORTICES IN CONFINEMENT

A Dissertation

Submitted to the Graduate Faculty of the
Louisiana State University and
Agricultural and Mechanical College
in partial fulfillment of the
requirements for the degree of
Doctor of Philosophy

in

The Department of Physics and Astronomy

by
Viorel - Andrei Alexandru
Licenţiat în Fizică, Universitatea Bucureşti, România, 1997
August 2001

UMI Number: 3021418

UMI Microform 3021418

Bell & Howell Information and Learning Company
300 North Zeeb Road
P.O. Box 1346
Ann Arbor, MI 48106-1346

Acknowledgments

I would like to thank the people that made it possible for me to write this dissertation: my advisor, Richard W. Haymaker, for his help and advice and, especially, for putting up with me for all these years, my friend, Paul N. Kirk, for his constant support, and the members of my committee for their suggestions and comments. I am also pleased to thank E. T. Tomboulis, J. Stack, S. Olejnic and S. Cheluvaraja for very interesting discussions related to my dissertation. Lastly, I would like to thank my wife, Delia, and my family for their love and support.

This work was supported in part by United States Department of Energy Grant No. DE-FG05-91 ER 40617.

Table of Contents

Abstract

The confinement property of quarks is still one of the puzzles of today's physics. Although QCD is believed to accurately describe the interaction between quarks, due to the peculiar nature of the theory we are still unable to prove that it confines the quarks. Most analytical efforts in QCD are based on perturbative techniques which are useless in studying confinement. Lattice gauge theory enables us to get non-perturbative results. We use lattice techniques to investigate one of the proposed mechanisms of quark confinement, namely the center vortex idea. We first present a cursory introduction to lattice theory and the methods used to detect confinement on the lattices. We then show how the center vortices are suppose to produce confinement using center vortices to study Z_2 lattice gauge theory. A review of the current studies regarding the idea of center vortices follows. The last chapter is dedicated to studying a particular definition of center vortices due to Tomboulis. We show how to implement this definition of vortices in numerical simulations and use numerical simulations to check the assumptions underlying the formalism. We also compare Tomboulis definition with other methods used to identify vortices on lattice.

Introduction

It is generally accepted that the strong interactions are described by a Yang-Mills type theory [1]. QCD is a $SU(3)$ gauge theory that couples the fermions (quarks) with the gauge field (gluons). In QCD we have six flavors of quarks, that differ by their masses and electric charges, and eight types of gauge bosons, the gluons, corresponding to the generators of the $SU(3)$ gauge group. The origin of the quark masses and their flavors lies outside the scope of QCD. QCD treats all flavors identically. It is believed that the quarks start out as massless fermions and their masses are treated as input parameters, presumably generated by a dynamical breaking of the chiral symmetry by some other interaction. The validity of QCD has been tested in deep inelastic scattering experiments. At high energy QCD is expected to be *asymptotically free* and the perturbative techniques can be employed to get analytical results that can be compared with the experimental results.

In spite of these successes, the fundamental particles of QCD, the quarks and gluons, have never been observed as free states. Moreover, all observed physical particles have zero color charge. These facts led to the conclusion that the strong forces have a confining behavior: the quarks interact in such a way that it is impossible to

separate them using a finite amount of energy. If QCD is indeed a theory describing the strong forces it needs to exhibit this type of behavior. Unfortunately, the perturbative techniques are useless in trying to address the confinement property of QCD. The problem stems from the fact that confinement is an infrared property and in the infrared regime the QCD effective coupling is no longer small. Lattice QCD [2, 3, 4] is a promising formulation for studying non-perturbative problems. As we will see, lattice simulations show that the static interquark potential is linearly increasing with distance [5]. This type of behavior will indeed explain the confinement of quarks.

Experimentally, the most stringent limit on the density of free quarks comes from Millikan type experiments where one looks for particles carrying fractional electric charge. The upper limit for the abundance of quarks, n_q, relative to the abundance of nucleons, n_p determined from these experiments [6] is:

$$\frac{n_q}{n_p} \leq 10^{-27}$$

On the other hand, if we are to assume that the quarks are unconfined, under reasonable assumptions, the concentration of relic quarks (remnant quarks from an early, hot universe) is [7]:

$$\frac{n_q}{n_p} \geq 10^{-12}$$

The 15 orders of magnitude discrepancy cannot be explained by any adjustment of the assumptions. It is therefore concluded that the quarks are indeed confined.

The QCD vacuum structure seems to be responsible for confinement. This vacuum is qualitatively different from an inert vacuum. In contrast with QED where the vacuum fluctuations are treated as perturbations, the QCD vacuum modifies essential properties of quarks. It is the gluon sea that is believed to be responsible for confinement. The sea quarks (the quark-antiquark pairs created and annihilated in the vacuum) seems to work against confinement. For $SU(3)$ we know that the β-function is, to the first order [8]:

$$\beta(g_0) = -\beta_0 g_0^3 + o(g_0^5)$$

where:

$$\beta_0 = \frac{1}{16\pi^2}(11 - \frac{2}{3}N_f)$$

where N_f is the number of flavors. We see then that if we have too many flavors the coefficient β_0 becomes negative and we lose asymptotic freedom and perhaps confinement also. The current thinking is that if we are to determine the properties of the gluon field we can insert the quarks perturbatively.

A number of "mechanisms" have been proposed to explain the confinement property of the gluon field. These models try to identify relevant degrees of freedom for confinement and use them to determine the long distance behavior of the full theory. The need for such models stems from a desire to understand how the vacuum acts to confine the quarks. Another reason for studying such mechanisms is to provide an outline for a definitive proof of the confinement property of QCD. An interesting

mechanism is the center vortex idea [9]. As we will see, the relevant degrees of freedom in this model are the center elements of the gauge group.

Center vortices are extended structures of the gluon field that carry a chromomagnetic flux given by a center element. They "disorder" the Wilson loop and produce the *area law*, the lattice equivalent of a linearly increasing interquark potential. A lot of effort has been put in identifying these structures on the lattice. The most popular approach is the projection methods [10, 11] which uses a gauge fixing procedure to locate vortices. The main objection against this prescription is its gauge dependence. A different approach has been proposed by Tomboulis [12, 13]. The Tomboulis method has the advantage of being gauge invariant but it seems difficult to implement.

The aim of our work is to find a definition for Tomboulis vortices that can be implemented numerically and to use this method to investigate the properties of center vortices. We will also try to see how vortices identified using Tomboulis' definition match with vortices identified by projection methods. Ultimately, we will try to see if vortices are the relevant configurations for confinement.

In our work we will be using the $SU(2)$ gauge group rather that the QCD's $SU(3)$. $SU(2)$ gauge theory is much easier to investigate numerically and it is believed that the $SU(2)$ theory differs only quantitatively from QCD. Since we are only interested in qualitative features of the non-Abelian gauge field we choose to work with $SU(2)$. Nevertheless, we tried to keep the discussion as general as possible so that most of the results can be easily extended to $SU(3)$.

The dissertation is organized as follows:

- in chapter 1 we show how to put a gauge theory on the lattice; without going into too much details we present the concepts relevant for our discussion.
- in chapter 2 a number of confinement criteria on the lattice are presented; we will see what are the requirements for a model proposed to explain confinement on the lattice.
- in chapter 3 we present the $Z(2)$ gauge theory; this is a well understood theory that is relevant for our presentation since its basic excitations are vortices.
- in chapter 4 we review the projection methods; we present the background, the results and the problems of the projection definition of vortices.
- in chapter 5 we present the Tomboulis definition of vortices; we show our derivation, the numerical results and compare Tomboulis vortices with the ones identified by the projection methods.
- in the Appendix we present some mathematical background and definitions that we will be using throughout the text. They are particularly relevant to the derivations in chapters 3 and 5.

Chapter 1

Introduction to Lattice Gauge Theory

1.1 Introduction

Field theories have been a very useful tool in understanding physics at different scales: from very large distances, where we have the general theory of relativity, to very short distances where we use the quantum field theories. There is even a certain hope among theorists that the ultimate physical theory, a theory that encompasses all scales, can be formulated as a field theory. The basic ingredients that a formulation of a physical theory needs, like locality and continuity, are easily implemented using the concept of a field.

However, the success of field theories was shadowed by the fact that they seem to be unsound mathematically. The perturbative treatment yields divergencies at different stages of the approximation process. The renormalization was introduced initially as a trick to solve this problem [14]. Although this procedure gets rid of the divergencies, at least for a certain category of systems, it seems to be rather ad-hoc. It was later that Wilson [15] showed that the divergencies and the renormalization procedure are quite natural. He argued that the problem arises from the fact that we

are expecting that a field theory that has a given behavior at a certain scale should have the same behavior at all scales. It is our extrapolation of the theory to all scales that creates the divergencies. This is by no means a problem associated only with quantum field theories. Classical electrodynamics shows divergencies when we are trying to compute things like the self-energy of the electron [16]. The explanation for this behavior was that the interaction at microscopic levels has new terms that cancel these divergencies. We know today that classical electrodynamics is only a macroscopic theory. It can be viewed as the limit of QED where at small distances the interaction is indeed different than the one predicted by the classical theory.

The brilliant contribution that Wilson made was to give a physical meaning to the renormalization procedure. He also showed why only a handful of quantum field theories are amenable to this procedure. The basic idea is that for a certain type of system, given any interaction that the system might have at microscopic distances, there are only few type of interactions that will still be manifest at large distances. Thus, for any effective field theory (the theory at large distances) to have a chance to be a fundamental theory at microscopic level, it has to be of a certain type. To make things clearer we will take an example: the scalar field theory is renormalizable only as a free theory. Thus, any system that exhibits the behavior of an interacting scalar field theory cannot be formulated in terms of scalar fields at microscopic level. The scalar of the theory has to be a composite particle.

The renormalization procedure, as described by Wilson, involves a regulator. The regulator is usually a parameter that alters the short distance behavior of the theory in such a way that will produce finite results. One then performs the

necessary computations in this altered theory and then removes the regulator in such a way that certain quantities are tuned to coincide with their measured values for all values of the regulator. These quantities that are kept fixed in the process of removing the regulator define the renormalization scheme. All other parameters of the theory are regarded as free parameters and they should be fixed by the requirement that the quantities that define the renormalization scheme assume their experimental value. The regulator of the theory can be a mass, like in Pauli-Villars renormalization procedure [17], some momentum cutoff or even a deviation from the number of space-time dimensions as in the procedure employed by 't Hooft [18].

We see then that by formulating a physical theory on a lattice, rather than in continuum, we do nothing more but regulate the theory by imposing a spatial cutoff which is the lattice spacing. This lattice cutoff is then not only common but it is required in order to make the theory well defined.

Another problem that we have in dealing with field theories is that we don't have methods to solve them exactly. It is only in very special cases that are trivial or at most of academic interest that we can solve them in a closed form. The only available treatment for theories of interest is a perturbative treatment. This treatment has been successfully employed for QED. Its success is due to the smallness of the coupling constant in the macroscopic regime. There we can treat the quantum fluctuations and their effects as a perturbation from an inert vacuum.

However, this treatment fails to work on a system that has a large coupling constant. In QCD the coupling constant in the large distance limit seems to be very large. Physically these theories cannot be described perturbatively since the

interacting theory is qualitatively different from the free theory. It is an experimental fact that quarks do not appear as asymptotic states – they are confined. The only place for perturbative treatment for non-Abelian gauge theories is at small distances since these theories are believed to be asymptotically free. The agreement between the perturbative results at high energy and experiment is quite good. However, very interesting features such as quark confinement depend essentially on the infrared regime.

Lattice gauge theories provide us with a non-perturbative approach. Although they are as difficult to solve analytically as the original theory we can use Monte-Carlo techniques to compute quantities on the lattice. This enables us to get non-perturbative results and, thus, to address questions regarding the infrared regime of the non-Abelian gauge theories.

The first success of lattice field theories was to show numerically that QCD provides for a linearly increasing interquark potential [5]. Lattice simulations have also been used in investigating hadron spectra [19], finite temperature QCD [20] and QCD vacuum structure [21]. The main problem facing today's studies is the limited computational power. However, we are rapidly approaching a stage where lattice QCD will be capable of producing very accurate predictions. For a detailed discussion of the methods employed and a review of numerical results the reader is referred to the Proceedings of the $XVIII^{th}$ International Symposium on Lattice Field Theory [22] and preceding conferences in the series.

1.2 Free Scalar Field on the Lattice

We will begin our presentation of lattice theories by showing how to implement the simplest field system: the free scalar field. We start with the Lagrangian density for the free scalar fields:

$$\mathcal{L} = \frac{1}{2}\partial_\mu\phi\partial^\mu\phi - \frac{1}{2}M^2\phi^2$$

where ϕ is a real scalar field. We know that the information about a field theory is contained in its Green functions:

$$G(x_1, x_2, ...) = \langle\Omega|T(\bar{\phi}(x_1)\bar{\phi}(x_2)...)|\Omega\rangle$$

where $\bar{\phi}$ is the operator representing the scalar field. These Green functions are the vacuum expectation values of the time ordered product of operators. Using the path-integral formalism we can write these functions as:

$$G(x_1, x_2, ...) = \frac{\int D\phi\, \phi(x_1)\phi(x_2)...e^{iS[\phi]}}{\int D\phi\, e^{iS[\phi]}}$$

where $D\phi$ is the measure on the space of all possible field configurations and $S[\phi]$ is the action associated with a particular configuration ϕ. We see that this expression looks very much like a classical statistical mechanics average where the Hamiltonian is replaced by the action. The essential difference is that we have an oscillatory integrand, e^{iS}, rather than a bounded one, $e^{-\beta H}$. To convert the above formula to a statistical mechanics average, which is suitable for numerical simulations, we

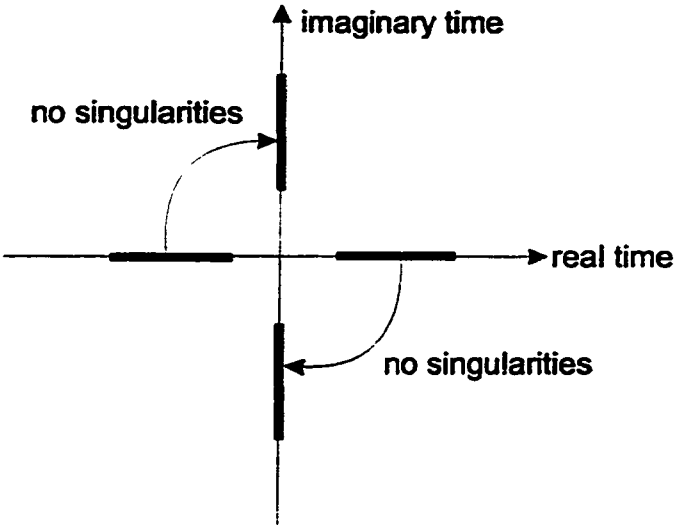

Figure 1.1: Real time to imaginary time rotation.

need to perform an analytic continuation to imaginary times: $x_i^0 \to -ix_i^4$. This is possible if the Green functions have no singularities in the path of this rotation (see Fig. 1.1).

Once the computations of the Green functions is completed in this "Euclidian formulation" we can rotate back to real times. Under this rotation the action changes:

$$S = \int \mathcal{L} d^4x \to iS_E = i \int \mathcal{L}_E d^4x$$

where:

$$\mathcal{L}_E = \frac{1}{2} \sum_{\mu=1}^{4} \partial_\mu \phi_E \partial_\mu \phi_E + \frac{1}{2} M^2 \phi_E^2$$

with $\phi_E(x^1, x^2, x^3, x^4) = \phi(-ix^4, x^1, x^2, x^3)$. We have then:

$$G_E(x_1, x_2, ...) = \frac{\int D\phi_E \, \phi_E(x_1)\phi_E(x_2)...e^{-S_E[\phi_E]}}{\int D\phi_E \, e^{-S_E[\phi_E]}}$$

We will be working in the Euclidian space from now on and we will drop the index.

To put the field on the lattice we will consider the values of the field at discreet points in the Euclidian space:

$$\begin{aligned} x_\mu &= n_\mu a \\ \phi_n &= \phi(na) \end{aligned}$$

The integral and differential operators will be:

$$\begin{aligned} \int d^4x &\rightarrow a^4 \sum_n \\ D\phi &\rightarrow \prod_n d\phi_n \\ \partial_\mu \phi &\rightarrow \frac{\phi_{n+\hat{\mu}} - \phi_n}{a} \end{aligned}$$

Using this we can write the discretized action:

$$S = \frac{1}{2} a^4 \sum_n \left[\left(\sum_\mu -\frac{2}{a^2} \phi_n \phi_{n+\hat{\mu}} \right) + \left(M^2 + \frac{8}{a^2} \right) \phi_n^2 \right]$$

We now introduce the dimensionless quantities:

$$\begin{aligned} \hat{\phi}_n &= a\phi_n \\ \hat{M} &= aM \end{aligned}$$

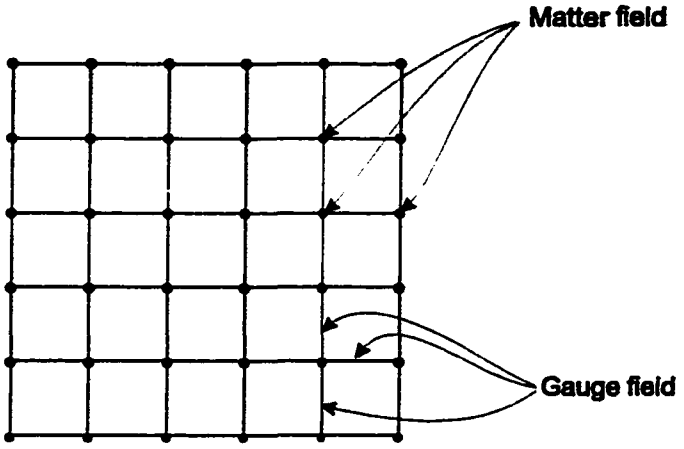

Figure 1.2: The matter field is defined on sites of the lattice and the gauge field is defined on links connecting the sites.

and the lattice action becomes:

$$\begin{aligned} S &= \frac{1}{2}\sum_n \left[-\sum_\mu \left(\hat{\phi}_n \hat{\phi}_{n+\hat{\mu}} + \hat{\phi}_n \hat{\phi}_{n-\hat{\mu}} \right) + (\hat{M}^2 + 8)\hat{\phi}_n^2 \right] \\ &= \frac{1}{2}\sum_n \left[\sum_\mu \left(\hat{\phi}_{n+\hat{\mu}} - \hat{\phi}_n \right)^2 + \hat{M}^2 \hat{\phi}_n^2 \right] \end{aligned} \tag{1.1}$$

The theory is now formulated in terms of a scalar field $\hat{\phi}_n$ defined at the sites of the lattice (see Fig. 1.2). The interaction is given by the action above which, as we can see, is formed out of a discretized Laplacian and a mass term. The vacuum expectation values are, in this framework, the correlation functions:

$$G(n_1, n_2, \ldots) = \langle \hat{\phi}_{n_1} \hat{\phi}_{n_2} \ldots \rangle = \frac{\int \prod_n d\hat{\phi}_n \, \hat{\phi}_{n_1} \hat{\phi}_{n_2} \ldots e^{-S[\hat{\phi}]}}{\int \prod_n d\hat{\phi}_n \, e^{-S[\hat{\phi}]}}$$

For this simple theory we can compute the correlation functions explicitly and see that in the limit $a \to 0$ we get the result expected from the continuum theory.

For example the two point correlation function (the equivalent of the propagator) will be:

$$G(n_1, n_2; \hat{M}) = \langle \hat{\phi}_{n_1} \hat{\phi}_{n_2} \rangle = \int_{-\pi}^{\pi} \frac{d^4k}{(2\pi)^4} \frac{e^{ik(n_1-n_2)}}{4\sum_\mu \sin^2 \frac{k_\mu}{2} + \hat{M}^2}$$

To recover the correlation function in the continuum we write:

$$\langle \phi(x_1)\phi(x_2) \rangle = \lim_{a\to 0} \frac{1}{a^2} G(\frac{x_1}{a}, \frac{x_2}{a}; Ma) = \int_{-\infty}^{\infty} \frac{d^4k}{(2\pi)^4} \frac{e^{ik(x_1-x_2)}}{k^2 + M^2}$$

which is exactly the Euclidian propagator.

It is interesting to see what happens if we are not able to compute the correlation functions explicitly. We can use numerical simulations to get the numbers for different values of n_1, n_2 and $\hat{M}$. How would we use these numbers to get the value of this Green function in the continuum? Since a does not enter directly in our discretized theory we need to use other parameters to adjust the value of a. The only parameter that we have in our theory is the dimensionless mass $\hat{M}$. Thus we can choose to compute $G(n_1, n_2; \hat{M})$ for different values of $\hat{M}$. Since $\hat{M} = Ma$ we can deduce the value of a for a particular $\hat{M}$ using the physical mass M:

$$a = \frac{\hat{M}}{M}$$

Using this value for a we can compute the continuum Green function:

$$\langle \phi(n_1 a)\phi(n_2 a) \rangle \simeq \frac{1}{a^2} G(n_1, n_2; \hat{M})$$

This is only an approximation since the lattice theory is only an approximation of the continuum theory. After all we neglected the short distance fluctuations. However, the smaller the lattice spacing the better the approximation. Thus all we have to do is to compute $G(n_1, n_2; \hat{M})$ for smaller and smaller values of $\hat{M}$ so that $a = \hat{M}/M$ goes to zero. There is, unfortunately, a limit for how small $\hat{M}$ can be. We see that in order to get a better and better approximation for $\langle \phi(x_1)\phi(x_2) \rangle$ for a physical distance $x_1 - x_2$ we need to compute $\langle \hat{\phi}_{n_1} \hat{\phi}_{n_2} \rangle$ at a distance $n_1 - n_2 = (x_1 - x_2)/a$ in the lattice. The smaller $\hat{M}$ gets the bigger will be the distance. Since we are limited in our simulations to lattices of a certain size, we cannot go to too small values for $\hat{M}$ if we are to compute effects at finite physical distances. The hope is that even though we cannot reach the limit $\hat{M} \to 0$, the asymptotic value of the continuum Green function can be inferred from the values achieved in the lattice simulations. The procedure that we just described here is the renormalization procedure on the lattice.

Returning to the lattice action (1.1) we see that in the "naive limit" when $a \to 0$ the action itself goes into the continuum action. This is the first requirement for a lattice action to describe the same system as the continuum action. There are an infinite number of different actions that have this property. We can add another term in the action (for example a term of the form $\hat{\phi}_n^6$) and still get an action that naively converges to the continuum action. This freedom of choosing the lattice action can be used to attenuate the lattice artifacts, as it is used in the renormalization improved action program [23], or to remove unwanted lattice features, as in the case of fermion doubling problem [24].

There is another requirement for a lattice theory. Let's take the two point correlation function. For sufficiently large distances it is:

$$\langle \hat{\phi}_{n_1} \hat{\phi}_{n_2} \rangle \sim e^{-|n_1 - n_2|/\hat{\xi}}$$

where $\hat{\xi}$ is the correlation length in lattice units. In order for the lattice theory to have a continuum limit where fields are interacting at non-zero distances we need $\hat{\xi} \to \infty$ as we approach the point in the parameter space that corresponds to $a = 0$. This corresponds to a second order phase transition for the lattice system. If the lattice theory doesn't have a second order phase transition at that point then there is no continuum limit for that theory. Moreover, the transition point has to occur at that particular place in the parameter space that corresponds to the values of the parameters that we expect from the continuum theory.

These are general requirements for a lattice field theory although the example that we used here was only for a free scalar theory. In particular, the lattice gauge theories have to fulfill these requirements too. The process of finding a lattice action for a gauge field is a little more complex than for scalar fields. We present it in the next section.

1.3 Gauge Fields on the Lattice

We will focus in this section only on pure gauge theories. In the continuum they are defined in terms of fields taking value in the Lie algebra associated with the gauge group. The most useful gauge theories are the ones generated by the $SU(N)$

gauge groups. The Euclidian action for these theories is:

$$S = \frac{1}{2}\int d^4x \sum_{\mu,\nu} \mathrm{Tr}(F_{\mu\nu}F_{\mu\nu})$$

where

$$F_{\mu\nu} = \partial_\mu A_\nu - \partial_\nu A_\mu + ig[A_\mu, A_\nu]$$

$F_{\mu\nu}$ and $A_{\mu\nu}$ are traceless hermitian matrices. The dynamical variables are the gauge fields A_μ valued in the $su(N)$ algebra. We see that g, the coupling constant, appears here although we have a pure gauge theory. This is due to the non-Abelian nature of the gauge group. The gauge fields in such a theory carry charge and thus they interact with each other. In an Abelian gauge theory the commutator $[A_\mu, A_\nu] = 0$ and then we have a free field theory.

The simple procedure that we used to derive the lattice version for the scalar fields doesn't work for gauge fields. To understand the implementation used for gauge fields we need to go back to their original motivation. The gauge fields are introduced in order to create theories that are invariant under local gauge transformations. The gauge field itself describes a connection between fields at different positions in space-time. For a vector field:

$$\phi(x) = \begin{pmatrix} \phi_1(x) \\ \phi_2(x) \\ \vdots \\ \phi_N(x) \end{pmatrix}$$

a change of basis at different space-time points produces a change in the values of the components. Such a change makes it difficult to compare fields at different points. On a lattice this problem is more obvious since the continuity is missing. In principle an interaction will try to arrange the field so that the field at neighboring sites on the lattice is parallel. However, a gauge transformation changes the basis at different points and thus we are forced to find a local basis invariant (gauge invariant) definition for parallelism. We introduce the gauge field to solve this problem. In the continuum a vector at a certain point x is parallel transported to another point y using the Schwinger line integral [3]:

$$\phi(x) \rightarrow Pe^{ig\int_C dx_\mu A_\mu}\phi(x)$$

where P stands for path-ordered product and the curve C starts at x and ends at y. This definition depends, of course, on the curve C. We need something to emulate this idea on the lattice. We can choose the Schwinger line integrals to represent the gauge field on the lattice:

$$U_n^\mu = e^{ig\int_{C_n^\mu} dx_\mu A_\mu} \tag{1.2}$$

where C_n^μ is the line connecting the points na and $(n+\hat{\mu})a$. We will use U_n^μ to describe the gauge field on the lattice. These variables will live on links (see Fig. 1.2) rather than sites. A link is an object characterized by the starting point n on the lattice and its direction μ. Our lattice theory will be formulated in terms of these link variables that take values in the gauge group.

We note here an important difference between the lattice and continuum theories: the link variables that characterize the gauge fields on the lattice are elements of the gauge group itself rather than its Lie algebra. Under a gauge transformation:

$$\phi(x) \rightarrow G(x)\phi(x)$$

the Schwinger line integral changes:

$$Pe^{ig\int_C dx_\mu A_\mu} \rightarrow G(y)Pe^{ig\int_C dx_\mu A_\mu}G^{-1}(x)$$

where C starts at x and ends at y. The gauge transformation on the lattice will then be:

$$\begin{aligned} \phi_n &\rightarrow G_n\phi_n \\ U_n^\mu &\rightarrow G_n U_n^\mu G_{n+\hat{\mu}}^{-1} \end{aligned}$$

In order to construct a gauge invariant theory on the lattice we need to have a gauge invariant action. Thus, in constructing the action, we need to use appropriate combinations of ϕ_n and U_n^μ. For a pure gauge theory we need to use gauge invariant combinations of U_n^μ. To see how we get these combinations consider a product of link variables such that they form a path in the lattice:

$$\prod U_{n_i}^{\mu_i} = U_{n_1}^{\mu_1}U_{n_2}^{\mu_2}...U_{n_3}^{\mu_3}$$

$$\prod_{i=1}^{k} U_{n_i}^{\mu_i} = U_{n_1}^{\mu_1}U_{n_2}^{\mu_2}...U_{n_3}^{\mu_3}$$

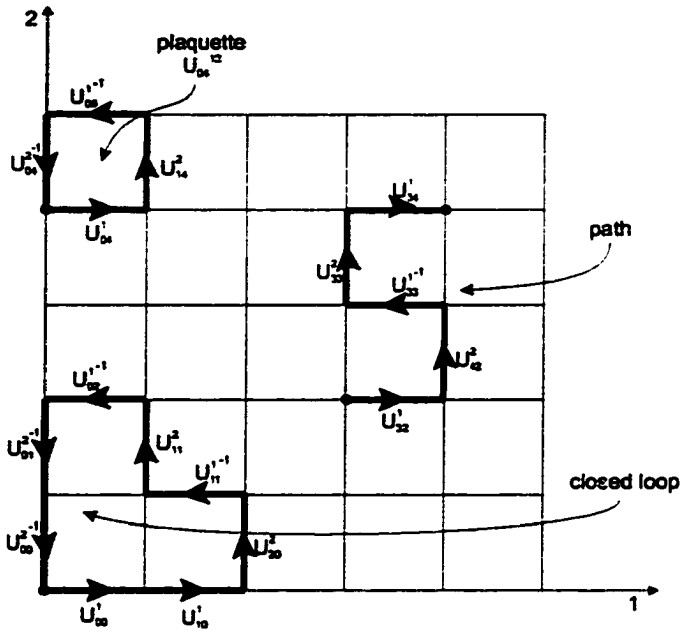

Figure 1.3: Paths, loops and plaquettes in a lattice pure gauge theory.

with $n_{i-1} = n_i - \hat{\mu}_i$ (see Fig. 1.3). We include here negative μ_k using the fact that for $\mu > 0$ we have:

$$U_n^{-\mu} = (U_{n-\hat{\mu}}^{\mu})^{-1}$$

since we are integrating the Schwinger line in the opposite direction. This product will change under a gauge transformation:

$$\prod_{i=1}^{k} U_{n_i}^{\mu_i} \to G_{n_1} \left(\prod_{i=1}^{k} U_{n_i}^{\mu_i} \right) G_{n_k}^{-1}$$

In order to get gauge invariant combinations we need to consider closed loops (i.e.

paths with $n_k + \hat{\mu}_k = n_1$). Such a product will change under a gauge transformation:

$$\prod_{i=1}^{k} U_{n_i}^{\mu_i} \to G_{n_1} \left(\prod_{i=1}^{k} U_{n_i}^{\mu_i} \right) G_{n_1}^{-1}$$

and its trace will be gauge invariant. These objects, the closed loop products, are the only gauge invariant objects defined in terms of U_n^μ alone. The simplest such loop is the *plaquette*:

$$U_n^{\mu\nu} = U_n^\mu U_{n+\hat{\mu}}^\nu U_{n+\hat{\mu}+\hat{\nu}}^{-\mu} U_{n+\hat{\nu}}^{-\nu} = U_n^\mu U_{n+\hat{\mu}}^\nu (U_{n+\hat{\nu}}^\mu)^{-1} (U_n^\nu)^{-1}$$

Using (1.2) for small lattice spacing we have:

$$\begin{aligned} U_n^\mu &= e^{iga A_\mu(na)} + o(a^2) \\ U_n^{\mu\nu} &= e^{iga^2 F_{\mu\nu}(na)} + o(a^4) = 1 + iga^2 F_{\mu\nu}(na) + o(a^4) \end{aligned}$$

Moreover:

$$U_n^{\mu\nu} + (U_n^{\mu\nu})^{-1} = 2 - g^2 a^4 F_{\mu\nu}(na) F_{\mu\nu}(na) + o(a^6)$$

and using this we can write the continuum action:

$$S = \frac{1}{2} \int d^4x \sum_{\mu,\nu} \mathrm{Tr}(F_{\mu\nu} F_{\mu\nu}) \to \frac{1}{2} a^4 \sum_n \sum_{\mu,\nu} \mathrm{Tr} \frac{2 - (U_n^{\mu\nu} + (U_n^{\mu\nu})^{-1})}{g^2 a^4}$$

The lattice action will then be:

$$S = \frac{N}{g^2} \sum_{n,\mu,\nu} (1 - \frac{1}{2N} \mathrm{Tr}(U_n^{\mu\nu} + (U_n^{\mu\nu})^{-1})) = \frac{2N}{g^2} \sum_p (1 - \frac{1}{2N} \mathrm{Tr}(U_p + U_p^{-1}))$$

The last sum runs over all plaquettes in the lattice (there is a factor of 2 that comes from the symmetry under interchange of μ and ν). For $SU(N)$ we have $U^{-1} = U^\dagger$ and thus the lattice action for $SU(N)$ can be written as:

$$S = \beta \sum_p \left(1 - \frac{1}{2N} \mathrm{Tr}(U_p + U_p^\dagger)\right)$$

where $\beta = \frac{2N}{g^2}$. The factor of 1 in the action due to each plaquette is just a normalization factor. It will not play any role in computing the averages:

$$\begin{aligned} \langle f(U) \rangle &= \frac{\int DU\, f(U) e^{-\beta \sum_p (1 - \frac{1}{2N} \mathrm{Tr}(U_p + U_p^\dagger))}}{\int DU\, e^{-\beta \sum_p (1 - \frac{1}{2N} \mathrm{Tr}(U_p + U_p^\dagger))}} \\ &= \frac{\int DU\, f(U) e^{\frac{\beta}{N} \sum_p Re\, \mathrm{Tr}(U_p)}}{\int DU\, e^{\frac{\beta}{N} \sum_p Re\, \mathrm{Tr}(U_p)}} \end{aligned}$$

where we $DU = \prod_{n,\mu} dU_n^\mu$.

From the lattice action we see that the only parameter for a $SU(N)$ pure lattice gauge theory is $\beta = \frac{2N}{g^2}$. In order to get to the continuum limit we need to take $g \to 0$ (since these theories are asymptotically free) and thus we need to let $\beta \to \infty$. The bare coupling, g, is dimensionless. We cannot use it to extract the lattice spacing as we did in the previous section using the physical mass M. We will need to fix other dimensionfull quantities to calibrate the lattice. For a pure gauge theory a

suitable observable can be the mass of the first glueball or the string tension. The most useful parameter to determine the lattice spacing is the string tension. We will introduce it in the next chapter and we will show its connection with confinement.

Chapter 2

Criteria of Confinement on the Lattice

2.1 Introduction

The confinement of quarks is an experimental fact: no free quarks have been observed up to the energies available in today's experiments. In non-Abelian gauge theories this is equivalent with saying that the theory should forbid all the states that carry color; only colorless configurations should be stable. The conventional wisdom is that a colored state will polarize the vacuum creating a quark-gluon cloud that will carry an infinite amount of energy. This is due to the fact that, in contrast with QED, the quark-gluon cloud is expected to increase the effective charge of the bare quark rather than screen it. It is also expected that this "anti-screening" behavior will survive even if we are to eliminate the dynamical quarks (the virtual quark-antiquark pairs). These conclusions are drawn from the behavior of the non-Abelian gauge theories close to the $g = 0$ point. These are perturbative results. No solutions of the renormalization group equation are known away from this $g = 0$ point. It is perfectly possible that, at a certain distance, a decreasing effective charge behavior sets in and eventually screens completely the charge of

the quark. Since we don't have a thorough understanding of these theories it is very difficult to predict how such an hypothetical particle will look. If the point where the screening overcomes anti-screening is far from the zero charge point, at energies much higher than those required to create a quark anti-quark pair, then, experimentally, the behavior of the quark at present energies will be the same.

From a practical point of view in order to determine the existence of confinement one needs to compute the static potential between a quark and an antiquark. Due to the fact that a dynamical quark-antiquark pair can be created which would lower the energy of the system it is difficult to investigate confinement in the full theory using numerical simulations. The expected increasing potential will flatten out once we reach energies higher than those needed for the quark antiquark pair. It is then impossible to test if there is a distance where a screening behavior sets in. One way to solve this problem is to use pure gauge theories. In pure gauge theories we have no dynamical quarks and the interquark potential is expected to increase indefinitely in a confined phase.

The lattice formulation has the advantage that it allows the calculation of non-perturbative results in numerical simulations. Moreover, the strong coupling regime, $\beta << 1$ can be investigated analytically (strong coupling expansion is not possible in the continuum). We will see that in the strong coupling region pure non-Abelian gauge theories exhibit confinement. However, this behavior is common to all gauge theories on the lattice in the strong coupling limit. This is not a problem since the physical theory will be recovered when we go to the continuum limit. The Abelian gauge theories like QED suffer a phase transition as we go to the weak coupling limit

and the fermions become deconfined. For non-Abelian gauge theories we expect no such phase transition to occur. Up to now there is no numerical evidence to suggest the existence of such a transition.

We will now introduce the operator that measures the interquark potential on the lattice.

2.2 Wilson Loop

Wilson [25] introduced an operator to measure the interquark potential. It is defined as:

$$W_C = \mathrm{Tr} \prod_{b \in C} U_b$$

where C is a closed loop in the lattice (see Fig. 1.3). The product is understood to follow the order of the path C and the trace is usually normalized so that it assumes values between -1 and 1. To see how the vacuum expectation value for this operator is related with the interquark potential consider the following expression:

$$I(\mathbf{x},\mathbf{y},\mathbf{x}',\mathbf{y}';t,t') = \langle\Omega|\bar{\Psi}(\mathbf{x}',t')U(\mathbf{x}',\mathbf{y}';t')\Psi(\mathbf{y}',t')\bar{\Psi}(\mathbf{y},t)U(\mathbf{y},\mathbf{x};t)\Psi(\mathbf{x},t)|\Omega\rangle$$

where $U(\mathbf{x},\mathbf{y};t) = P\exp(ig\int_C A_\mu(x)dx^\mu)$ and C is the line starting at $\mathbf{y}$ and ending at $\mathbf{x}$. This expression represents the probability that a gauge invariant state, $\bar{\Psi}(\mathbf{y},t)U(\mathbf{y},\mathbf{x};t)\Psi(\mathbf{x},t)|\Omega\rangle$, formed out of a massive pair of quark and antiquark at $\mathbf{x}$ and $\mathbf{y}$ at time t propagates to $\mathbf{x}'$ and $\mathbf{y}'$ at time t'. This massive fermionic field couples with the gauge field in the minimal way. It can be shown [3] that in the

limit of infinitely massive quarks we have:

$$I(\mathbf{x},\mathbf{y},\mathbf{x}',\mathbf{y}';t,t') \sim \delta(\mathbf{x}-\mathbf{x}')\delta(\mathbf{y}-\mathbf{y}')e^{-2iM(t'-t)}\langle\Omega|\,\mathrm{Tr}\,Pe^{ig\int_C dx^\mu A_\mu}|\Omega\rangle$$

where M is the mass of the quarks and C is the rectangle defined by $(\mathbf{x},t)$, $(\mathbf{y},t)$, $(\mathbf{y}'=\mathbf{y},t')$ and $(\mathbf{x}'=\mathbf{x},t')$. The $e^{-2iM(t'-t)}$ term is due to the rest mass of the quark pair. The energy of the interaction is included in the last term of the expression above and it is expected to behave as:

$$\langle\Omega|\,\mathrm{Tr}\,Pe^{ig\int_C dx^\mu A_\mu}|\Omega\rangle = \sum_k c_k e^{-iE_k(t'-t)}$$

where E_k are the eigenvalues of the Hamiltonian and c_k represent the overlaps of the gauge invariant state $\bar{\Psi}(\mathbf{y},t)U(\mathbf{y},\mathbf{x};t)\Psi(\mathbf{x},t)|\Omega\rangle$ with the eigenvectors of the Hamiltonian. In the Euclidian formulation this term will be:

$$\langle\Omega|\,\mathrm{Tr}\,Pe^{ig\int_C dx^\mu A_\mu}|\Omega\rangle = \sum_k c_k e^{-E_k(t'-t)}$$

and we see that for large time separations we have:

$$\langle\Omega|\,\mathrm{Tr}\,Pe^{ig\int_C dx^\mu A_\mu}|\Omega\rangle \sim c_0 e^{-E_0(t'-t)}$$

where E_0 is the energy of the lowest state that has a non-zero overlap with our gauge invariant state. Thus from studying the asymptotic behavior of this operator we can extract the potential energy of the quark-antiquark pair, E_0.

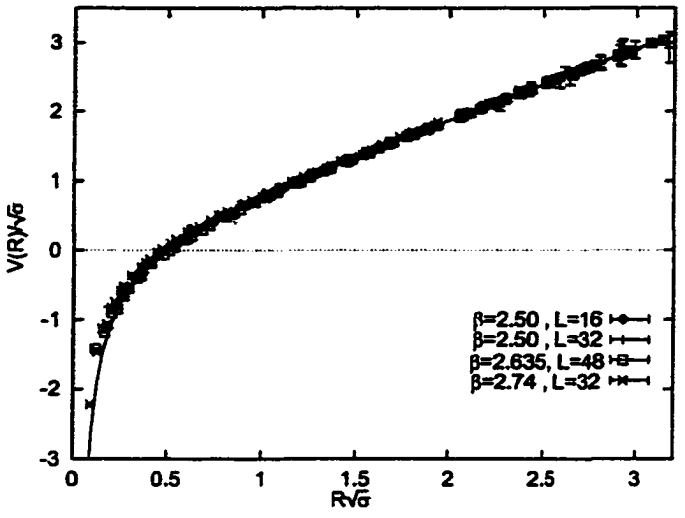

Figure 2.1: Interquark potential for pure $SU(2)$ theory. Note that the potential is measured at different values of β and for different lattice sizes and is scaled in units of the string tension. The solid line is the string picture expectation $V(R) = \sigma R - \frac{\pi}{12R}$ [26].

On the lattice the operator $\mathrm{Tr}\, P e^{ig\int_C dx_\mu A_\mu}$ is represented by the Wilson loop W_C. Using its average we can define the interquark potential as:

$$V(R) = -\lim_{T\to\infty} \frac{1}{T} \ln\langle W(R,T)\rangle$$

where $W(R,T)$ is the Wilson loop measured around the rectangle of length R in the spatial direction and T in the time direction.

In a pure gauge theory this potential is expected to grow indefinitely if we are to have confinement. The state of the art lattice simulations [26, 27] show that this is indeed the case (see Fig. 2.1 and Fig. 2.2). We see that up to the available lattice sizes the potential is indeed increasing. Moreover, in Fig. 2.1 we observe the scaling of the interquark potential: the potential is computed at different values of

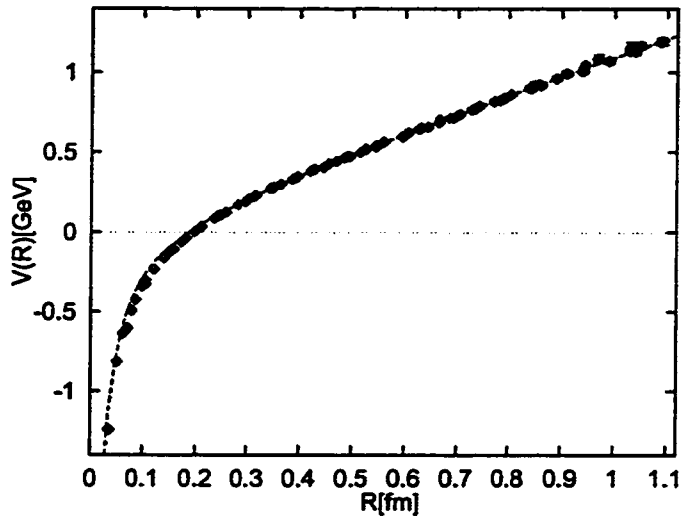

Figure 2.2: Interquark potential for pure $SU(3)$ theory. The simulation was run on a $48^3 \times 64$ lattice at $\beta = 6.8$ corresponding to a lattice spacing $a \simeq 0.035fm$. The graph is scaled in physical units. The solid line represents the string potential $V(R) = \sigma R - \frac{e}{R}$ [27].

β but after calibrating the lattice using the string tension we see that the shape of the potential is the same, the points fall on the same curve. We also see that at sufficiently large distances a linear behavior sets in. We define:

$$\sigma = \lim_{R\to\infty} \frac{\partial V(r)}{\partial R} = -\lim_{A\to\infty} \frac{1}{A} \ln\langle W_C \rangle$$

where A is the minimal area spanned by the Wilson loop. This observable is called the *string tension*. Its name comes from the string picture of confinement. The gluon field is believed to be squeezed in thin tubes that run between color charges. Thus a quark-antiquark pair looks like a string with finite density per unit length. This energy density can be interpreted as the tension in the string σ. The measured string tension is $\sigma \simeq (440MeV)^2$. This value is determined using a Cornell potential

to fit the spectrum of heavy quarks mesons [28]. This is one of the parameters most used to calibrate the lattice.

Thus in a confined phase the Wilson loop is:

$$W_C \sim e^{-\sigma A}$$

when $A \to \infty$. This behavior is called the *area law* since the average Wilson loop vanishes exponentially with the area enclosed. Hence we have our first criterion of confinement:

If the Wilson loop exhibits an area law then we have confinement.

In an unconfined phase the Wilson loop is expected to have a *perimeter law* behavior:

$$W_C \sim e^{-\alpha P}$$

where P is the perimeter of the loop C. This is expected since even for a constant interquark potential there will be an exponential decay due to the time-like legs of the Wilson loop. In the Euclidian formulation the time and space directions are on the same footing and thus we should expect the same attenuation as in the space direction. Thus the perimeter will drive the decay in the large loop limit in the absence of confinement. In this phase the string tension, $\sigma = 0$. Thus, the string tension can be used as an order parameter to signal the confined phase.

One question that can arise is whether the potential can increase in a different fashion. It has been shown that for gauge theories on the lattice the potential cannot increase faster than linearly. Tomboulis [29] has shown that:

$$\langle W(1,1)\rangle \leq \langle W(I,J)\rangle^{1/IJ}$$

for all theories that have reflection positivity. Reflection positivity [4, 30] is a fundamental requirement for lattice theories. Without it we cannot construct a positive definite transfer matrix and we cannot recover the Minkowski Green functions from the Euclidian ones. The action that we will use in this text obeys this requirement. Using the relation above we can write:

$$V(r) = -\lim_{T\to\infty}\frac{1}{T}\ln\langle W(\frac{r}{a},T)\rangle \leq \frac{-\ln\langle W(1,1)\rangle}{a}r$$

and we see that the potential cannot increase faster than linearly. $-\ln\langle W(1,1)\rangle \geq 0$ always since the Wilson loop is normalized to have values between -1 and 1. It can also be shown that $\langle W(1,1)\rangle \geq 0$.

It is worth mentioning that even if $\sigma = 0$ we can still have confinement. It is possible to have a potential that increases slower than linearly (for example $V(r) \sim \sqrt{r}$) and then the string tension is zero. However, we can always determine if we have confinement by simply looking at the potential.

On the practical side there is a useful quantity connected with the string tension. Most of the time the area law is accompanied by a background perimeter law. The

dominant behavior will be the area law behavior in the large loops limit. However, for small loops the perimeter law can have an important effect. To cancel this background we define the Creutz Ratio [2]:

$$\chi(I,J) = -\ln \frac{\langle W(I,J)\rangle \langle W(I-1,J-1)\rangle}{\langle W(I,J-1)\rangle \langle W(I-1,J)\rangle}$$

For a Wilson loop average with an area law and a perimeter law:

$$\langle W(I,J)\rangle = e^{-\sigma A - \alpha P} = e^{-\sigma IJ - 2\alpha(I+J)}$$

we have:

$$\chi(I,J) = \sigma$$

The advantage of using this ratio is that it converges faster to the string tension since it eliminates the perimeter term.

In the strong coupling limit ($\beta \to 0$) we can use perturbation theory to compute the Wilson loop. Using the Wilson action for $SU(N)$ pure gauge theories:

$$S = \frac{\beta}{N} \sum_p Re\,\mathrm{Tr}\, U_p$$

we get [2, 3]:

$$\langle W(I,J)\rangle \to \begin{cases} \left(\frac{\beta}{2N^2}\right)^{IJ} & N > 2 \\ \left(\frac{\beta}{4}\right)^{IJ} & SU(2) \end{cases}$$

in the limit $\beta \to 0$. We see then that in the strong coupling regime $SU(N)$ theories

have an area law. The string tension, in this limit, is:

$$\sigma \to \begin{cases} -\ln \frac{\beta}{2N^2} & N > 2 \\ -\ln \frac{\beta}{4} & SU(2) \end{cases}$$

The only question that remains to be settled is whether in going to the continuum limit ($\beta \to \infty$) we encounter any phase transitions. The numerical simulations suggest that we have no such phase transitions. However, no analytical proof has been put forth. This is one reason why different mechanisms for confinement have been developed. The hope is to find the degrees of freedom that are relevant for confinement. Center vortices represent such an attempt. In the next section we will introduce a different operator that is related both to the Wilson loop and to center vortices.

2.3 Center Vortices and the 't Hooft Loop

The 't Hooft loop is closely connected with the center vortices. We will see that the 't Hooft loop inserts a vortex slice in a configuration. Let us take an $SU(N)$ field in the continuum. Under a gauge transformation:

$$A_\mu \to A_\mu^\Omega = \Omega A_\mu \Omega^\dagger - \frac{i}{g}\Omega \partial_\mu \Omega^\dagger$$

We see that the gauge field doesn't change under the $Z(N)$ transformations (i.e. Ω and $Z\Omega$ have the same effect when $Z \in Z(N)$). Let us take the field in an x, y plane and define a gauge transformation that doesn't depend on z, t. In the x, y pane define a cut-line going from the origin to infinity (see Fig. 2.3). Define a gauge

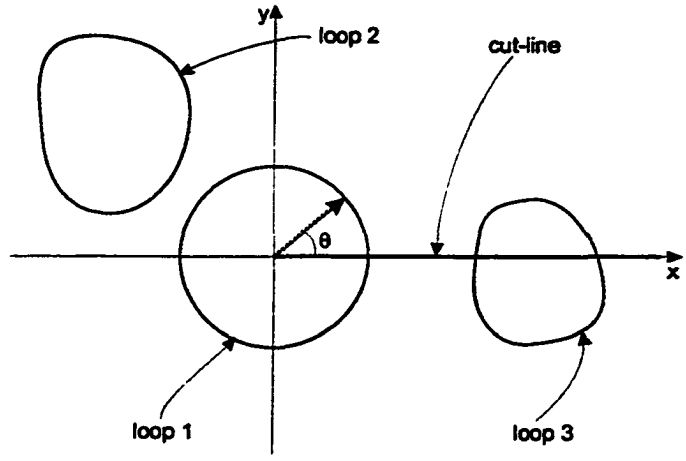

Figure 2.3: An $x-y$ plane in the four dimensional space. The cut-line is the place where our gauge transformation is singular. We also show a number of different types of loops in this plane.

transformation $\Omega(x,y) = \Omega(r,\theta)$ such that $\Omega(r,2\pi) = Z\Omega(r,0)$ where $Z \in Z(N)$. This is not exactly a gauge transformation since it has a discontinuity at the cut-line. However, if we are to look at the gauge field itself we see that:

$$\lim_{\theta \nearrow 2\pi} A_\mu^\Omega(r,\theta) = \lim_{\theta \searrow 0} A_\mu^\Omega(r,\theta)$$

since we started with a continuous gauge field and at the cut-line the gauge transformation differs by a center element. In order for A_μ^Ω to be gauge equivalent to A_μ we need to introduce a singular field on the cut-line. However, we are not interested in producing a gauge equivalent configuration. We will only be interested in our new gauge configuration A_μ^Ω which we know is continuous all over the plane except, maybe, at the cut-line. We know that at the cut-line the field is continuous too. The only point where the field is singular is at the origin. We will show this below.

Let us compare the new gauge field A_μ^Ω with the original field A_μ. To see where they differ let's consider the closed Schwinger lines in this plane. Under a gauge transformation they change to:

$$Pe^{ig\oint_C A_\mu dx^\mu} \to \Omega(x) Pe^{ig\oint_C A_\mu dx^\mu} \Omega(x)^\dagger$$

where C is a curve starting and ending at x. This is true for a gauge transformation. Ours is only an approximate gauge transformation. To be precise as long as the curve C doesn't cross the cut-line (for example loop 2 in Fig. 2.3) the above formula is true. However, if the loop crosses the cut-line we need to be more careful. Let's consider a loop crossing the cut-line once (like loop 1 in Fig. 2.3). Then the Schwinger line integral changes to:

$$Pe^{ig\oint_C A_\mu dx^\mu} \to \Omega(r,0) Pe^{ig\oint_C A_\mu dx^\mu} \Omega(r,2\pi)^\dagger = \Omega(r,0) Pe^{ig\oint_C A_\mu dx^\mu} \Omega(r,0)^\dagger Z^\dagger$$

The Wilson loop for such a curve will then change:

$$W_C(A_\mu) = \mathrm{Tr}\, Pe^{ig\oint_C A_\mu dx^\mu} \to W_C(A_\mu^\Omega) = \mathrm{Tr}\left(\Omega(r,0) Pe^{ig\oint_C A_\mu dx^\mu} \Omega(r,0)^\dagger Z^\dagger\right) = Z^\dagger W_C(A_\mu)$$

We see then that the Wilson loop on this curve gains a factor due to a center element.

For a loop that crosses the cutline but doesn't encircle the origin (like loop 3 in Fig. 2.3) the Wilson loop doesn't change. To see this we write:

$$W_C(A_\mu^\Omega) \;=\; \mathrm{Tr}\left[Pe^{ig\int_{C_1} A_\mu dx^\mu} Pe^{ig\int_{C_2} A_\mu dx^\mu}\right]$$

$$= \mathrm{Tr}\left[\Omega(r,0)Pe^{ig\int_{C_1}A_\mu dx^\mu}\Omega(r',0)^\dagger\Omega(r',2\pi)Pe^{ig\int_{C_2}A_\mu dx^\mu}\Omega(r,2\pi)^\dagger\right]$$

$$= \mathrm{Tr}\left[\Omega(r,0)Pe^{ig\int_{C_1}A_\mu dx^\mu}ZPe^{ig\int_{C_2}A_\mu dx^\mu}\Omega(r,0)^\dagger Z^\dagger\right] = W_C(A_\mu)$$

In general a Wilson loop will have the same value in the new configuration as in the original configuration. The only exception are the loops that circle the origin. Their value will be altered with Z^n where n is the number of times they circle the origin in clockwise fashion minus the number of times they circle the origin in anticlockwise fashion. Since we can define the field strength $F_{\mu\nu}$ using small Wilson loops (we can write formally $F_{\mu\nu} = \lim_{C_{\mu\nu}\to 0}\frac{1-W_{C_{\mu\nu}}}{Area(C_{\mu\nu})}$ where $C_{\mu\nu}$ is a small loop circling a rectangle in the μ,ν directions) we conclude that the field strength is the same everywhere except at the origin. We can also see that the field is singular at the origin since smaller and smaller loops do not approach 1 but rather an element in the center of the gauge group. This singularity can be removed by "smearing" it around the origin. For example we can retain the new configuration A^Ω_μ only for $r > r_0$ and define A_μ in the disc $r < r_0$ such that the field is continuous. Such a configuration will have the same properties as A^Ω_μ except around the origin. 't Hooft [9] calls this a "renormalization" issue and we are not going to deal with it here.

Going back to four dimensions we see that our A^Ω_μ field matches the original A_μ field except on loops circling the (z,t) plane at $x = y = 0$. On this plane the field is singular (or has a large action density after renormalization). This is the salient feature of our new configuration. By going from A_μ to A^Ω_μ we have inserted a *center vortex* lying on the $x = y = 0$ plane. We can see now that these vortices have to

carry a center element since if we are using a different group element to introduce the discontinuity the gauge field will be discontinuous as well.

The center vortices can lie on an infinite plane but they can also be defined on a closed surface. If we look at such a closed surface in a three dimensional slice of the space we will see a closed loop C^*. As in the case of the infinite plane if we measure a Wilson loop C we get the same value except when C winds around C^*. In this case the Wilson loop will pick an element from the center of the gauge group. In the operator picture we can talk about an operator $B(C^*)$ defined on closed loops C^* that inserts this distortion in the field. This operator was introduced by 't Hooft [9] and has these commutation relations with the Wilson loop:

$$W(C)B(C^*) = B(C^*)W(C)Z(C,C^*)$$

where $Z(C,C^*) \in Z(N)$ and depends on the number of times the 't Hooft loop C^* winds around the Wilson loop C. If the loops are unlinked then $Z(C,C^*) = 1$. The commutation relations are evaluated at the same time (i.e. the loops C and C^* lie in the same three dimensional slice). They assert that if we are to measure the Wilson loop first and then insert a center vortex, linked with the measured Wilson loop, we will get a result that differs by a center element from the result that we get when we first insert the center vortex. In general we have:

$$Z(C,C^*) = Z_0^{n(C,C^*)}$$

where $n(C, C^*)$ is the number of times C^* winds around C. Z_0 is the center element used to define the singular gauge transformation Ω. For the 't Hooft operator we will always choose

$$Z_0 = \epsilon = e^{i2\pi/N}$$

where ϵ is the generator for $Z(N)$.

't Hooft [9] argued that we can deduce the behavior of the Wilson loop using the 't Hooft loop. His argument starts by considering two large loops C and C^* that are linked and far away from each other (the curve C never comes close to the curve C^*). Relaxing the constraint to the three dimensional slice we can deform C^* (or C) continuously to another curve $\bar{C}^*$, that lives in the original three dimensional slice, but it is not linked with C. Moreover, we can do this deformation and keep the curves C and C^*_τ (the deformed curve with $C^*_0 = C^*$ and $C^*_1 = \bar{C}^*$) still far apart at all stages of the transformation. Since C and C^*_τ are far apart we can assume declustering and write:

$$\langle B(C^*_\tau)W(C)\rangle \simeq \langle B(C^*_\tau)\rangle\langle W(C)\rangle e^{i\alpha(C,C^*_\tau)}$$

where we used the commutation relations. $\alpha(C, C^*_\tau)$ does not have to be a multiple of $2\pi/N$ since the two loops are not in the same three dimensional slice. However, it varies from $\alpha(C, C^*) = 2\pi/N$, the linked situation, to $\alpha(C, \bar{C}^*) = 0$ for the unlinked situation. If there are no massless particles in the theory, 't Hooft asserts that α cannot vary continously. Where will the jump take place? We know that α has

to change when C^* pierces a surface S bounded by C or when C pierces a surface S^* bounded by C^*. In either case a physical quantity, α, suffers a change and thus there is a physical sheet S (or S^*) that carries a finite action density.

From this we infer that at least one of the loops needs to have an area law. We are then able to state a second criterion for confinement:

> If the 't Hooft loop has a perimeter law behavior, then we have confinement.

In order to find the lattice implementation for the 't Hooft loop operator we need to introduce the transfer matrix for the lattice. This is necessary since the definition for the 't Hooft loop is given in the operator approach (the Wilson loop and 't Hooft loop commutation relations have to be evaluated at the same time). Following Yaffe [31] we construct the Hilbert space for a lattice gauge theory using the kets $|U_\Sigma\rangle$ where U_Σ is an $SU(N)$ gauge configuration defined on the spatial links at a certain time. The scalar product is defined to be:

$$\langle U_\Sigma^1 | U_\Sigma^2 \rangle = \delta(U_\Sigma^1 U_\Sigma^{2\dagger}) e^{-\frac{\beta}{N}\sum_{p\in\Sigma} Re\,\mathrm{Tr}\,U_p}$$

where Σ is a three dimensional slice in the lattice at a fixed time. All plaquettes included in Σ are spatial plaquettes. The transfer matrix is then:

$$\langle U_{\Sigma_2} | e^{-H} | U_{\Sigma_1} \rangle = \int dU_\Xi e^{\frac{\beta}{N}\sum_{p\in\Xi} Re\,\mathrm{Tr}\,U_p}$$

where Ξ includes the time plaquettes starting in U_{Σ_1} and ending in U_{Σ_2}, one time

step away. Using this we can write the partition function:

$$Z = \mathrm{Tr}\, e^{-TH}$$

where T is the extent of the lattice in the time direction. The lattice averages will be:

$$\langle A \rangle = \frac{\mathrm{Tr}(Ae^{-TH})}{\mathrm{Tr}\, e^{-TH}}$$

for any operator A. To see this all we have to do is to consider:

$$Z = \int dU_{\Sigma_T} \langle U_{\Sigma_T} | e^{-TH} | U_{\Sigma_T} \rangle e^{\frac{\beta}{N} \sum_{p \in \Sigma_T} Re\, \mathrm{Tr}\, U_p}$$

and insert the identity operator:

$$I = \int dU_{\Sigma} |U_{\Sigma}\rangle \langle U_{\Sigma}| e^{\frac{\beta}{N} \sum_{p \in \Sigma} Re\, \mathrm{Tr}\, U_p}$$

in the appropriate places. The extra factors appearing in the last two expressions are due to the fact that the kets are not normalized. We write:

$$\begin{aligned} Z &= \int dU_{\Sigma_1} ... dU_{\Sigma_T} \langle U_{\Sigma_T} | e^{-H} | U_{\Sigma_{T-1}} \rangle e^{\frac{\beta}{N} \sum_{p \in \Sigma_{T-1}} Re\, \mathrm{Tr}\, U_p} ... \langle U_{\Sigma_1} | e^{-H} | U_{\sigma_T} \rangle \\ &= \int dU_{\Sigma_1} ... dU_{\Sigma_T} dU_{\Xi_1} ... dU_{\Xi_T} e^{\frac{\beta}{N} \sum_{p \in \Xi_T} Re\, \mathrm{Tr}\, U_p} e^{\frac{\beta}{N} \sum_{p \in \Sigma_{T-1}} Re\, \mathrm{Tr}\, U_p} ... e^{\frac{\beta}{N} \sum_{p \in \Xi_1} Re\, \mathrm{Tr}\, U_p} \\ &= \int dU_{\Lambda} e^{\frac{\beta}{N} \sum_{p \in \Lambda} Re\, \mathrm{Tr}\, U_p} \end{aligned}$$

which is exactly the usual partition function. In this formalism we can define the

Wilson loop by its action on the kets:

$$W_C|U_\Sigma\rangle = \mathrm{Tr}\left(\prod_{b\in C} U_b\right)|U_\Sigma\rangle$$

and we see that the Wilson loop operator is diagonal in this base. The 't Hooft loop cannot be diagonal in this base since it doesn't commute with the Wilson loop. We know that its action is to change the value of the Wilson loop when the Wilson loop winds around C^*. We can implement this type of action starting with a set of links L^* and writing:

$$B(C^*)|U_\Sigma\rangle = |U'_\Sigma\rangle$$

where the configuration U'_Σ is given by:

$$U'_b = \begin{cases} U_b & b \notin L^* \\ \epsilon U_b & b \in L^* \end{cases}$$

The set L^* will play the role of the interior of loop C^*. Every time the Wilson loop crosses it in the positive direction it will pick up an ϵ factor. We will show later that the expectation value of $B(C^*)$ doesn't depend on our choice of L^*. The average of this operator will be:

$$\begin{aligned}
\langle\Omega|B(C^*)|\Omega\rangle &= \frac{\mathrm{Tr}\left(e^{-TH}B(C^*)\right)}{\mathrm{Tr}\,e^{-TH}} \\
&= \frac{1}{Z}\int dU_{\Sigma_T}\langle U_{\Sigma_T}|e^{-TH}B(C^*)|U_{\Sigma_T}\rangle e^{\frac{\beta}{N}\sum_{p\in\Sigma_T} Re\,\mathrm{Tr}\,U_p} \\
&= \frac{1}{Z}\int dU_{\Sigma_1}...dU_{\Sigma_2}...e^{\frac{\beta}{N}\sum_{p\in\Sigma_1} Re\,\mathrm{Tr}\,U_p}...e^{\frac{\beta}{N}\sum_{p\in\Sigma_T} Re\,\mathrm{Tr}\,U_p}\langle U_{\Sigma_1}|e^{-H}|U'_{\Sigma_T}\rangle
\end{aligned}$$

In the last bracket we have $|U'_{\Sigma_T}\rangle = B(C^*)|U_{\Sigma_T}\rangle$. We write:

$$\langle U_{\Sigma_1}|e^{-H}|U'_{\Sigma_T}\rangle = \int dU_{\Xi_1} e^{\frac{\beta}{N}\sum_{p\in\Xi_1} Re\,\mathrm{Tr}\,U'_p}$$

where the values of U'_p are the same as those generated by $\langle U_{\Sigma_1}|e^{-H}|U_{\Sigma_T}\rangle$ except on the plaquettes that start in the set $L^* \subset \Sigma_T$ and extend one unit in the positive time direction. We will denote the set form by these plaquettes with S^*. For these plaquettes there is an extra ϵ factor. Summing up we write:

$$\begin{aligned}
\langle\Omega|B(C^*)|\Omega\rangle &= \frac{1}{Z}\int dU_\Lambda e^{\frac{\beta}{N}\sum_{p\notin S^*} Re\,\mathrm{Tr}\,U_p} e^{\frac{\beta}{N}\sum_{p\in S^*} Re\,\mathrm{Tr}(\epsilon U_p)} \\
&= \frac{1}{Z}\int dU_\Lambda e^{\frac{\beta}{N}\sum_{p\in\Lambda} Re\,\mathrm{Tr}\,U_p} e^{\frac{\beta}{N}\sum_{p\in S^*} Re((\epsilon-1)\,\mathrm{Tr}\,U_p)} \\
&= \left\langle e^{\frac{\beta}{N}\sum_{p\in S^*} Re[(\epsilon-1)\,\mathrm{Tr}\,U_p]}\right\rangle
\end{aligned}$$

Due to the Haar invariance of the measure we know that the average is invariant under the transformation $U_b \to \epsilon U_b$. Thus:

$$\left\langle e^{\frac{\beta}{N}\sum_{p\in S_1^*} Re[(\epsilon-1)\,\mathrm{Tr}\,U_p]}\right\rangle = \left\langle e^{\frac{\beta}{N}\sum_{p\in S_2^*} Re[(\epsilon-1)\,\mathrm{Tr}\,U_p]}\right\rangle$$

as long as the sets S_1^* and S_2^* form a co-closed surface. Thus we can change the surface S^* to any other surface $S^{*\prime}$ as long as their coboundary are the same: $\hat{\partial}S^* = \hat{\partial}S^{*\prime}$. The only thing that is invariant is the set of cubes $\hat{\partial}S^*$. This is obviously a co-closed set since it is the co-boundary of another set. On the dual lattice it is represented by a closed loop. This will be our 't Hooft loop C^*.

To sum up, the 't Hooft loop lives on the dual lattice. We showed how to construct it for a special case where it lies in a three dimensional spatial slice. However, we can now extend this definition to any loop C^* on the dual lattice. For any such loop we take a surface tiling it $\hat{\partial} S^* = C^*$ and we define its expectation value to be:

$$\langle B(C^*) \rangle = \left\langle e^{\frac{\beta}{N} \sum_{p \in S^*} Re[(\epsilon - 1) \operatorname{Tr} U_p]} \right\rangle$$

If this operator exhibits a perimeter law then the Wilson loop is expected to have an area law (assuming, of course, no massless particles) and we should have confinement.

We have to mention here that although some analytical results support the argument presented by 't Hooft there is no definitive proof that in a theory without massless particle the 't Hooft loop and the Wilson loop are forbidden to have a perimeter law simultaneously. Mack and Petkova [32] and Yaffe [31] proved that in the presence of certain constraints the 't Hooft loop exhibits an area law. However, the Wilson loop still has an area law. This is, of course, allowed by the 't Hooft argument but it shows that the Wilson loop and the 't Hooft loop are not perfectly dual to each other in an $SU(N)$ theory (in $Z(2)$ we will show that they are dual). A further analysis by Tomboulis [12] shows that the perimeter law of the 't Hooft loop is due to screening provided by the $Z(2)$ monopoles (these objects will be introduced in a latter chapter).

On the numerical side, there are very few simulations focusing on the 't Hooft loop. The reason is that it is difficult to measure with sufficient accuracy. The main

problem is that the 't Hooft loop can vary over a wide range of values and the bigger its area the more wild the variations. There are only a few numerical studies of the 't Hooft loop and they focus primarily on the $Z(2)$ monopole potential [33].

2.4 Magnetic and Electric Free Energies

The physical interpretation of the 't Hooft loop is that it introduces a magnetic loop on the curve C^* that acts as a source of magnetic flux. 't Hooft [34] considered a periodic boundary condition box and extended the 't Hooft loop to wrap around the lattice. The advantage of this procedure is that you get rid of the magnetic loop but you still retain the magnetic flux running through the lattice.

To see how this is implemented on the lattice we present a derivation due to Yaffe [31]. We will again use the operator approach. On a periodic lattice the physical states $|\Psi\rangle$ are represented by vectors in the Hilbert space constructed out of the kets $|U_\Sigma\rangle$. The vectors representing physical states have to be gauge invariant i.e.:

$$\langle U_\Sigma|\Phi\rangle = \langle U_\Sigma^G|\Psi\rangle$$

where $|U_\Sigma^G\rangle$ is the gauge transformed ket of $|U_\Sigma\rangle$. The gauge transformations G have the same boundary conditions as the lattice. However, we can consider a transformation that looks like a non-periodic gauge transformation. The transformations that we will consider here are formed out of the center elements that are defined on links rather than sites (the regular gauge transformations are defines on sites). Such a transformation will be 1 everywhere except on a certain set of links that we now define. We will take the $1,2$ directions in the three dimensional slice Σ and

consider:

$$L_{12}^{*} = \{b^{3}_{(n_1,n_2,0)} \in \Sigma\}$$

This is the set of links that start in the $1,2$ plane and extend one unit in the positive 3 direction. The operator associated with this transformation is:

$$B_{12}|U_{\Sigma}\rangle = |U'_{\Sigma}\rangle$$

where:

$$U'_b = \begin{cases} U_b & b \notin L_{12}^{*} \\ \epsilon U_b & b \in L_{12}^{*} \end{cases}$$

This operator is said to introduce a unit magnetic flux ϵ in the $1,2$ direction. $B_{12}^{m_{12}}$ will introduce m_{12} units of magnetic flux. We see that m_{12} is defined only modulo N since $B_{12}^{N} = 1$. This transformation is not a proper gauge transformation and the physical states $|\Psi\rangle$ need not be invariant under this transformations. We will say about a state $|\Psi\rangle$ that it carries e_{12} units of electric flux in the 12 direction if:

$$B_{12}|\Psi\rangle = \epsilon^{e_{12}}|\Psi\rangle$$

We see that e_{12} has to be an integer since $B_{12}^{N} = 1$. The electric flux is also defined only modulo N. We can define a projection operator on the subspace with e_{12} units of electric flux:

$$P(e_{12}) = \sum_{m_{12}=0}^{N-1} \epsilon^{e_{12}m_{12}} B_{12}^{m_{12}} \tag{2.1}$$

Going back to the usual lattice formulation we can see that the operator B_{12} is very

much like the 't Hooft operator described in the previous section and following the same steps we can write:

$$\langle \Omega | B_{12} | \Omega \rangle = \left\langle e^{\frac{\beta}{N} \sum_{p \in S^*_{12}} Re[(\epsilon - 1) \operatorname{Tr} U_p]} \right\rangle$$

where $S^*_{12} = \hat{\partial} L^*_{12}$ is a co-closed plane of 34 plaquettes wrapping around the lattice in the 12 direction. Since we know that we can shift the plane without affecting the average as long as the plane remains wrapped in the 12 directions the choice of the surface S^*_{12} is immaterial.

We can now extend this definition to any pair $\mu\nu$ of directions in the lattice. We will have then the operators $B_{\mu\nu}$ with the expectation values:

$$\langle \Omega | B_{\mu\nu} | \Omega \rangle = \left\langle e^{\frac{\beta}{N} \sum_{p \in S^*_{\mu\nu}} Re[(\epsilon - 1) \operatorname{Tr} U_p]} \right\rangle$$

These operators commute and they are related with the projections operators $P(\vec{e})$ (where $\vec{e} = (e_{01}, ..., e_{23})$ is the electric flux running through the lattice in all possible directions) by a generalization of equation (2.1):

$$P(\vec{e}) = \sum_{\vec{m}} \epsilon^{\vec{e} \cdot \vec{m}} B_{\vec{m}}$$

where $\vec{m} = (m_{01}, ..., m_{23})$ is the six component magnetic flux and $B_{\vec{m}} = \prod_{\mu\nu} B_{\mu\nu}^{m_{\mu\nu}}$.

Using the averages of these operators we can define the electric flux free energy:

$$e^{-F_m(\vec{m})} = \langle \Omega | B_{\vec{m}} | \Omega \rangle = \left\langle e^{\frac{\beta}{N} \sum_{\mu\nu} \sum_{p \in S^*_{\mu\nu}} Re[(\epsilon^{m_{\mu\nu}} - 1) \operatorname{Tr} U_p]} \right\rangle$$

and magnetic flux free energy:

$$e^{-F_e(\vec{e})} = \langle \Omega | P(\vec{e}) | \Omega \rangle = \sum_{\vec{m}} \epsilon^{\vec{m}\cdot\vec{e}} e^{-F_m(\vec{m})}$$

To make things clearer we will specialize these formulae to the case of $SU(2)$:

$$\begin{aligned} e^{-F_m(\vec{m})} &= \left\langle e^{-\beta \sum_{\mu\nu} \sum_{p \in S^*_{\mu\nu}} \mathrm{Tr}\, U_p} \right\rangle \\ e^{-F_e(\vec{e})} &= \sum_{\vec{m}} (-1)^{\vec{m}\cdot\vec{e}} e^{-F_m(\vec{m})} \end{aligned}$$

where $m_{\mu\nu}$ and $e_{\mu\nu}$ assume only values of 0 and 1. Since the electric flux free energy is the Fourier transform of the magnetic flux free energy we can invert it and write:

$$e^{-F_m(m_{34})} = \sum_{\vec{e}} (-1)^{m_{34}\cdot\vec{e}} e^{-F_e(\vec{e})} = 1 - e^{-F_e(e_{34})}$$

where m_{34} is a flux in the 34 direction. We see that if $F_e \to \infty$ as we increase the size of the box (heavy electric flux as defined by 't Hooft [34]) then $F_m \to 0$ (the magnetic flux is light). For confinement to occur we expect the electric flux to be heavy and its free energy will be:

$$F_e(e_{34}) \sim \sigma A_{12} - \ln(\alpha A_{34})$$

where $A_{\mu\nu}$ is the area of a plane in the $\mu\nu$ direction. 't Hooft argued that this type of behavior is expected for the free energy of the electric flux since such a flux is introduced by a Wilson loop acting in the 12 plane. The second term is just an

entropy factor due to the fact that there are a number of A_{34} positions in the lattice where the flux sheet can be inserted. Using the relation between the electric and magnetic fluxes we can infer that:

$$e^{-F_m(m_{34})} \simeq 1 - F_m(m_{34}) = 1 - e^{-F_e(e_{34})}$$

and thus:

$$F_m(m_{34}) \simeq \alpha A_{34} e^{-\sigma A_{12}} \tag{2.2}$$

In the vortex picture $F_m(m_{34})$ measure the free energy of a vortex wrapping around the lattice in the 34 direction. To see that this is indeed a center vortex we just need to realize that the operator B_{34} associated with $F_m(m_{43})$ introduces a center element on a co-closet set of plaquettes p^{12}. A Wilson loop in a 12 plane will then be unchanged except when it circles around the p^{12} plaquette that belongs to the vortex inserted by B_{34}.

We can then formulate a criterion of confinement in terms of the vortex free energy (or magnetic flux free energy):

> If the vortex free energy varies with the size of the box like in equation (2.2) then we have confinement.

Unlike for the 't Hooft loop there are analytical results that such a behavior leads indeed to confinement. Tomboulis and Yaffe [29] have proved that:

$$\langle \mathrm{Tr}(\prod_{b \in C} U_b) \rangle \leq \left(e^{-F_e(e_{34})}\right)^{Ac/A_{12}}$$

where A_C is the minimal area spanned by the Wilson loop C and A_{12} is the area of the plane 12 in which the loop C lies. $F_e(e_{34})$ measures the free energy of an electric flux running through this plane. For a vortex free energy of the type (2.2) and for a large area A_{12} we have:

$$e^{-F_e(e_{34})} = 1 - e^{-F_m(m_{34})} \simeq \alpha A_{34} e^{-\sigma A_{12}}$$

and thus:

$$\langle \mathrm{Tr}(\prod_{b \in C} U_b) \rangle \leq (\alpha A_{34})^{A_C/A_{12}} e^{-\sigma A_C} = e^{-(\sigma - \frac{\ln \alpha A_{34}}{A_{12}}) A_C}$$

For large lattices we have $\frac{\ln \alpha A_{34}}{A_{12}} \to 0$ and thus the Wilson loop will be bounded from above by $e^{-\sigma A_C}$. Then we have an area law for the Wilson loop with the string tension at least σ.

This type of behavior for the vortex free energy is particular to non-Abelian gauge theories. The expected behavior for a $Z(2)$ theory is [35]:

$$F_m(m_{34}) \sim \alpha(\beta) A_{34}$$

and for an $U(1)$ gauge theory:

$$F_m(m_{34}) \sim \beta\alpha \frac{A_{34}}{A_{12}}$$

The first type of behavior corresponds to a vortex that remains thin and cannot be spread by quantum fluctuations (we will see that this is indeed the case for a

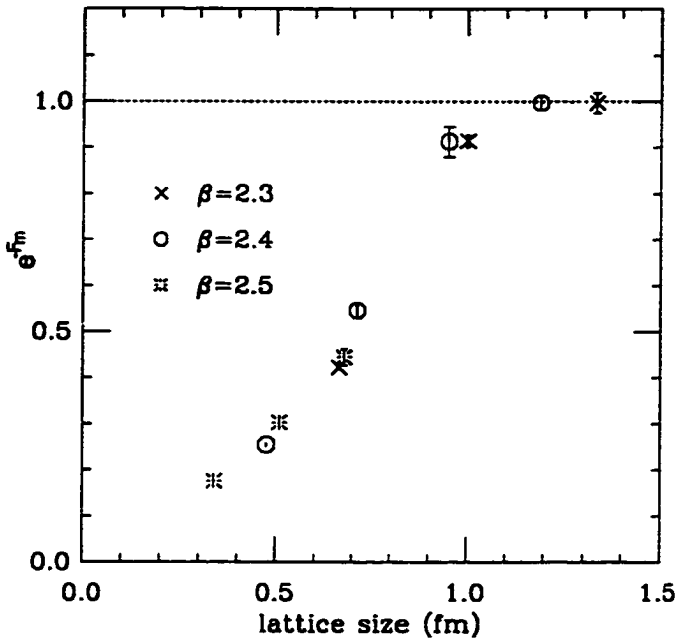

Figure 2.4: SU(2) vortex free energy. Notice that the simulations were run at different β and that the points fall on a universal curve [35].

$Z(2)$ system). The second type of behavior corresponds to a flux that spreads in a Coulomb like fashion. Both these types correspond to theories that are deconfined in the weak coupling limit.

If we look at the possible type of behavior we see that for large lattices it is only the confining behavior (2.2) that predicts a zero free energy for the vortex. Numerical simulations have been performed [35] and we see in Fig. 2.4 that the free energy behaves exactly as expected for a confined phase. It is also interesting to note that the free energy becomes zero at a lattice size of roughly 1 fm and thus we should expect a vortex thickness of around 1 fm.

In conclusion we presented three methods to detect confinement on the lattice. The most widely used operator to detect confinement is the Wilson loop. The 't

Hooft loop is promising but it doesn't have the analytical support. The free energy of the magnetic flux has analytical backing as a criterion for confinement and numerical simulations have started to investigate its behavior. We also note here that the 't Hooft loop and magnetic flux free energy are intimately connected with the idea of center vortices.

We will now explore these ideas in the context of $Z(2)$ gauge theory, a theory that is very well understood.

Chapter 3

$Z(2)$ Lattice Gauge Theory

3.1 Introduction

The discretization makes the idea of continuity difficult to implement on the lattice. One introduces interactions that have the correct continuum limit. These interactions between neighbors on the lattice tend to give a continuous behavior. However, the fact that we are not dealing with continuous quantities makes possible to investigate a new type of systems: systems with discreet gauge groups.

We can use such systems to gain a better insight in the dynamics of the models that use a continuous group. Another reason to study such systems is to use them as a testing ground for new techniques.

We will focus, in this chapter, on the simplest of such groups: the $Z(2)$ group. We present this model because it will help us understand the dynamics of vortices: this system has vortices as its basic excitation. Moreover, the methods used to identify vortices in $SU(2)$ will use some of the results derived in this chapter.

In this chapter we will introduce the concept of duality (and self-duality), we will show how vortices can disorder the Wilson loop to create an area law and we will show that in this theory the 't Hooft loop is exactly dual to the Wilson loop.

3.2 The $Z(2)$ Gauge Theory

Let us take a lattice Λ that has $Z(2)$ variables living on the links: $U_b \in Z(2)$. We write the partition function as [25, 2, 3]:

$$Z = \sum_{\{U\}} e^{S(U)}$$

where:

$$S(U) = \sum_{p \in \Lambda} S_p(U_p)$$

S_p being the action due to a plaquette. The most general type of plaquette action has to be a class action to be invariant under gauge transformations. Any such action admits a character expansion:

$$S_p(U) = \sum_l c_l \chi_l(U) \tag{3.1}$$

where χ_l is the trace in the l^{th} irreducible representation of the gauge group. Now, for $Z(2)$ we have only two such representations:

$$\begin{aligned} \chi_+(U) &= U^0 = 1 \\ \chi_-(U) &= U^1 = U \end{aligned}$$

where $+$ labels the trivial representation and $-$ label the other respresentation. Our action can be written as $S_p(U) = \beta_+ + \beta_- U$. Let us do a character expansion for

$e^{S_p(U)}$. We have:

$$e^{S_p(U)} = b_+ + b_- U$$

The relationship between b and β can be inferred if we write down the equations for $U = \pm 1$:

$$\begin{aligned} e^{\beta_+ + \beta_-} &= b_+ + b_- \\ e^{\beta_+ - \beta_-} &= b_+ - b_- \end{aligned}$$

We solve these equations and find:

$$\begin{aligned} b_+ &= e^{\beta_+} \cosh \beta_- \\ b_- &= e^{\beta_+} \sinh \beta_- \end{aligned}$$

and, conversely:

$$\begin{aligned} \beta_+ &= \frac{1}{2} \ln(b_+^2 - b_-^2) \\ \beta_- &= \frac{1}{2} \ln \frac{b_+ + b_-}{b_+ - b_-} \end{aligned}$$

Now, let us see how to find the dual of this theory. First we will give an outline of the procedure. We will show that the $Z(2)$ gauge theory is approximately self-dual. We start by rewriting the action using the character expansion for $e^{S(U)}$. We then group the terms that are initially defined on links to variable defined on plaquettes. We then notice that we can generate the plaquette variables using configurations

defined on cubes. These variables defined on cubes live on links on the dual lattice. We see then that the final action defined on links in the dual lattice has the same form as the action that we started from. The only difference is in the coefficients that define this action. We will now show the mathematical derivation of this procedure.

Consider the partition function:

$$Z = \sum_{\{U_b\}} e^{\sum_p S_p(U_p)} = \sum_{\{U_b\}} \prod_{p\in\Lambda} \sum_{i_p=\pm 1} b_{i_p} \chi_{i_p}(U_p)$$

where we used the expansion (3.1). We will now rewrite this using our notation in Appendix section A.4. In the partition function we sum over all $Z(2)$ configurations defined on links and thus $\{U_b\} \to C^1(\Lambda)$. Moreover, the product

$$\prod_{p\in\Lambda} \sum_{i_p=\pm 1} \to \sum_{i\in C^2(\Lambda)}$$

since we sum again over all $Z(2)$ configurations defined on plaquettes; we can also write U_p as $\hat{\partial} U(p)$ where $U \in C^1(\Lambda)$. Using these we write:

$$Z = \sum_{U\in C^1(\Lambda)} \sum_{i\in C^2(\Lambda)} \prod_p b_{i(p)} \prod_p \chi_{i(p)}(\hat{\partial} U(p))$$

We will denote $\prod_p b_{i(p)}$ with $b(i)$ and notice that the last term in the expression above is nothing but the bracket, $\{\cdot,\cdot\}$, we introduced in the Appendix section A.5. We write:

$$Z = \sum_{U\in C^1(\Lambda)} \sum_{i\in C^2(\Lambda)} b(i)\{i, \hat{\partial} U\}$$

We use now the property (A.5) and we have:

$$Z = \sum_{i \in C^2(\Lambda)} b(i) \sum_{U \in C^1(\Lambda)} \{\partial i, U\} \tag{3.2}$$

Now using equations (A.6) and (A.7) we have:

$$Z = \sum_{i \in C^2(\Lambda)} b(i) |C^1(\Lambda)| \delta(\partial i)$$

The δ function asserts that the boundary of the i configuration is zero. Then we have:

$$Z = \sum_{i \in Z^2(\Lambda)} b(i) |C^1(\Lambda)|$$

where we remember that $Z^2(\Lambda)$ is the group of all closed configurations of dimension 2. We know that this group can be written as:

$$Z^2(\Lambda) = H^2(\Lambda) \times B^2(\Lambda)$$

where $H^2(\Lambda)$ is the homology group of order 2 and $B^2(\Lambda)$ is the group of boundary configurations of dimension 2. The equality above asserts that all closed configurations can be written as a product of a configuration in $H^2(\Lambda)$ and one in $B^2(\Lambda)$. We have then:

$$Z = |C^1(\Lambda)| \sum_{\alpha \in H^2(\Lambda)} \sum_{\beta \in B^2(\Lambda)} b(\alpha\beta)$$

Now, since $\beta \in B^2(\Lambda)$ there is at least one configuration $\gamma \in C^3(\Lambda)$ such that $\beta = \partial\gamma$. In fact for one such configuration γ we have an entire set $\gamma\tau$ with $\tau \in Z^3(\Lambda)$ such

that $\partial(\gamma\tau) = \partial\gamma\partial\tau = \beta\phi_2 = \beta$ and thus if we are to replace the sum over $B^2(\Lambda)$ with the sum over $C^3(\Lambda)$ we need to take care of this multiplicity. We will have:

$$Z = \frac{|C^1(\Lambda)|}{|Z^3(\Lambda)|} \sum_{\alpha \in H^2(\Lambda)} \sum_{\gamma \in C^3(\Lambda)} b(\alpha\partial\gamma)$$

In order to recover the original form of the action we need to go to the dual lattice. We have:

$$Z = \frac{|C^1(\Lambda)|}{|Z^3(\Lambda)|} \sum_{\alpha \in H^2(\Lambda)} \sum_{\gamma^* \in C^1(\Lambda^*)} b(*\alpha\hat{\partial}\gamma^*)$$

where $*\alpha \in C^2(\Lambda)$ is the image of α on the dual lattice. The isomorphism $* : C^3(\Lambda) \to C^1(\Lambda^*)$ ensures that the summation is the same.

We now remember that:

$$b(*\alpha\hat{\partial}\gamma^*) = \prod_{p \in \Lambda} b_{*\alpha(p)\hat{\partial}\gamma^*(p)}$$

and we write $b_{\pm}$:

$$b_U = ae^{\bar{S}_p(U)} \tag{3.3}$$

where a is a normalization constant. Then we can write:

$$Z = \frac{|C^1(\Lambda)|}{|Z^3(\Lambda)|} \sum_{\alpha \in H^2(\Lambda)} \sum_{\gamma^* \in C^1(\Lambda^*)} a^{N_p} exp\left(\sum_p \bar{S}_p(*\alpha(p)\hat{\partial}\gamma^*(p)\right)$$

where N_p is the number of plaquettes in the lattice. By switching Λ and Λ^* and

reverting to a more familiar notation we get:

$$Z = \frac{|C^1(\Lambda)|}{|Z^3(\Lambda)|} a^{N_p} \sum_{\alpha \in H^2(\Lambda^*)} \sum_{\{U_b\}} e^{\sum_p \bar{S}_p(\alpha_p^* U_p)}$$

where α^* is the image on the direct lattice of α. We choose now a to cancel the factor in front:

$$a = \left[\frac{|C^1(\Lambda)|}{|Z^3(\Lambda)|}\right]^{-1/N_p} = 2^{-\frac{1}{2}\frac{N_s-1}{N_s}}$$

where N_s is the number of sites in the lattice. We finally get:

$$Z = \sum_{\alpha \in H^2(\Lambda^*)} \sum_{\{U_b\}} e^{\sum_p \bar{S}_p(\alpha_p^* U_p)} \tag{3.4}$$

This looks just like the starting partition function where we replaced S_p with $\bar{S}_p$. There is, however, another difference: the summation over the elements of the homology group $H^2(\Lambda^*)$. These elements correspond to configurations that are co-closed (closed on the dual lattice) but are not the co-boundary of any link configuration. The number of such distinct configurations is $|H^2(\Lambda)| = 2^6$. They represent planes on the dual lattice that wrap around the lattice. There are six such planes; one for every pair of directions. We call this configurations twists. We can determine the twist in a given pair of directions $\mu\nu$ for an arbitrary configuration U by taking the bracket $\{U, P_{\mu\nu}\}$. $P_{\mu\nu}$ is a configuration that is everywhere 1 except on a plane that wraps around the lattice in the $\mu\nu$ direction. If the bracket is -1 we say that we have a twist in the $\mu\nu$ direction – this corresponds to a flux running through the

lattice. We can now write:

$$Z = \sum_{\{U_b\}} e^{\sum_p \bar{S}_p(U_p)} + \sum_{\alpha \in H^2(\Lambda^*), \alpha \neq \phi_2} \sum_{\{U_b\}} e^{\sum_p \bar{S}_p(\alpha_p^* U_p)}$$

where we have isolated the sum over configurations with no twist. We want to show that we can safely neglect the sum over twisted configurations. To prove this lets take a simple twist α^* in the $(1,2)$ direction:

$$\alpha^*(p) = \begin{cases} 1 & p \notin P_{12}^* \\ -1 & p \in P_{12}^* \end{cases}$$

where

$$P_{12}^* = \{p^{12}_{0,0,n_3,n_4} | n_3, n_4 \in Z_{N_3,N_4}\}$$

It is easy to see that this configuration is the image on the direct lattice of a configuration that wraps around the dual lattice. We see then that we have:

$$\sum_{\{U_b\}} e^{\sum_p \bar{S}_p(\alpha_p^* U_p)} = \sum_{\{U_b\}} e^{\sum_{p \notin P_{12}^*} \bar{S}_p(U_p) + \sum_{p \in P_{12}^*} \bar{S}_p(-U_p)} = \sum_{\{U_b\}} e^{\sum_p \bar{S}_p(U_p)} e^{\sum_{p \in P_{12}^*} [\bar{S}_p(-U_p) - \bar{S}(U_p)]}$$

We have: $\bar{S}_p(-U_p) - \bar{S}(U_p) = \bar{\beta}_+ - \bar{\beta}_- U_p - \bar{\beta}_+ - \bar{\beta}_- U_p = -2\bar{\beta}_- U_p$. We can write:

$$\sum_{\{U_b\}} e^{\sum_p \bar{S}_p(\alpha_p^* U_p)} = \sum_{\{U_b\}} e^{\sum_p \bar{S}_p(U_p)} e^{-2\bar{\beta}_- \sum_{p \in P_{12}^*} U_p}$$

It is easy to see that $e^{\sum_p \bar{S}_p(U_p)} e^{-2\bar{\beta}_- \sum_{p \in P_{12}^*} U_p}$ will have the upper bound $e^{-2\bar{\beta}_- N_3 N_4}$ times the upper bound of $e^{\sum_p \bar{S}_p(U_p)}$ (N_3, N_4 are the dimensions of the lattice in the

3 and 4 directions). If $\bar{\beta}_-$ is positive (which is always true if we start with a positive β_-) the sum over the twist configurations will be roughly $e^{-2\bar{\beta}_- N_3 N_4}$ times the sum over the no twist configurations. For N_3 and N_4 large enough we can safely neglect this contribution to the partition function.

We are allowed to write then:

$$Z \simeq \sum_{\{U_b\}} e^{\sum_p \bar{S}_p(U_p)}$$

To compute $\bar{S}_p$ we use equation (3.3) to write:

$$\begin{aligned} b_+ &= a e^{\bar{\beta}_+ + \bar{\beta}_-} \\ b_- &= a e^{\bar{\beta}_+ - \bar{\beta}_-} \end{aligned}$$

where $a = 2^{-\frac{1}{2}\frac{N_s-1}{N_s}}$. For N_s large enough we have $a \simeq 1/\sqrt{2}$ and we get:

$$\begin{aligned} \bar{\beta}_+ &= \beta_+ + \frac{1}{2} \ln \sinh 2\beta_- \\ \bar{\beta}_- &= \frac{1}{2} \ln \coth \beta_- \end{aligned} \tag{3.5}$$

In conclusion we see that the four dimensional $Z(2)$ gauge theory is self-dual (the dual of the theory is of the same type). The change in action is given by equation (3.5). We note here that β_+ is a trivial factor in the action; it introduces only a multiplicative factor in the partition function that doesn't change the averages at all.

The parameter that characterizes different points of the theory is β_-. We see that under duality transformations (3.5) small values of the β_- are mapped into large values for $\bar{\beta}_-$ and vice versa. Also we see that there is a point that is mapped into itself:

$$\beta_c = \frac{1}{2}\ln(1+\sqrt{2}) \simeq 0.44$$

3.3 Dual Observables

Now, that we have the dual theory a natural question arises: what is the use of it? All we know thus far is that for a $Z(2)$ gauge theory given by coupling constants (β_+, β_-) there is another pair of coupling constants $(\bar{\beta}_+, \bar{\beta}_-)$, connected with the original pair by the equations (3.5), that yields the same partition function. In what respect is the new point $(\bar{\beta}_+, \bar{\beta}_-)$ dual to the original one? A naive answer will be that the observables have the same value at the dual points. However, this is not true. To make a definite statement about a certain observable we will need to compute its dual observable. To show how this is done we will derive the dual of the Wilson loop.

To define the Wilson loop let's take a closed curve C in the lattice (we will require that this curve is actually the boundary of a surface). We will then define the Wilson loop on a particular configuration U_b to be:

$$W_C(U_b) = \mathrm{Tr}(\prod_{b \in C} U_b)$$

where the product is ordered following the path C through the lattice (in an Abelian

theory the order is not important) and the trace is in the fundamental representation. The average of the Wilson loop will then be:

$$\langle W_C \rangle = \frac{1}{Z} \sum_{\{U_b\}} e^{\sum_p S_p(U_p)} W_C(U_b)$$

We will cast this operator in a form that fits our notation in Appendix (see sections A.4, A.5). We know that $\chi_+(U) = 1$ and $\chi_-(U) = U$. Then we can write the Wilson loop as:

$$W_C(U) = \{i_C, U\}$$

where $i_C \in C^1(\Lambda)$ is defined as:

$$i_C(b) = \begin{cases} 1 & b \notin C \\ -1 & b \in C \end{cases}$$

Using this notation and equation (3.2) we get:

$$\langle W_C \rangle = \langle \{i_C, U\} \rangle = \frac{1}{Z} \sum_{U \in C^1(\Lambda)} \sum_{i \in C^2(\Lambda)} b(i) \{\partial i \cdot i_C, U\}$$

Now, since i_C is a boundary configuration there is $s \in C^2(\Lambda)$ such that $i_C = \partial s$. Then:

$$\langle W_C \rangle = \frac{1}{Z} \sum_{U \in C^1(\Lambda)} \sum_{i \in C^2(\Lambda)} b(i) \{\partial i \cdot \partial s, U\} = \frac{1}{Z} \sum_{U \in C^1(\Lambda)} \sum_{i \in C^2(\Lambda)} b(i) \{\partial (i \cdot s), U\}$$

Using group summation invariance we can write:

$$\langle W_C \rangle = \frac{1}{Z} \sum_{U \in C^1(\Lambda)} \sum_{i \in C^2(\Lambda)} b(i \cdot s^{-1}) \{\partial i, U\}$$

From here on we can apply the same steps as in the previous section and we get an expression similar with equation (3.4):

$$\langle W_C \rangle = \frac{1}{Z} \sum_{\alpha \in H^2(\Lambda^*)} \sum_{\{U_b\}} e^{\sum_p S_p(\alpha_p^* s_p^{*-1} U_p)}$$

where s^{-1} lies in the dual lattice and s^{*-1} is its image in the direct lattice. Using the same approximations as before (neglecting the sum over twist configurations) we get:

$$\langle W_C \rangle = \frac{1}{Z} \sum_{\{U_b\}} e^{\sum_p S_p(s_p^{*-1} U_{1\cdot})}$$

We note here that there is no orientation in $Z(2)$ (since $U^{-1} = U$) and thus $s^{*-1} = s^*$. We see that s^* is a co-surface that has as its co-boundary the co-loop C^*. We can then write in a more usual notation:

$$\langle W_C \rangle = \frac{1}{Z} \sum_{\{U_b\}} e^{\sum_{p \notin S^*} \tilde{S}_p(U_p) + \sum_{p \in S^*} \tilde{S}_p(-U_p)}$$

This operator is exactly the 't Hooft operator as defined in the previous chapter. Thus, the 't Hooft loop is the dual of the Wilson loop. It is dual in the sense that the vacuum expectation value for the Wilson loop for a certain value of β is equal

with the vacuum expectation value for the 't Hooft loop at the dual point $\bar{\beta}$:

$$\langle W_C \rangle_\beta = \langle B_{C^*} \rangle_{\bar{\beta}}$$

where C^* is the image on the dual lattice of the loop C.

3.4 Behavior of the Wilson Loop

We will now focus on understanding the physics of the $Z(2)$ gauge theory. One might wonder why did we choose to focus on the Wilson loop in the previous section: the answer is that the Wilson loop will provide us with an order parameter for the gauge theories. It is known that gauge theories do not have a local order parameter. We usually employ asymptotic values of certain operators or global objects to detect various phases of the system. Using the Wilson loop we define the string tension:

$$\sigma(\beta) = -\lim_{A\to\infty} \frac{1}{A} \ln\langle W_C \rangle$$

where A is the minimal area spanning the Wilson loop. As argued in a previous chapter the physical meaning of the string tension comes from pure $SU(3)$ gauge theory where the Wilson loop is used to measure the static potential between a quark-antiquark pair. The string tension will be our order parameter: it will be zero in the deconfined phase and non-zero in the confined phase.

In $Z(2)$ gauge theory we can have only two types of behavior for the Wilson loop. If we are to find out that the Wilson loop has different types of behavior at two different values of β then we know that we have a phase transition somewhere

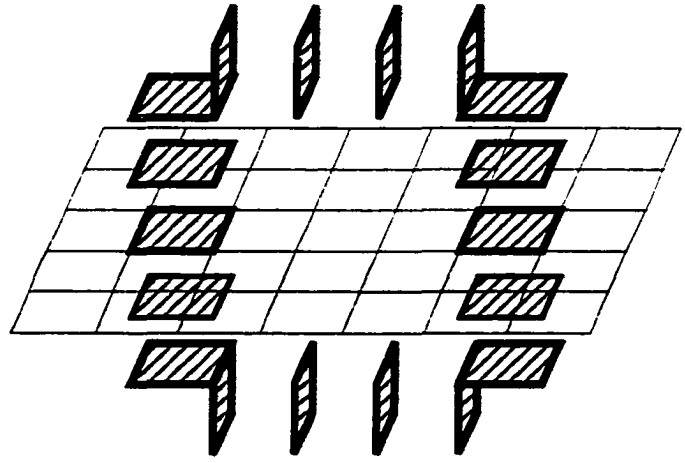

Figure 3.1: A typical vortex in a $2+1$ dimensional lattice. The hashed plaquettes have a -1 value and all the others are $+1$.

between these two values. We will investigate now the behavior of the Wilson loop for different extreme values of β.

At small β we can use a power expansion in β. Using this so called strong coupling expansion we get:

$$\langle W_C \rangle \simeq \frac{1}{Z}\beta^A$$

to the first order in β. We see then that the string tension for $\beta \to 0$ is:

$$\sigma(\beta) = -\ln\beta \tag{3.6}$$

We see that in this regime the Wilson loop has an area law.

We will now present an argument on how vortices can explain this behavior for the Wilson loop. Due to the Abelian nature of the gauge group the product of links around a contour C is equal with the product of the plaquettes tiling that contour.

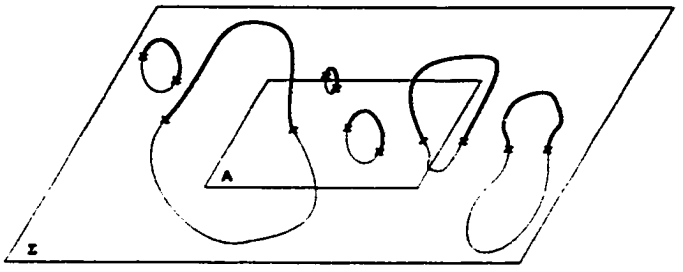

Figure 3.2: Vortices in a $2+1$ theory intersecting the plane Σ. The value of the Wilson loop is given by the number of intersection points trapped inside the Wilson loop.

We can then write the Wilson loop as:

$$W_C = \prod_{p \in S} U_p$$

where $\partial S = C$. It is obvious that the Wilson loop is a counter of how many times the area S is pierced by a vortex (i.e. a plaquette is negative): if the number of times is odd we will get -1 and 1 otherwise.

Since the configurations of -1 are produced by link configurations ($U_p = \hat{\partial} U_b$) we see that they have to be co-closed since $\hat{\partial} U_p = \hat{\partial}^2 U_b = \phi_3$. We will call these configurations, defined on a co-closed set of plaquettes, *vortex configurations*. The $Z(2)$ gauge theory is, in this sense, a vortex theory. A configuration S that is co-closed and irreducible (there is no subset $A \subset S$ that can be removed such that the remaining configuration is still co-closed) will be called a *vortex* (see Fig. 3.1). All vortex configurations can be defined as a product of vortices. Following a standard argument [36] we how it is possible for vortices to create an area law. Each vortex

configuration S has a definite linkage with an Wilson loop:

$$W_C(S) = (-1)^{\alpha(C,S)}$$

where $\alpha(C, S)$ is the number of plaquettes that belong to a surface spanning the Wilson loop and are -1 in the S configuration. The number, $(-1)^{\alpha(C,S)}$, is independent of our choice of the area spanning the Wilson loop.

Imagine now a planar section in the lattice of area Σ (see Fig. 3.2). Take a Wilson loop of area A in this plane. Consider N vortices piercing this plane randomly (assume no correlation). The probability of n such vortices piercing the area A of the Wilson loop is:

$$P_n = C_N^n \left(\frac{A}{\Sigma}\right)^n \left(1 - \frac{A}{\Sigma}\right)^{N-n}$$

The average value of the Wilson loop will be:

$$\langle W_C \rangle = \sum_{n=0}^{N} (-1)^n P_n = \sum_{n=0}^{N} (-1)^n C_N^n \left(\frac{A}{\Sigma}\right)^n \left(1 - \frac{A}{\Sigma}\right)^{N-n} = \left(1 - \frac{2A}{\Sigma}\right)^N$$

Define now $\rho = \frac{N}{\Sigma}$ to be the density of vortices piercing the plane. Then, take the limit $\Sigma \to \infty$ but keep the density ρ fixed. We get:

$$\langle W_C \rangle = \lim_{\Sigma \to \infty} \left(1 - \frac{2A}{\Sigma}\right)^{\rho\Sigma} = e^{-2\rho A}$$

We see that the Wilson loop, in this simple model, is expected to have an area law.

Furthermore, the string tension is related with the planar density of vortices by:

$$\sigma = 2\rho$$

However, this simple model is misleading: for one it will seem that $\langle W_C \rangle$ depends on the area of the surface chosen to span the perimeter C. We know that this is not true. We arrive to this false conclusion because we neglected a very important fact: the vortices have to pierce the plane in pairs since they have to co-closed. We see that it is important to treat the piercing points in pairs generated by the same vortex rather than separately. The model that we showed before has as a sufficient condition for an area law to set in a finite planar density of vortices. We will show that, while this is necessary, it is certainly not enough.

Consider a random distribution of N_p pairs of piercing points on the surface Σ. Furthermore, suppose that the points in a pair cannot be separated by a distance greater than d. We will now look at a Wilson loop that has the area much bigger that this distance ($A \gg d^2$). If the pair is either completely outside or completely inside the Wilson loop it has no effect on its value. In order for the pair to have any effect it has to pierce the plane once inside the Wilson loop and once outside. In order for this to happen we need the midpoint of the pair to lie in a band of width d around the contour C of the loop. Let us denote with p the probability of such a pair lying in this particular band to actually affect the Wilson loop. Then the probability of n_p such pairs to pierce the band (to the first order the area of the

band is Pd where P is the perimeter of the loop) and affect the Wilson loop is:

$$P_{n_p} = C_{N_p}^{n_p} \left(\frac{pPd}{\Sigma}\right)^{n_p} \left(1 - \frac{pPd}{\Sigma}\right)^{N_p - n_p}$$

Using the same steps as before and denoting $\rho = \frac{2N_p}{\Sigma}$ we get:

$$\langle W_C \rangle = \left(1 - \frac{2pPd}{\Sigma}\right)^{N_p} \to e^{-\rho p P d}$$

and thus the Wilson loop has a perimeter law.

We see now that it is not enough to have a non-zero planar density ρ for area law to set in. We need also to require the vortices of any length to have a non-zero probability in the action (it is actually the planar density of vortices of infinite length that will give us the string tension).

Thus we have two possible phases for the system: one in which the vortices *percolate* (we have a non-zero probability for infinitely long vortices) and we have an area law for the Wilson loop; another phase is when the vortices are limited in length and we have a perimeter law for the Wilson loop.

We can understand better the structure of a vortex if we look on the dual lattice. There a vortex is a closed surface and the cost in action for such a vortex is $-2\beta A$ where A is the surface of the vortex. In statistical mechanics terms we have a competition between the cost to excite such a vortex:

$$E(A) \sim e^{-2\beta A}$$

and the entropy or the number of surfaces that have the same area:

$$N(A) \sim e^{kA}$$

The probability to excite a vortex of area A is:

$$P(A) \sim e^{(k-2\beta)A}$$

We see know that the vortices will percolate when $k > 2\beta$ and they don't when $k < \beta$. If we can determine k then we can determine the transition point (we need k for asymptotically large surfaces only to determine the transition point).

This problem is very complicated but we can use some simple arguments to put some bounds on k and implicitly on the transition point.

For an upper bound we can use this argument [37]. Consider the lattice and number the links in the lattice such that you introduce a total ordering among the links. We want now to compute the number $N_{C_0}(A)$ of connected irreducible surfaces S that have the same area A and $\partial S = C_0$. Start with the contour C_0 and pick the lowest ranked link in the contour; attach a plaquette to this link; you have six different choices. Define a new contour C_1 defined by the contour C_0 and the plaquette you just introduced. Repeat the steps for the contour C_1 and arrive to C_2. We can do this until we arrive at C_A and we have included A plaquettes. If C_A is void we have produced an irreducible connected set with area A and $\partial S = C_0$. We see that by using this procedure we are going to generate all surfaces that interest

us. We will also produce some other surfaces but since we are only interested in an upper bound this is not a problem. Since we have six choices at every step we see that we can write:

$$N_{C_0}(A) \leq 6^A$$

We can refine this bound further using the fact that when we are to select the new plaquette there will be only five choices if the lowest ranked link in C_k is actually in the boundary of one of the k plaquettes already selected. We will have then:

$$N_{C_0}(A) \leq 5^{A-|C_0|}6^{|C_0|}$$

where $|C_0|$ is the number of links in C_0. By selecting C_0 to be the contour of a plaquette p_0 we realize that the number of closed surfaces containing p_0 with area A is actually bounded by:

$$N(A) \leq 5^{A-4}6^4$$

For $A \to \infty$ we see that $N(A) \leq 5^A$ and thus we have an upper bound on k:

$$k \leq \ln 5$$

For a lower bound we can count only the non-intersecting strings of cubes starting at a particular cube. In order to insure the fact that the string doesn't self intersect we will start with a cube (let's say c^{123}_{0000}) and consider only the same type of cubes (c^{123}) connected to the "positive" faces (i.e. only c^{123}_{1000} or c^{123}_{0100} or c^{123}_{0010}). By repeating

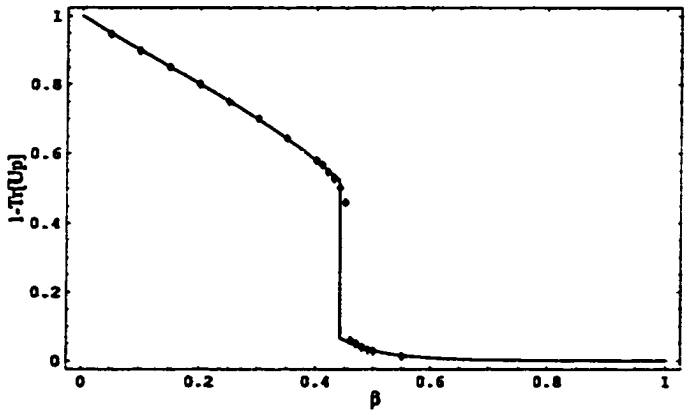

Figure 3.3: The plaquette in $Z(2)$ theory. The line represents analytical results that are computed using the strong coupling expansion and duality. The dots are results from numerical simulations in a 6^4 lattice.

this l times we get a string of cubes with area $A = 4l + 2$. The number of such strings is:

$$N_l = 3^l$$

and they provide us with a lower bound for $N(A)$ i.e.:

$$3^{\frac{A}{4}} \leq N(A)$$

for large enough A.

In conclusion we have:

$$\frac{\ln 3}{8} \leq \beta_c \leq \frac{\ln 5}{2}$$

$$0.137 \leq \beta_c \leq 0.805$$

The knowledge of this coupled with the self-duality of the system enables us to

assert that the fixed point of the duality transformation (3.5) is the critical point. There is, of course, the possibility that there are 3 or another odd number of phase transitions in the interval $(0.137, 0.805)$. This is, however, impossible since $N(A)$ is independent of β and $E(A)$ depends monotonically on β. Thus from the point of view of the string tension there is only one phase transition and this occurs at:

$$\beta_c = \frac{1}{2}\ln(1+\sqrt{2}) \simeq 0.441$$

which is within the bound we found. The transition point can be seen in Fig. 3.3 where we plotted the average plaquette $1 - \mathrm{Tr}(U_p)$ as a function of β.

As a final note we can find more restrictive bounds on beta using the duality transformations: for $\beta = 0.805$ we have $\tilde{\beta} = 0.203$ and then we know that $0.203 \leq \beta_c \leq 0.805$.

3.5 't Hooft Loop Behavior

Since the 't Hooft loop is dual to the Wilson loop we know its behavior in the two phases of the theory: it will have a perimeter law for $\beta < \beta_c$ and will have an area law for $\beta > \beta_c$. However, it is interesting to see if we can infer its behavior using the vortex picture.

For high β a simple argument shows that we have an area law. Consider, on the dual lattice, the 't Hooft loop C^*. Choose a surface S^* spanning the loop. The excitation of the theory are closed surfaces S and the 't Hooft loop is:

$$B_{C^*}(S) = e^{-2\beta\sum_{p\in S^*} U_p} = e^{-2\beta A(S^*)} e^{4\beta A(S\cap S^*)}$$

where $A(S)$ is the area of surface S. The average of the operator will be:

$$\langle B_{C^*} \rangle = \frac{1}{Z} \sum_S e^{-2\beta A(S)} e^{4\beta A(S \cap S^*)} e^{-2\beta A(S^*)}$$

In order to get the first order contribution we need to find the configuration that minimizes $A(A) + A(S^*) - 2A(S \cap S^*)$ where S is a closed surface. It is easy to see that S has to be the closed surface formed by S^* and S^*_{min} with S^*_{min} the minimal surface spanning the 't Hooft loop. Then for $\beta \to \infty$ we have:

$$\langle B_{C^*} \rangle \simeq \frac{1}{Z} e^{-2\beta(A(S^*)+A(S^*_{min})-2A(S^*)+A(S^*))} = \frac{1}{Z} e^{-2\beta A(S^*_{min})}$$

since $A(S^* \cup S^*) = A(S^*) + A(S^*_{min})$ and $A((S^* \cup S^*_{min}) \cap S^*) = A(S^*)$.

We see then that for high β we have an area law for the 't Hooft loop. the string tension extracted from this approximation is:

$$\sigma(\beta) = 2\beta$$

This string tension should match the string tension for the Wilson loop at:

$$\bar{\beta} = \frac{1}{2} \ln \coth \beta - \frac{1}{2} \ln \frac{1 + 2^{-2\beta}}{1 - e^{-2\beta}}$$

Since $\beta \to \infty$ we have $e^{-2\beta} \simeq 0$ and then:

$$\bar{\beta} \simeq \frac{1}{2} \ln(1 + 2e^{-2\beta}) \simeq \frac{1}{2} 2e^{-2\beta} = e^{-2\beta}$$

Since $\bar{\beta}$ is very small we can use the strong coupling expansion (3.6) and write:

$$\bar{\sigma} = -\ln\bar{\beta} = -\ln e^{-2\beta} = 2\beta$$

which is exactly the result we expected.

In the low β regime the arguments are, unfortunately, not that simple and we will not pursue it here.

3.6 Conclusion

In this chapter we showed that the $Z(2)$ gauge theory is self-dual and has a phase transition at the fixed point of the duality transformation. Moreover, we showed that in this theory the Wilson loop is dual to the 't Hooft loop.

We also employed the vortex picture to explain the behavior of the Wilson and 't Hooft loop. Although this picture doesn't enable us to get a quantitative understanding of the theory it gives us a qualitative description of the physics of the system. We were also able to set some limits on the critical point of the theory and we determined that the transition point is actually a percolation-depercolation transition point.

Our limited possibility to investigate this system, in spite of its self-duality, stems from the fact that the duality of this system is dynamical rather than kinematical: there is no way to attach a dual configuration to a particular configuration in the original theory. Thus we are unable to identify the basic excitation of the system in the strong coupling (low β) regime and that is why we have a limited description of this phase.

Chapter 4

Projection Vortices

4.1 Introduction

We will present in this chapter a number of methods designed to identify center vortices on the lattice. $Z(2)$ gauge theory exhibits vortices as its fundamental excitations and there we have no problem identifying them. However, when we are dealing with a continuous group (like $SU(N)$) the identification of center vortices becomes a key issue.

First of all let's try to answer the question: why center vortices at all? The standard argument [38, 39] is the following. Let's take a loop C in the lattice and then break it down into smaller loops $\{C_i\}$ like in Fig. 4.1. Define a function F such that: $F(C) = \prod_i F(C_i)$. If we are to find that for sufficiently large loops we have:

$$\langle F(C) \rangle = \langle \prod_{i=1}^{n} F(C_i) \rangle \simeq \prod_{i=1}^{n} \langle F(C_i) \rangle$$

then we can say that the sub loops C_i vary independently (they have no correlation

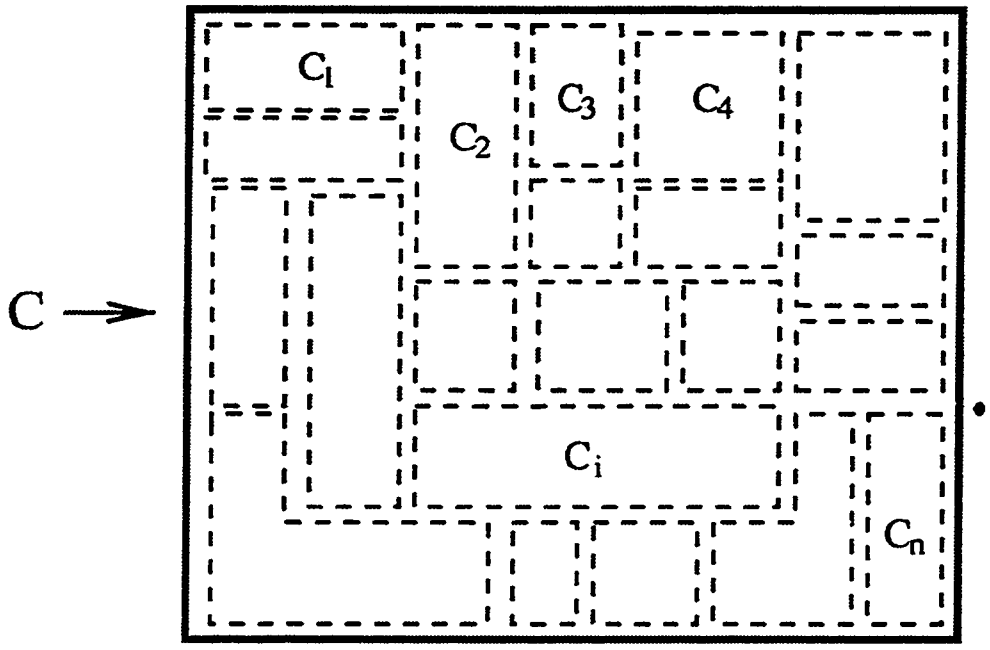

Figure 4.1: Breaking down of a large loop C into smaller sub loops $\{C_i\}$.

with respect to the function F). We can then take any large loop and break it down into loops still large enough so that they are uncorrelated. Then we can write:

$$\langle F(C)\rangle \simeq \langle F(C_{min})\rangle^k$$

where $k = \frac{A(C)}{A(C_{min})}$ and C_{min} is the minimal size loop that varies independently (we assumed that we divided the big loop C into a lot of identical C_{min} loops). In this simple picture we get an area law since:

$$\langle F(C)\rangle \simeq \alpha^{A(C)}$$

where $\alpha = \langle F(C_{min})\rangle^{1/A(C_{min})}$. We will say that the Wilson loop is *disordered* (with respect to the function F) since different pieces of it vary independently.

To make this argument more substantial let F be a class function with the following character expansion:

$$F(g) = \sum_{j \neq 0} f_j \chi_j(g)$$

where the summation runs over both integer and half-integer representations. We have neglected a factor f_0 since we wanted to have $\langle F(U) \rangle = 0$ when U is completely random. In two dimensions, where the SU(2) theory can be solved exactly, we have:

$$\langle \prod_{i=1}^{n} F(U(C_i)) \rangle \simeq (\prod_{i=1}^{n} 2 f_{1/2}) e^{-\sigma_{1/2} A(C)} = \prod_{i=1}^{n} \langle F(U(C_i)) \rangle$$

where:

$$\sigma_{1/2} = -\ln \frac{I_2(\beta)}{I_1(\beta)}$$

and here we have different loops varying independently.

However, if we go to more than two dimensions, we find that at least in the strong coupling limit (which can be treated perturbatively) we have:

$$\langle \prod_{i=1}^{n} F(U(C_i)) \rangle \simeq \left(\frac{1}{3}\right)^{n-1} f_i^n \langle \chi_1(U(C)) \rangle = \left(\frac{1}{3}\right)^{n-1} f_1^n e^{-\mu P(C)}$$

where $\mu = 4\sigma_{1/2}$. On the other hand we have:

$$\prod_{i=1}^{n} \langle F(U(C_i)) \rangle \simeq \prod_{i=1}^{n} f_1 \langle \chi_1(U(C_i)) \rangle = f_1^n e^{-\mu \sum_i P(C_i)}$$

For n large enough we have:

$$\sum_{i=1}^{n} P(C_i) \gg P(C)$$

and then:

$$\langle \prod_i F(U(C_i)) \rangle \gg \prod_i \langle F(U(C_i)) \rangle$$

and we no longer have independent variations of $F(C_i)$. We see that the correlation is brought on by the fact that F has a non-zero f_1 in the character expansion. In fact the leading term will still have a perimeter law behavior (and correlation) as long as there is at least one $f_i \neq 0$ for an integer representation i. In particular let's define the probability density function for the Wilson loop:

$$P_C[g] = \langle \delta(g, U(C)) \rangle = \langle \sum_j \chi_j(g) \chi_j(U(C)) \rangle = \sum_j \chi_j(g) W_j(C)$$

where the summation runs over all irreducible representation of $SU(2)$ and $W_j(C) = \langle \chi_j(U(C)) \rangle$. Since $\chi_1(g) \neq 0$ we have a strong correlation among the probabilities distributions $P_{C_I}[g]$ for different sub loops. Thus, although in the limit $C \to \infty$ we have $P_C[g] \to 1$ (the random distribution) this randomness cannot be brought on by vortices and it cannot explain the area law. Moreover, $P_C[g]$ approaches the random distribution in a perimeter law fashion.

We mentioned before that the existence of any f_j for integer representations will bring on a correlation among $F(U(C_i))$. What if we were to chose a function that has no integer representation coefficients? Let us focus on the center projection

function. We have for $SU(2)$:

$$Z(U) = \text{sign}\,\text{Tr}(U) = \sum_{j=1/2,3/2,\ldots} a_j \chi_j(U)$$

where:

$$a_j = \int dg\, \text{sign}\,\text{Tr}(g) x_j(g)$$

For this function we have (in the strong coupling expansion):

$$\langle \prod_i Z(U(C_i)) \rangle \simeq \left(\frac{3}{4\pi}\right)^n e^{-\sigma_{1/2} A(C)}$$

and

$$\prod_i \langle Z(U(C_i)) \rangle \simeq \prod_i \frac{3}{4\pi} e^{-\sigma_{1/2} A(C_i)}$$

and thus:

$$\langle \prod_i Z(U(C_i)) \rangle \simeq \prod_i \langle Z(U(C_i)) \rangle$$

which tells us that $Z(U(C_i))$ fluctuate independently.

Thus, we see that it is only the center part of $U(C_i)$ that shows no correlation (in the strong coupling limit). Moreover, the mechanism that brings this about has to be somehow dependent on the number of dimensions in the lattice. Center vortices seem to be the appropriate type of object to explain this behavior.

Now that we have a reason to pursue this type of object let us try to define it. We know that they carry a center group element (-1 for $SU(2)$) and that they have the topology of the vortices in $Z(2)$ theory (they should be defined on a co-closed

surface). We also know how to insert a vortex in the lattice: all we have to do is to flip a certain number of links from 1 to -1 and we get a vortex structure. However, the dynamics of a continuous group allows for a relaxation of the -1. In $Z(2)$ we could introduce only *thin* vortices (i.e. vortices that have the thickness of a plaquette). If we had all the plaquettes positive then no Wilson loop was negative. In $SU(2)$ we can have all plaquettes positive and still have negative Wilson loops. This is due to the continuous nature of the gauge group. The vortex can spread on a number of plaquettes. This type of structures will be called *thick* vortices.

The thin structures cannot be responsible for confinement in the weak coupling limit. They have basically the dynamics of the $Z(2)$ theory and they will (as in the $Z(2)$ case) depercolate for β high enough. The structures that are believed to be responsible for confinement are the thick vortices.

In this chapter we will present two methods to identifying vortices in $SU(2)$ gauge theory. They are both projection methods and differ only in the gauge fixing method.

4.2 Maximum Center Gauge

The basic idea behind maximum center gauge is to define a method that brings the gauge field to a smooth enough representation in which we can identify the vortex structure. To understand the problem let's try to see what happens when we go to large values of β (weak coupling limit). Since β is high we expect that the plaquettes are very close to 1. However, we can still have Wilson loops (they have to be large enough) that have values significantly different from 1. We can have even

negative values for certain Wilson loops. In the vortex picture this is due to the fact that there is a center vortex piercing the loop. However, it is difficult to spot where this piercing actually happens since the gauge configuration is quite noisy. There are two sources of noise: one is the gauge freedom; we can have all the plaquettes close to 1 and still have the link variables of any value. The second source of noise is the ultraviolet quantum fluctuations.

The first source of noise can be eliminated by gauge fixing. This is exactly what the projection methods use as a first step. The general idea is to find a gauge fixing method that is blind to the center of the gauge group. We fix the link variables in such a way that the $SO(3)$ part is attenuated as much as possible and the remaining $Z(2)$ gauge transformations will be irrelevant since they are not going to affect the vortex structure. Moreover, we leave the $Z(2)$ part alone so that we can recover the vortex structure.

To see how this procedure works imagine a Wilson loop that has the value -1. By changing the gauge we cannot alter the value of the Wilson loop. However, after a gauge transformation that is trying to maximize the absolute value of the trace of the links it is most likely that this Wilson loop will have all links very close to 1 except for an odd number of links very close to -1. The place that has the links -1 is very likely to be part of a vortex.

In the maximum center gauge method we define the functional:

$$F(U) = \sum_b [\mathrm{Tr}(U_b)]^2 \tag{4.1}$$

We will try then to fix the gauge such that this functional is maximized under gauge transformations. It is clear that this procedure fixes the gauge only up to a $Z(2)$ gauge transformation since for any configuration ${}^gU$ a $Z(2)$ transform of this configuration will produce the same value for the functional.

After we fixed the gauge we will try to get rid of the ultraviolet fluctuations (short distance fluctuations). After gauge fixing most links are very close to center elements ± 1. However, they will not be exactly ± 1. They will fluctuate around these center elements. In the hope that the long distance fluctuations were picked up by the gauge fixing procedure and locked into the center elements we can assume that these link fluctuations are important only for short distance physics. We will then get rid of them by doing a projection: we will replace the link value with the center value that they are closest to:

$$Z_b = \text{sign}\,\text{Tr}(U_b)$$

The resulting configuration will be a $Z(2)$ configuration. Vortices are easy to identify: they are made out of plaquettes that are negative on co-closed surfaces. They will be called *P-vortices*. However, these are thin objects. The hope is that these thin structures will lie in the middle of thick vortices.

To understand the gauge fixing procedure better we use the following argument [40]: let's take two gauge configurations U_b and V_b. Using the standard metric on

the $SU(2)$ manifold we can define a distance between U_b and V_b:

$$d(U,V) = \sum_b \mathrm{Tr}((U_b - V_b)(U_b - V_b)^\dagger) = 2\sum_b (\mathrm{Tr}(I) - \mathrm{Tr}(U_b V_b^\dagger))$$

where we used the fact that $\mathrm{Tr}(U_b V_b^\dagger) = \mathrm{Tr}(U_b^\dagger V_b)$ for $U_b, V_b \in SU(2)$. If we ask the question what is the pure gauge configuration (zero field configuration) that is closest in metric d to a particular configuration U_b we get:

$$\begin{aligned} d(U,G) &= 2\sum_{\vec{n},\mu} (\mathrm{Tr}(I) - \mathrm{Tr}(U_{\vec{n}}^\mu G_{\vec{n}}^{\mu\dagger})) = 2\sum_{\vec{n},\mu} \{\mathrm{Tr}(I) - \mathrm{Tr}[U_{\vec{n}}^\mu (g_{\vec{n}} g_{\vec{n}+\hat{\mu}}^\dagger)^\dagger]\} \\ &= 2\sum_{\vec{n},\mu} \{\mathrm{Tr}(I) - \mathrm{Tr}[g_{\vec{n}}^\dagger U_{\vec{n}}^\mu g_{\vec{n}+\hat{\mu}}]\} = 2\sum_{\vec{n},\mu} \{\mathrm{Tr}(I) - \mathrm{Tr}({}^g U_{\vec{n}}^\mu)\} \end{aligned}$$

where G is a pure gauge field generated from identity by the gauge transformation g: $G_{\vec{n}}^\mu = g_{\vec{n}} g_{\vec{n}+\hat{\mu}}^\dagger$. ${}^g U_{\vec{n}}^\mu$ is the gauge transformed configuration equivalent with $U_{\vec{n}}^\mu$. We see that in order to minimize the distance d we have to maximize:

$$\hat{F}({}^g U) = \sum_b \mathrm{Tr}({}^g U)$$

with respect to g. The next step that brings us closer to our problem is to ask what is the configuration of the form:

$$V_{\vec{n}}^\mu = g_{\vec{n}} Z_{\vec{n}}^\mu g_{\vec{n}+\hat{\mu}}^\dagger \tag{4.2}$$

that is closest to U_b (above we have $Z^\mu \in Z(2)$). V^μ is a gauge configuration equivalent with a $Z(2)$ configuration. We can break this problem in two parts. First

we try to determine g up to a residual $Z(2)$ gauge transformation by using the distance d defined in terms of the adjoint representation:

$$d_A(U,V) = \sum_b \mathop{\mathrm{Tr}}_A[(U_b - V_b)(U_b - V_b)^\dagger]$$

The advantage of using this representation is that the configurations like V look like a pure gauge configuration in the adjoint representation. Since we solved this problem we know that the solution for g will be given by maximizing:

$$\hat{F}(g^\dagger U) = \sum_b \mathop{\mathrm{Tr}}_A(g^\dagger U_b) \tag{4.3}$$

with respect to gauge transformation g. Since:

$$\mathop{\mathrm{Tr}}_A(U) = \mathrm{Tr}(U)^2 - 1$$

maximizing $\hat{F}$ in equation (4.3) is equivalent to maximizing:

$$F(g^\dagger U) = \sum_b \mathrm{Tr}(g^\dagger U_b)^2$$

Here we see that the gauge transformation needed to go to the maximum center gauge is just the inverse of the gauge transformation g needed to define V_b in equation (4.2).

Once we found g we are left with only one problem: determining Z_n^μ. To find it we will need to minimize each term of the sum over links. Thus we need to find the

minimum of:

$$\mathrm{Tr}[(U^{\mu}_{\vec{n}} - g_{\vec{n}} Z^{\mu}_{\vec{n}} g^{\dagger}_{\vec{n}+\hat{\mu}})(U^{\mu}_{\vec{n}} - g_{\vec{n}} Z^{\mu}_{\vec{n}} g^{\dagger}_{\vec{n}+\hat{\mu}})^{\dagger}] = 2(\mathrm{Tr}(I) - \mathrm{Tr}(^{g^{\dagger}} U^{\mu}_{\vec{n}} Z^{\mu}_{\vec{n}}))$$

This is obviously minimized when $\mathrm{Tr}(^{g^{\dagger}} U^{\mu}_{\vec{n}} Z^{\mu}_{\vec{n}})$ is maximized which happens for:

$$Z^{\mu}_{\vec{n}} = \mathrm{sign}\,\mathrm{Tr}(^{g^{\dagger}} U^{\mu}_{\vec{n}})$$

This is exactly the projection step involved in defining the projected $Z(2)$ configuration in the maximum center gauge. We see now that the configuration produced by the maximum center gauge projection is that $Z(2)$ configuration that is closest to the family of configurations that are gauge equivalent with our original $SU(2)$ configuration.

In conclusion, this method associates a $Z(2)$ configuration to an $SU(2)$ configuration. The procedure is hard to control analytically: the gauge fixing is not a problem since it doesn't alter the physical content of the configuration; however, the projection step involves approximations that cannot be estimated. The only way to support such an approach is by empirical means. For example, one will chose an observable that is supposed to depend on the long distance physics and check the agreement between the values of the observable in the full theory and on the projected configurations. If these values agree then we have reasons to believe that the procedure is justified and, furthermore, that the values extracted from the projected configurations for some other observables, that depend on the same physics, should

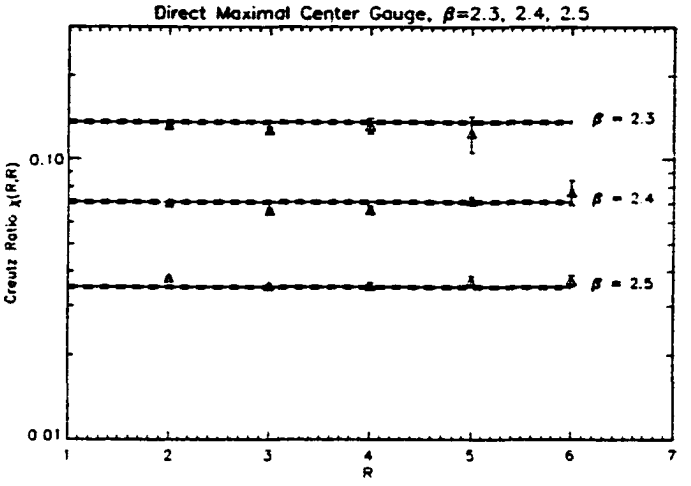

Figure 4.2: Creutz Ratios $\chi(R,R)$ extracted from the projected configurations at different values of β. The solid lines represent the string tension in the full theory [41, 10].

agree with the values computed in the full theory. Another test will be the scaling of the observables measured on the projected configuration.

To see that this is indeed the case we will make a survey of the results obtained using this method.

Survey of Results in Maximum Center Gauge

We say that an observable is center dominated if its value computed in the projected configurations is consistent with the value computed in the full theory.

The first test of center domination was performed on the long range part of the interquark potential [41, 10]. It was found that the string tension was center dominated. The values of Creutz ratios extracted from the projected configurations closely matched the values in the full theory (see Fig. 4.2). It was further found that the string tension scales as expected. Moreover, the string tension showed

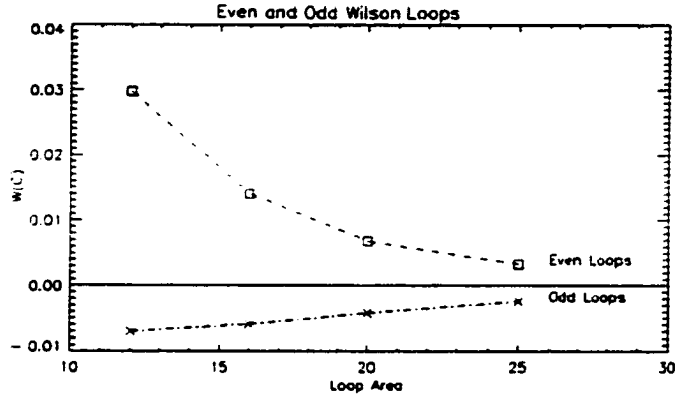

Figure 4.3: Wilson loop averages measured for even and odd loops. The numbers are for $\beta = 2.3$ [41, 10].

"precocious linearity": the area law sets in much faster for projected configurations than for the full theory. This property is assumed to be due to the projection step where it is believed that we get rid of the short distance effects, hence less noise and early set in of the asymptotic behavior.

A number of other tests have been performed to check the validity of the vortex mechanism. For example the Wilson loop in the full theory was tagged by the parity of the number of vortices piercing it. We produce two bins: one with an even number of trapped vortices and another one with an odd number of trapped vortices. The averages for each bin will be denoted by: $W_{even}(C)$ and $W_{odd}(C)$. For $C \to \infty$ we expect that:

$$\lim_{C\to\infty} \frac{W_{even}(C)}{W_{odd}(C)} = -1$$

if the vortex mechanism is right. This seems to be the case (see Fig. 4.3). We remember that this is a prerequisite for the argument used in the $Z(2)$ gauge theory for vortices to produce an area law. The value of the Wilson loop should come from

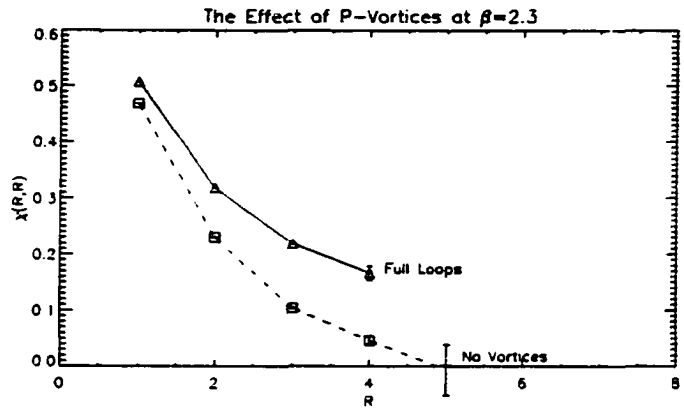

Figure 4.4: Creutz Ratios for the Wilson loop with and without P-vortices [41, 10].

the number of trapped vortices. There is also a decrease in the absolute value:

$$\lim_{C\to\infty} W_{even,odd}(C) = 0$$

but this decrease does not produce the area law. It is the fraction of even and odd trapped vortices that is responsible for the area law. To see that this is indeed the case another test was performed: we remove the vortex degree of freedom by multiplying the Wilson loop in the full configuration with the one on the projected configuration. We write:

$$\bar{W}(C) = W(C)(-1)^n$$

where n is the number of vortices trapped inside the loop C. We expect that the average of this operator doesn't exhibit an area law if the vortex picture is right. It was indeed observed that this operator doesn't have an area law (see Fig. 4.4). Other studies regarding long-distance physics using P-vortices were performed as

well: finite temperature studies where the string tension of the spatial loops is explained by the P-vortices running through the lattice in the time direction, and the lack of string tension for loops in the space time direction is due to finite length of the vortices in spatial directions; the phase transition was studied using P-vortices and it was found to be a percolation-depercolation phase transition [36].

It seems that P-vortices do indeed signal the presence of a physical object that is relevant for confinement. However, a number of problems plague this definition for vortices.

The first problem with P-vortices is their lack of theoretical support. The procedure is supported by numerical simulations but there are no analytical results backing it up. The only arguments supporting P-vortices are numerical results. It is hard to understand how P-vortices can pick up thick vortices in the lattice: if the thick vortices are really spread over the lattice then by gauge fixing we cannot alter them. It is in the process of projecting, the process that we have no means to control (we cannot estimate the approximations introduced), that the signal is picked up.

The second problem with P-vortices is due to "Gribov copies" [42] in the gauge fixing process. From a technical point of view the maximal center gauge is found using iterative methods. This methods try to maximize the functional (4.1) by maximizing with respect to the gauge transformation at each site until a sweep through the lattice doesn't change the gauge configuration too much. This methods are bound to find local maxima rather than global one. However, this will not be a problem if the results do not depend strongly on how close to the maximum you get.

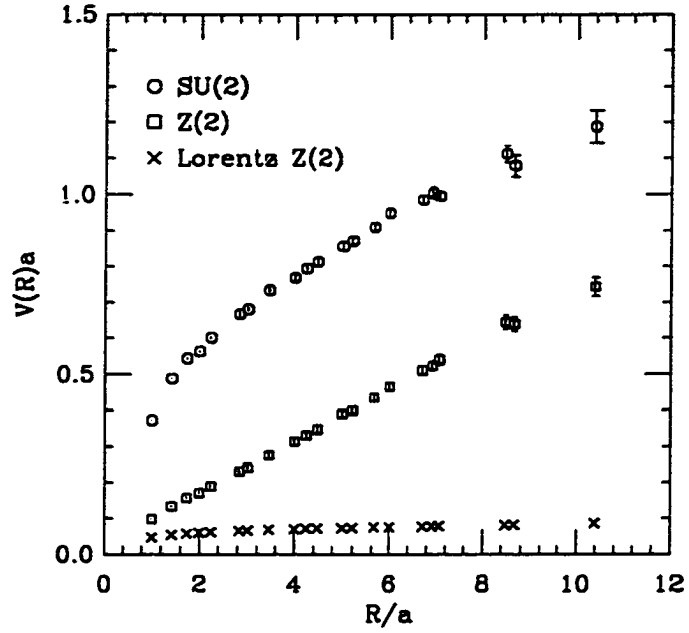

Figure 4.5: Interquark potential for the full Wilson loop ,$SU(2)$, the projected Wilson loop using the regular gauge fixing procedure, $Z(2)$, and the indirect one that fixes first to Lorentz gauge, Lorentz $Z(2)$. The measurements are performed on a 12^4 lattice at $\beta = 2.4$ [44].

Unfortunately this is not the case. Studies [43] have showed that by refining the method and getting closer to the global maximum the string tension extracted from the projected configuration decreases significantly. One method involved generating a number of gauge equivalent copies of the original configuration. Then a local maximum was found for each copy. The one that had the highest value for the function (4.1) was kept. This study found that the value of the string tension decreased with the number of copies used.

More severely, a study by Kovacs and Tomboulis [44] showed that if you precondition the configurations by gauge fixing first to the Lorentz gauge and then going to the maximum center gauge you lose the string tension completely (see Fig. 4.5).

Another problem that P-vortices have is that they are unstable under cooling. Cooling is a procedure that smooths out the gauge field (the simplest procedure will be to replace each link with the value that maximizes the action locally). This procedure is supposed to influence only the short distance physics. Measurements of the string tension in the full theory have showed that after a small number of cooling steps the string tension remains the same. Stack [45] has showed that after one cooling step the string tension in the projected configuration loses half its value. This is too big a change considering that the string tension is unchanged in the full theory.

These last two problems raise serious questions about P-vortices. Since the center dominance of the string tension is dependent on the way you choose to go to the maximum center gauge one can argue that there is no true physics in these objects. The successes of P-vortices seem to be a mere accident.

However, we cannot disregard the results obtained using P-vortices completely. Even if they are poorly defined objects they seem to signal some physical structure that matches our understanding of vortices. It is argued [46] that we can get the same behavior even if we are not going to use the maximum center gauge. All we have to use is a gauge fixing procedure that has the following properties:

- the gauge fixing depends only on the adjoint link variables
- the procedure fixes completely the gauge in the adjoint variables
- at weak coupling the gauge fixing transforms most of the link into values close to the center of the group

The problem with the maximum center gauge is to fix uniquely the gauge. Thus it may be possible to find another gauge fixing method that fixes the gauge uniquely, is easy to implement and obeys all the requirements above. In fact such a method exists and we will present it in the next section.

4.3 Laplacian Center Gauge

We saw that the gauge fixing to maximum center gauge involved finding the maximum of the functional (4.1). The main problem in implementing this condition is due to non-linear nature of the problem. The maximum center gauge is equivalent with the Landau gauge in the adjoint representation. The problem of fixing to Landau gauge in the fundamental representation was solved in [47]. We present here the solution without proving it. To find the gauge transformation to maximize the functional:

$$\hat{F}({}^{g}U) = \sum_{\vec{n},\mu} \mathrm{Tr}({}^{g}U^{\mu}_{\vec{n}})$$

we construct the covariant Laplace operator using the configuration U:

$$\Delta_{\vec{n},\vec{m}} = 8\delta_{\vec{n},\vec{m}} - \sum_{\mu}(U^{\mu}_{\vec{n}}\delta_{\vec{n}+\hat{\mu},\vec{n}} + U^{\mu\dagger}_{\vec{n}-\hat{\mu}}\delta_{\vec{n}-\hat{\mu},\vec{n}})$$

This Laplacian is just the lattice discretization of the covariant Laplacian. This operator acts on color fields, defined on the sites of the lattice, that transform in the fundamental representation of the gauge group. Under a gauge transformation:

$U^{\mu}_{\vec{n}} \rightarrow {}^{g}U^{\mu}_{\vec{n}} = g_{\vec{n}} U^{\mu}_{\vec{n}} g^{\dagger}_{\vec{n}+\hat{\mu}}$ the Laplacian changes:

$$\Delta_{\vec{n},\vec{m}} \rightarrow {}^{g}\Delta_{\vec{n},\vec{m}} = g_{\vec{n}} \Delta_{\vec{n},\vec{m}} g^{\dagger}_{\vec{m}}$$

Denote with ϕ^0 the eigenvector corresponding to the smallest eigenvalue of the Laplacian:

$$\sum_{\vec{m}} \Delta_{\vec{n},\vec{m}} \phi^0_{\vec{m}} = \lambda_0 \phi^0_{\vec{n}}$$

We see that under a gauge transformation the eigenvalues do not change and the eigenvectors change covariantly:

$$\sum_{\vec{m}} {}^{g}\Delta_{\vec{n},\vec{m}} {}^{g}\phi^0_{\vec{m}} = g_{\vec{n}} \sum_{\vec{m}} \Delta_{\vec{n},\vec{m}} \phi^0_{\vec{m}} = \lambda_0 {}^{g}\phi^0_{\vec{n}}$$

where ${}^{g}\phi^0_{\vec{n}} = g_{\vec{n}} \phi^0_{\vec{n}}$. To find the gauge rotation that maximizes $\hat{F}({}^{g}U)$ we need to find the rotation that orients ${}^{g}\phi^0$ in the $(0,0,1)$ direction at all sites.

Our problem is very similar. The only difference is that we need to replace the fundamental representation with the adjoint representation. We then proceed to define the Laplacian in the adjoint representation using:

$$\dot{U}_{ab} = \frac{1}{2} \mathrm{Tr}[U \sigma^a U^{\dagger} \sigma^b]$$

where $\dot{U}^{ab}$ si the matrix in the adjoint representation for the group element U. We define the Laplacian exactly like before only that we use the adjoint representation

for the links:

$$\Delta^A_{\vec{n},\vec{m}} = 8\delta_{\vec{n},\vec{m}} - \sum_\mu (\dot{U}^\mu_{\vec{n}} \delta_{\vec{n}+\hat{\mu},\vec{m}} + \dot{U}^{\mu\dagger}_{\vec{n}-\hat{\mu}} \delta_{\vec{n}-\hat{\mu},\vec{m}})$$

This Laplacian acts on a color field in the adjoint representation. This field has three real components at each site. We find the eigenvector ϕ^{A0} corresponding to minimal eigenvalue and make a gauge transformation that rotates this field in a arbitrary chosen direction (for sake of definitiveness we will chose the third direction). However, this doesn't fix the gauge completely. There is a remnant $U(1)$ gauge transformation that rotates the field around the third axis. To fix this left-over gauge invariance we will pick a second eigenvector ϕ^{A1} (corresponding to the second lowest eigenvalue of the Laplacian) and fix completely the gauge by rotating the field such that the first eigenvector is along the third direction and the second eigenvector lies in the plane given by the second and third directions in the color space. This should fix the gauge completely except, of course, for a $Z(2)$ gauge transformation that is impossible to fix in the adjoint representation.

There are, however, places where degeneracies might occur. It may happen that $|\phi^{A0}| = 0$ at a certain site. The gauge rotation at that site is completely undefined. The manifold of such places is one dimensional since there are three constraints to obey ($\phi^{A0}_1 = \phi^{A0}_2 = \phi^{A0}_3 = 0$). These defects will be identified with monopoles. We are not interested in monopoles so will not pursue them here.

The other type of degeneracy that can occur is to have ϕ^{A0} and ϕ^{A1} parallel at certain sites. There it is impossible to fix the remnant $U(1)$ degree of gauge freedom. The manifold of such places is two dimensional since there are only two constraints

in this case ($\frac{\phi_1^{A0}}{\phi_1^{A1}} = \frac{\phi_2^{A0}}{\phi_2^{A1}} = \frac{\phi_3^{A0}}{\phi_3^{A1}}$). We identify this type of degeneracy with vortices.

The advantage of this gauge fixing is that you have a linear problem to solve in order to fix the gauge and thus the "Gribov copies" problem is solved. We will say that a vortex passes through a site on the lattice when ϕ^{A0} is parallel with ϕ^{A1} at that site. Since we expect the vortices to pierce a plaquette some kind of interpolation has to be employed. The only interpolation that preserves the idea of closed vortices (co-closed surfaces) has been found [11] to be equivalent with taking the center projection on the gauge configuration.

To sum up the step involved in this method we first fix the gauge using the two eigenvectors of the Laplacian and then we do a regular center projection ($Z_b = \text{sign}\,\text{Tr}(U_b)$).

It has been shown that using this method we get an increase in the number of P-vortices. The string tension found in the projected configurations is consistent with the one extracted from the full theory. Moreover, the removal of the P-vortices (by multiplying the Wilson loop in the full theory with the Wilson loop in the projected configuration) produces a zero string tension [48]. On the downside this method seems to lack the scaling of the vortex density [49] and also the string tension is recovered from relatively large loops (it doesn't exhibit the "precocious linearity" of the maximum center gauge method).

Chapter 5

Tomboulis Method

5.1 Introduction

We will present now a method that is substantially different from the methods presented in the previous chapter. The main objection against the vortex definitions already presented is that they involve a gauge fixing. Gauge fixing in itself is not questionable as long as the results derived are gauge invariant. However, the projection step depends on the gauge you choose and thus the entire procedure is suspicious. We would prefer, if possible, to have a vortex definition that is gauge invariant.

Such a definition has been put forth by Tomboulis [12, 13]. The basic idea is to split the $SU(2)$ variables living on links into $SU(2)/Z(2)$ variables living on links and $Z(2)$ variables living on plaquettes. This procedure is supported by the following argument. In continuum the vortices are configurations of the gauge field. However, since in continuum the field variables are valued in the Lie algebra $su(2)$, rather than

the Lie group $SU(2)$, there is no distinction between the pure $SU(2)/Z(2)$ and $SU(2)$ gauge theory. For pure gauge theories in continuum the gauge group is $SU(2)/Z(2)$ rather than $SU(2)$ since the fields are invariant under the center of the group. Vortices, in continuum, will be topologically classified by $\pi_1(SU(2)/Z(2)) = Z(2)$ (the first homotopy group for $SU(2)/Z(2)$). We have seen this classification when we first introduced the 't Hooft loop.

In a lattice gauge theory the variables are the group elements themselves. Thus besides the $SU(2)/Z(2)$ degrees of freedom we have excitations of the $Z(2)$ degrees of freedom. This excitations are thin (one plaquette across) and they are exactly the vortices that we've seen in the $Z(2)$ gauge theory. However, for large value of β they are strongly suppressed and they "froze out" gradually as we go to continuum limit. Thus the lattice gauge theory becomes an $SU(2)/Z(2)$ gauge theory as we are approaching the continuum limit which is exactly what we expect. The only objects left to disorder the Wilson loop in the weak coupling limit will be the thick vortices which are the analog of the center vortices in the continuum.

It is then interesting to study such a formalism that removes the center of the group from the link variables. We will follow here a variant of the standard derivation [12, 13, 50].

5.2 Derivation

We will start by writing the usual Wilson action for $SU(2)$:

$$Z = \int \prod_b dU_b e^{\frac{\beta}{2}\sum_p \mathrm{Tr}(U_p)}$$

We will now separate for each plaquette the $Z(2)$ part:

$$\eta_p = \text{sign}\,\text{Tr}(U_p)$$

We see that $\eta \in C^2(\Lambda)$ where the group used to define the homology groups is $Z(2)$. We will use the Haar invariance of the measure on the group $SU(2)$ under the transformations $U_b \to \gamma_b U_b$ where $\gamma_b \in Z(2)$. We have then:

$$Z = \int \prod_b dU_b e^{\frac{\beta}{2}\sum_p |\text{Tr}(U_p)|(\hat{\partial}\gamma)_p \eta_p}$$

where we used the fact that $\gamma \in C^1(\Lambda)$ and $\hat{\partial}\gamma \in C^2(\Lambda)$ is the configurations generated on plaquettes by γ. Since for every $\gamma \in C^1(\Lambda)$ the relation above is true we can write:

$$Z = \frac{1}{|C^1(\Lambda)|}\sum_{\gamma \in C^1(\Lambda)} \int \prod_b dU_b e^{\frac{\beta}{2}\sum_p |\text{Tr}(U_p)|(\hat{\partial}\gamma)_p \eta_p}$$

We introduce the variable σ defined on plaquettes ($\sigma \in C^2(\Lambda)$) to replace $(\hat{\partial}\gamma)\eta$ in the exponent:

$$Z = \frac{1}{|C^1(\Lambda)|}\int \prod_b dU_b \sum_{\gamma \in C^1(\Lambda)} \sum_{\sigma \in C^2(\Lambda)} \delta(\sigma^{-1}(\hat{\partial}\gamma)\eta) e^{\frac{\beta}{2}\sum_p |\text{Tr}(U_p)|\sigma_p}$$

where the δ function is over the group $C^2(\Lambda)$. It is different from zero only when $\sigma(p) = \hat{\partial}\gamma(p)\eta(p)$ for all p. We can write the δ function (see Appendix):

$$\delta(\sigma^{-1}(\hat{\partial}\gamma)\eta) = \frac{1}{|C^2(\Lambda)|}\sum_{\tau \in C^2(\Lambda)} \{\tau, \sigma^{-1}(\hat{\partial}\gamma)\eta\} = \frac{1}{|C^2(\Lambda)|}\sum_{\tau \in C^2(\Lambda)} \{\tau, \hat{\partial}\gamma\}\{\tau, \sigma^{-1}\eta\}$$

We perform now the summation over γ:

$$\sum_{\gamma \in C^1(\Lambda)} \{\tau, \hat{\partial}\gamma\} = \sum_{\gamma \in C^2(\Lambda)} \{\partial\tau, \gamma\} = |C^1(\Lambda)|\delta(\partial\tau)$$

The partition function will be:

$$Z = \frac{1}{|C^2(\Lambda)|} \int \prod_b dU_b \sum_{\sigma \in C^2(\Lambda)} \sum_{\tau \in C^2(\Lambda)} \{\tau, \sigma^{-1}\eta\} \delta(\partial\tau) e^{\frac{\beta}{2} \sum_p |\mathrm{Tr}(U_p)|\sigma_p}$$

We sum over τ:

$$\sum_{\tau \in C^2(\Lambda)} \{\tau, \sigma^{-1}\eta\}\delta(\partial\tau) = \sum_{\tau \in Z^2(\Lambda)} \{\tau, \sigma^{-1}\eta\} = \sum_{\alpha \in H^2(\Lambda)} \sum_{\rho \in B^2(\Lambda)} \{\alpha\rho, \sigma^{-1}\eta\}$$

where we used the fact that if $\partial\tau$ is zero (due to the δ function) then $\tau \in Z^2(\Lambda)$ (it is a closed configuration). We also used the fact that a closed configuration can be written as the product between a member of the homology group and a member of the boundary group. The sum over boundary configuration can be written as:

$$\sum_{\rho \in B^2(\Lambda)} f(\rho) = \frac{1}{|Z^3(\Lambda)|} \sum_{\rho \in C^3(\Lambda)} f(\partial\rho)$$

since there are $|Z^3(\Lambda)|$ configurations in $C^3(\Lambda)$ that have the same boundary ρ. We write then:

$$\sum_{\tau \in C^2(\Lambda)} \{\tau, \sigma^{-1}\eta\}\delta(\partial\tau) = \frac{1}{|Z^3(\Lambda)|} \sum_{\alpha \in H^2(\Lambda)} \sum_{\rho \in C^3(\Lambda)} \{\alpha\partial\rho, \sigma^{-1}\eta\}$$

$$= \frac{1}{|Z^3(\Lambda)|} \sum_{\alpha \in H^2(\Lambda)} \sum_{\rho \in C^3(\Lambda)} \{\alpha, \sigma^{-1}\eta\}\{\partial\rho, \sigma^{-1}\eta\}$$
$$= \frac{1}{|Z^3(\Lambda)|} \sum_{\alpha \in H^2(\Lambda)} \sum_{\rho \in C^3(\Lambda)} \{\alpha, \sigma^{-1}\eta\}\{\rho, \hat{\partial}(\sigma^{-1}\eta)\}$$
$$= \frac{|C^3(\Lambda)|}{|Z^3(\Lambda)|} \sum_{\alpha \in H^2(\Lambda)} \{\alpha, \sigma^{-1}\eta\}\delta(\hat{\partial}(\sigma^{-1}\eta))$$

Summing everything up we write the partition function:

$$Z = \frac{|C^3(\Lambda)|}{|C^2(\Lambda)||Z^3(\Lambda)|} \int \prod_b dU_b \sum_{\sigma \in C^2(\Lambda)} \delta(\hat{\partial}(\sigma^{-1}\eta)) e^{\frac{\beta}{2}\sum_p |\mathrm{Tr}(U_p)|\sigma_p} \sum_{\alpha \in H^2(\Lambda)} \{\alpha, \sigma^{-1}\eta\}$$

We see that there is no dependence on the sign of any particular link in the terms summed above (all the terms are invariant under $U_b \to -U_b$) and then we can restrict the integration to $SU(2)/Z(2)$. We have:

$$Z = \frac{|C^3(\Lambda)||C^1(\Lambda)|}{|C^2(\Lambda)||Z^3(\Lambda)|} \int \prod_b d\hat{U}_b \sum_{\sigma \in C^2(\Lambda)} \delta(\hat{\partial}(\sigma^{-1}\eta)) e^{\frac{\beta}{2}\sum_p |\mathrm{Tr}(\hat{U}_p)|\sigma_p} \sum_{\alpha \in H^2(\Lambda)} \{\alpha, \sigma^{-1}\eta\} \tag{5.1}$$

where $\hat{U}$ denotes the equivalence class of U.

Having written the partition function let us discuss the various terms in the action. We first have an integration over $\hat{U}_b$. This integration is unconstrained. Then we have a summation over σ. However, this summation is constrained by:

$$\delta(\hat{\partial}(\sigma^{-1}\eta)) = \prod_{c \in \Lambda} \delta(\sigma_c^{-1}\eta_c)$$

where σ_c^{-1} and η_c are the products over all six faces of the cube c of σ_p^{-1} and η_p. We see that the σ variables have to obey the constraint $\sigma_c = \eta_c$. These variables are

associated with the thin ($Z(2)$) part of the theory. The η variables play a special role that will be disscused later. The σ_p variables describe a thin flux crossing the plaquette p. This flux is conserved except for the places where $\sigma_c = -1$. When $\sigma_c = -1$ we say that we have a *thin monopole* on the cube C. This monopoles are forced in by the $SO(3)$ part of the theory since we start with $\hat{U}_b$, we compute η_p and then we require a thin monopole where $\eta_c = -1$. From this respect these thin monopoles can be viewed as thick monopoles two since they are produce by the $\hat{U}_b$ configuration.

The other constraint comes from the last term of the partition function (5.1):

$$\sum_{\alpha \in H^2(\Lambda)} \{\alpha, \sigma^{-1}\eta\}$$

This constraint require that $\{\alpha, \sigma^{-1}\eta\} = 1$ for all $\alpha \in H^2(\Lambda)$. Now, the members of $H^2(\Lambda)$ are the six planes wrapping around the lattice. This constraints then asserts that there should be no $\sigma^{-1}\eta$ flux running through the lattice.

We see that $\sigma^{-1}\eta$ forms a co-closed surface (since $\hat{\partial}(\sigma^{-1}\eta) = \phi_3$) and thus it has the topology of a vortex. The objects of this type are called hybrid vortices since they are formed from patches of thin and thick vortices. This patches end up in a co-closed monopole loop.

The η part can be moved anywhere in the lattice without any cost in action. They will still have to obey the constraint but other than that they are free to move. This moving actually amounts to nothing else but a change of representatives for the classes $\hat{U} \in SU(2)/Z(2)$. They appear in this formalism only to ensure that

operators defined in terms of $\hat{U}_b$ are well defined (they don't depend on our choice of representative). However, there are variables defined only in terms of η that are invariant under a change of representatives. As an example we have:

$$\eta_c = \prod_{p \in \partial c} \eta_p$$

This type of operators are meaningful. In fact the only operators that involve η alone and are meaningfully are the ones defined on close surfaces. Those surfaces that are boundary configurations can be written as a product over cube variables, η_c, and since the σ variables obey the constraint $\sigma_c = \eta_c$ we can express this type of operators in terms of σ variables. The same argument can be made for surfaces wrapping around the lattice using the second constraint. Thus the only role for η variables is to make operators that depend on $\hat{U}_b$ well defined.

5.3 Wilson Loop and Vortex Counters

We have seen in the previous section how to produce a formulation where the $SU(2)$ variables are split in $SU(2)/Z(2)$ and $Z(2)$ parts. This new formalism has the same partition function as the original formalism. The only thing left is to define the operators in these new variables. Using the same steps as in the previous section we can write he Wilson loop as:

$$W_C(\hat{U}, \sigma) = \mathrm{Tr}(\prod_{b \in C} \hat{U}_b) \prod_{p \in S} \eta_p \sigma_p^{-1} \tag{5.2}$$

where S is any surface with $\partial S = C$. The product over link is understood to be ordered. This operator represents the Wilson loop in our formulation in the sense that:

$$\langle W_C(U)\rangle_{SU(2)} = \langle W_C(\hat{U},\sigma)\rangle_{SO(3)\times Z(2)}$$

We will show latter that it is not only the averages that are the same but also the probability distribution is the same for any loop C and any value of β. The sign of the Wilson loop is given by two parts:

$$N_{thick}(S) = \text{sign}\,\text{Tr}(\prod_{b\in C}\hat{U}_b)\prod_{p\in S}\eta_p$$

and

$$N_{thin}(S) = \prod_{p\in S}\sigma_p^{-1}$$

Using this operators Tomboulis defines three types of vortices linking the Wilson loop:

- Thin vortices when $N_{thin}(S) = -1$ for all S with $\partial S = C$.
- Thick vortices when $N_{thick}(S) = -1$ for all S with $\partial S = C$.
- Hybrid vortices when $N_{hybrid}(S) = N_{thin}(S)N_{thick}(S) = -1$ for all S but $N_{thin,thick}$ have different signs for different surfaces.

These operators will be called vortex counters. They are only defined modulo 2. The thin vortices will be highly suppressed for large β. They thin degrees of freedom will form then only small patches in hybrid vortices.

In contrast with the projection methods these vortices are not well localized. Also, they do not obey a Stokes theorem since we did not project the configuration into an Abelian configuration. To detect vortices we use the Wilson loop and we say that when the sign flips we trapped a vortex inside. This ambiguity in defining a location for a vortex is the main objection to this definition of vortices. However, once you accept this definition the separation into thin and thick vortices appears natural. By removing the spurious thin degrees of freedom from the sign of the Wilson loop it is hoped that we will have a better counter for thick vortices.

Among the three counters that are defined above it is only the hybrid counter that it is guaranteed by the theory to be the same for all surfaces chosen to span the Wilson loop. The other two counters can change sign when we change the surface, but always simultaneously, so that the hybrid counter is unchanged. It is actually interesting to realize that these counters will change sign when the volume defined by the old surface and the new surface contains an odd number of monopoles. Since the thin monopoles lie on top of cubes that have $\eta_c = 1$ it is easy to see why the counters change signs simultaneously. We can also see from here that we cannot talk of pure thin or thick vortices as long as we have at least one monopole in the lattice. A more careful definition for pure vortices may be designed so that they are well defined even in the presence of monopoles that are somehow disconnected or far away. We will not attempt such a definition here.

If we are to remove the monopoles then we are able to talk of pure thin and thick vortices. In such a theory it is be obvious that the thin vortices will die down (exactly like in the $Z(2)$ gauge theory) with increasing β. The thin vortices will

depercolate at around twice the value of β_c in $Z(2)$. However, we know that by removing the thin monopoles we do not change the value of the string tension. It is only the behavior if the 't Hooft loop that will be changed. The thick vortices that are the only one left to disorder the Wilson loop. In the next section we will present an algorithm that will help us investigate these ideas numerically.

5.4 Alternative Definition

Tomboulis formulation, in the form presented above, is very cumbersome to implement numerically. The problem is the constraint on the σ variables. To generate configurations randomly and then check the constraints is very inefficient. We have showed [50, 51, 52, 53] that the constraints in the σ variables can be satisfied very easily if we cast the expression (5.1) in the form:

$$Z = const \times \int \prod_b dU_b \sum_{\sigma^{-1}\eta \in \mathcal{D}} e^{\frac{\beta}{2}\sum_p |\mathrm{Tr}(U_p)|\sigma_p}$$

where the constraints are defined by set $\mathcal{D}$. If we are able to find a suitable definition for $\mathcal{D}$ then we might me able to simulate this system numerically. The "constraint" definition for $\mathcal{D}$ can be read of from the partition function (5.1):

$$\mathcal{D} = \{\alpha \in C^2(\Lambda) | \delta(\hat{\partial}\alpha) = 1 \ and \sum_{\beta \in H^2(\Lambda)} \{\alpha, \beta\} \neq 0\}$$

This definition is obviously not useful for numerical simulations. We will show now how to find a more useful definition. The first constraint asserts that $\alpha = \sigma^{-1}\eta$ is a co-closed configuration. Thus its image on the dual lattice is going to be a close

configuration. Thus any configuration in $\alpha \in \mathcal{D}$ can be written as $\alpha = *^{-1}\rho$ where $\rho \in Z^2(\Lambda^*)$ the set of all two dimensional closed configurations on the dual lattice. If α has such a form the first constraint is automatically obeyed. However there is a second constraint to obey:

$$H[\alpha] = \sum_{\beta \in H^2(\Lambda)} \{\alpha, \beta\} \neq 0.$$

To see the effect of this additional constraint we write down the general for, for $\rho \in Z^2(\Lambda^*)$. Since it is a closed configuration it can always be written as the product between a boundary configuration and a configuration in the homology group. Thus we have $\rho = \tau\gamma$ with $\tau \in B^2(\Lambda^*)$ and $\gamma \in H^2(\Lambda^*)$. We have then:

$$\begin{aligned} H[\alpha] &= H[*^{-1}(\tau\gamma)] = \sum_{\beta \in H^2(\Lambda)} \{*^{-1}(\tau\gamma), \beta\} = \sum_{\beta \in H^2(\Lambda)} \{\tau, *\beta\}\{\gamma, *\beta\} \\ &= \sum_{\beta \in H^2(\Lambda)} \{\gamma, *\beta\} = H[*^{-1}\gamma] \end{aligned}$$

where we used the fact that τ is a boundary configuration and thus:

$$\{\tau, *\beta\} = \{\partial\pi, *\beta\} = \{\pi, \hat{\partial} * \beta\} = \{\pi, *(\partial\beta)\} = 1$$

since $\beta \in H^2(\Lambda)$ and thus $\partial\beta = \phi_2$. We see then that the second constraint acts only on the γ part of ρ. In fact since $\gamma \in H^2(\Lambda^*)$ we have:

$$H[*^{-1}\gamma] = \begin{cases} 0 & \gamma \neq \phi_2 \\ |H^2(\Lambda^*)| & \gamma = \phi_2 \end{cases}$$

Since for every co-plane $*^{-1}\gamma_0 \neq \phi_2$ wrapped around the lattice there is a plane $\beta_0 \in H^2(\Lambda)$ such that they have only one plaquette in common so that $\{*^{-1}\gamma_0, \beta_0\} = -1$ and thus $H[*^{-1}\gamma_0] = 0$.

We see then that any element $\alpha \in \mathcal{D}$ can be written as $\alpha = *^{-1}\rho$ where ρ is not only a closed configuration but also a boundary configuration (since its homotopically equivalent with the identity ϕ_2). Thus the set $\mathcal{D}$ is the image under duality transformation of the set $B^2(\Lambda^*)$, the set of all two dimensional boundary configuration. The constant factor in our partition function is:

$$\frac{|H^2(\Lambda)||C^3(\Lambda)|}{|C^2(\Lambda)||Z^3(\Lambda)|} = \frac{1}{|B^2(\Lambda^*)|} = \frac{1}{|\mathcal{D}|}$$

and we can write the partition function:

$$Z = \int \prod_b dU_b \frac{1}{|\mathcal{D}|} \sum_{\sigma^{-1}\eta \in \mathcal{D}} e^{\frac{\beta}{2}\sum_p |\mathrm{Tr}(U_p)|\sigma_p} \tag{5.3}$$

where $\mathcal{D} = *^{-1}B^2(\Lambda^*)$.

This set is easy to generate numerically. Since all configurations are images of two dimensional boundary configurations we can generate it by taking the three dimensional configurations on the dual lattice and multiply their boundaries and transport this product on the direct lattice. More practically we can take the images of the three dimensional configurations on the dual lattice which are actually the one dimensional configurations on the direct lattice. We will then take the coboundary of link configurations to define the set $\mathcal{D}$. The smallest such configuration is the one

generated by a link b. We call it a star transformation. We can write it explicitely as:

$$\alpha_b(p) = \begin{cases} 1 & p \notin \hat{\partial} b \\ -1 & p \in \hat{\partial} b \end{cases}$$

All the products of generated by such star transformations will be included in $\mathcal{D}$. Moreover, they will cover completely the set. Thus we have a "constructive" definition for the set $\mathcal{D}$ which allows us to implement it numerically. The algorithm is the following:

- Do a regular $SU(2)$ simulation to thermalize the lattice.
- Compute η and then put σ on top of η so that $\sigma^{-1}\eta = \phi_2 \in \mathcal{D}$.
- Do a $SU(2)$ update and for every changed η change the corresponding σ.
- Do a $Z(2)$ update that is realized by changing all six σ's on the plaquettes surrounding a link at once.
- Repeat the last two steps as many time as possible.

The first step ensures that we have a thermalized lattice in terms of U_b. The second step sets σ such the constraint is obeyed. The third step update the U_b variables. The forth step allows η and σ to drift apart but keeps the constraint obeyed. Furthermore, it will generate all possible configurations if you run it indefinitely.

This algorithm generates full $SU(2)/Z(2) \times Z(2)$ configurations. We can use it to measure the vortex counters and various products of the Wilson loop with vortex counters. In a latter section we will present numerical results produced with

this algorithm. However, there are certain operators that are defined in the $SU(2)$ formulation that are difficult, if not impossible, to measure using this method. Of special interest for us is the P-vortex counter that is defined on $SU(2)$ configurations. In the next section we will show how to measure the Tomboulis vortex counters on regular $SU(2)$ configurations which will allow us to compare them with P-vortices.

5.5 Tomboulis Vortex Counters in $SU(2)$ Theory

In trying to compare the vortex counters as defined by Tomboulis with P-vortices on a particular configuration we are faced with the following problem: Tomboulis vortices are defined on an $SU(2)/Z(2) \times Z(2)$ configuration whereas the P-vortices are defined on an $SU(2)$ configuration. An one-to-one mapping between these two sets of configurations is not possible since the configuration space for Tomboulis variables is bigger that the set of $SU(2)$ configurations. We can, of course, define an arbitrary mapping between these two sets but this will be useless unless this mapping maps one configuration into a physically equivalent configuration. Defining this equivalence is not a trivial task.

Another way to impose this requirement is to ask that two operators that are equivalent, for example the Wilson loop in the regular $SU(2)$ formulation and the Wilson loop defined in Tomboulis formulation (5.2), respond identically on these equivalent configurations. The problem is then defining equivalent operators. In fact, as soon as we have defined what equivalent operators are, we no longer need this mapping since we can use the equivalent operator for the vortex counters directly on the $SU(2)$ configurations.

For the Wilson loop Tomboulis has shown that the average of the Wilson loop can be reproduced exactly if we use the operator:

$$W_T(U,\sigma) = \mathrm{Tr} \prod_{b\in C} U_b \prod_{p\in S}(\eta_p\sigma_p) = W_W(U) \prod_{p\in S}(\eta_p\sigma_p)$$

where the subscript T stands for the $SO(3)\times Z(2)$ formulation and W for the $SU(2)$ formulation. These operators have not only the averages equal but also any function of these operators will have the same average. To see this we write:

$$\begin{aligned}\langle f(W_T)\rangle &= \frac{1}{Z}\int DU \frac{1}{|\mathcal{D}|}\sum_{\sigma\eta\in\mathcal{D}} f(W_T(U,\sigma)) e^{\frac{\beta}{2}\sum_p |\mathrm{Tr}\, U_p|\sigma_p} \\ &= \frac{1}{Z}\int DU \frac{1}{|\mathcal{D}|}\sum_{\sigma\eta\in\mathcal{D}} f(W_W(U)\sigma_S\eta_S) e^{\frac{\beta}{2}\sum_p \mathrm{Tr}\, U_p\eta_p\sigma_p}\end{aligned}$$

where we have written $|\mathrm{Tr}\, U_p| = \mathrm{Tr}\, U_p\eta_p$. We notice that σ and η appear only in a $\sigma\eta$ combination. Thus we can make a change of variables $\tau = \sigma\eta$ and write:

$$\langle f(W_T)\rangle = \frac{1}{Z}\int DU \frac{1}{|\mathcal{D}|}\sum_{\tau\in\mathcal{D}} f(W_W(U)\tau_S) e^{\frac{\beta}{2}\sum_p \mathrm{Tr}\, U_p\tau_p}$$

Since the summation over τ does not depended on η any more we can write:

$$\langle f(W_T)\rangle = \frac{1}{|\mathcal{D}|}\sum_{\tau\in\mathcal{D}} \frac{1}{Z}\int DU f(W_W(U)\tau_S) e^{\frac{\beta}{2}\sum_p \mathrm{Tr}\, U_p\tau_p}$$

Due to the fact that $\tau \in \mathcal{D}$ we can always find a configuration $\gamma_b \in C^1(\Lambda)$ such that $(\hat{\partial}\gamma)(p) = \tau_p$ and we make the change of variable: $U_b \to \gamma_b U_b$. Using the Haar

invariance over $SU(2)$ we can write:

$$\langle f(W_t)\rangle = \frac{1}{|\mathcal{D}|}\sum_{\tau\in\mathcal{D}}\frac{1}{Z}\int DU f(W_W(U)\prod_{p\in S}\hat{\partial}\gamma(p)\tau_S)e^{\frac{\beta}{2}\sum_p \mathrm{Tr}\, U_p\hat{\partial}\gamma(p)\tau_p}$$

Since $\hat{\partial}\gamma(p)=\tau_p$ we have:

$$\begin{aligned}\langle f(W_T)\rangle &= \frac{1}{|\mathcal{D}|}\sum_{\tau\in\mathcal{D}}\frac{1}{Z}\int DU f(W_W(U))e^{\frac{\beta}{2}\sum_p \mathrm{Tr}\, U_p}\\ &= \frac{1}{|\mathcal{D}|}\sum_{\tau\in\mathcal{D}}\langle f(W_W)\rangle = \langle f(W_W)\rangle\end{aligned}$$

for any function f. We see then that the operators W_W and W_T are equivalent in the sense that we can measure the average $\langle f(W_T)\rangle$ on a regular $SU(2)$ configuration using $f(W_W)$. Moreover, we can show in a similar fashion, that any product of Wilson operators: $f_1(W_T^{C_1})\cdot ....\cdot f_n(W_T^{C_n})$ is equivalent with $f_1(W_W^{C_1})\cdot ....\cdot f_n(W_W^{C_n})$. Thus we see that we can use W_W in the original $SU(2)$ formulation as an equivalent for the operator W_T defined in the $SO(3)\times Z(2)$ formulation. These operators produce the same averages for all possible products and functions defined on them.

This property has been used to transport operators from the regular $SU(2)$ theory to Tomboulis formulation. We will use this property here to find the equivalent for the Tomboulis vortex counters in the regular $SU(2)$ theory.

The hybrid counter, N_{hybrid}, is defined as:

$$N_{hybrid} = \mathrm{sign}\left(\mathrm{Tr}\left(\prod_{b\in C}U_b\right)\prod_{p\in S}\eta_p\sigma_p^{-1}\right) = \mathrm{sign}(W_T)$$

Since sign(W_T) is just a function of W_T we can define the hybrid counter in $SU(2)$ to be:

$$N_{hybrid}^{SU(2)} = \text{sign}(W_W)$$

For the thin counter we notice that:

$$\sigma_p^{-1} = \eta_p \eta_p \sigma_p^{-1} = \text{sign}\,\text{Tr}\, U_p \eta_p \sigma_p^{-1} = \text{sign}(\text{Tr}\, U_p \eta_p \sigma_p^{-1})$$

The last term is just the sign of the smallest Wilson loop in Tomboulis formulation. We can then define:

$$(\sigma_p^{-1})^{SU(2)} = \text{sign}\,\text{Tr}\, U_p$$

and then the thin vortex counter in $SU(2)$ becomes:

$$N_{thin}^{SU(2)} = \prod_{p \in S} (\sigma_p^{-1})^{SU(2)} = \prod_{p \in S} \text{sign}\,\text{Tr}\, U_p$$

Here we used the fact that not only functions of W produce the same averages but also the products of different Wilson loops.

For the thick counter we have to use the fact that $N_{thick} = N_{hybrid} \times N_{thin}$ and we write:

$$N_{thick}^{SU(2)} = N_{hybrid}^{SU(2)} \times N_{thin}^{SU(2)} = \text{sign}\left(\prod_{b \in C} \text{Tr}\, U_b\right) \times \prod_{p \in S} \text{sign}\,\text{Tr}\, U_p$$

We have now the equivalent vortex counters in the $SU(2)$ formulation of the theory. We can use them to compute averages using the regular algorithms for $SU(2)$

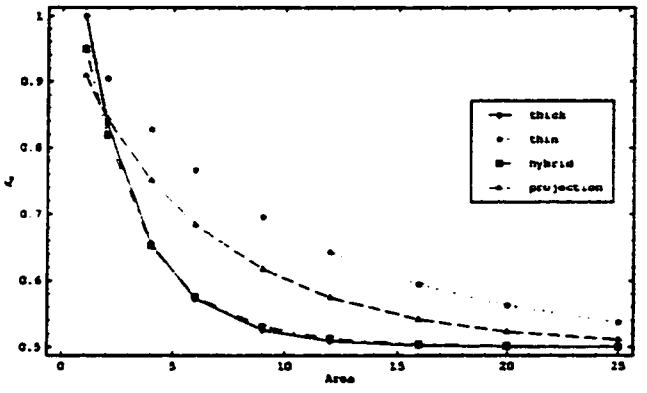

Figure 5.1: Fraction of Wilson loops trapping an even number of vortices inside.

or, more interestingly, to compare the signal that the Tomboulis vortex counters produce with the signal produced by other vortex counters, in particular, the P-vortex counters. In the next section we will present the result of the numerical investigations.

5.6 Numerical Results

The definition of Tomboulis vortex counters in section 5.4 is difficult to implement numerically due to the fact that it is very time consuming to generate all possible surfaces that tile a particular Wilson loop. Moreover, in a configuration that has monopoles pure vortex counters are difficult to define (according to the definition in section 5.4 all vortices will be hybrid). Due to these problems we used only the minimal surface to define the vortex counters. If the vortex counter is -1 for the minimal surface we say that we trapped a vortex inside that particular Wilson loop.

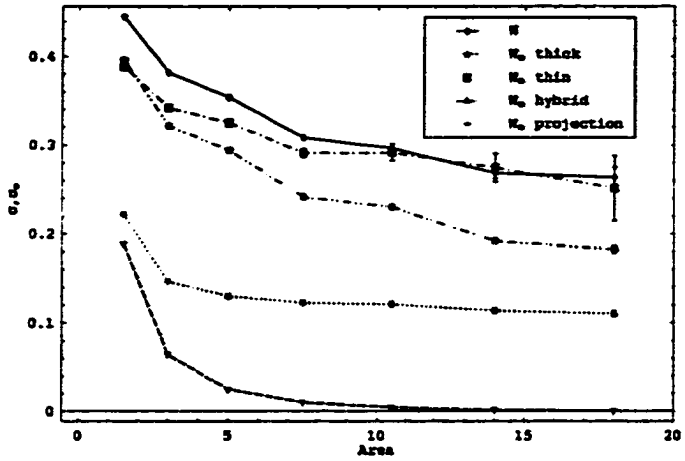

Figure 5.2: String tension for the full Wilson loop and the tagged Wilson loops.

Tagged Wilson Loops

We first looked at the density of vortices in a typical configuration. At $\beta = 2.3$ we see from Fig. 5.1, where we plotted the fraction of Wilson loops that produce a positive vortex counter, that thick and hybrid vortices are more dense that the projection vortices which in turn are more dense than the thin vortices. All fractions converge to 50% in the large loop limit. This is a necessary condition for the vortices to disorder the Wilson loop. The thick and hybrid vortex density are almost the same. This would suggest that the thick and hybrid counters are closely related. This would be good since we expect the hybrid counter to follow closely the signal produced by the Wilson loop.

A logical next step was to look at the string tension of the "tagged" Wilson loops. Using a vortex counter we measure the average of only those Wilson loops that produce a positive signal for this vortex counter. Thus we do not include in the average process the Wilson loops that have a -1 vortex counter. By doing this we

effectively remove the disordering mechanism associated with that particular vortex type. If that particular vortex is relevant for confinement we expect that the tagged Wilson loop will show a smaller string tension or even no string tension at all.

In Fig. 5.2 we plotted the logarithmic derivative $(-\frac{\ln W(A_{i+1})-\ln W(A_i)}{A_{i+1}-A_i})$ of the tagged Wilson loops at $\beta = 2.3$. The logarithmic derivative should converge to the string tension in the large area limit. We see from the picture that the Wilson loop tagged by the hybrid vortex has no area law. This is expected since we know that the hybrid counter is kinematically connected with the full Wilson loop (we will see numerical evidence of this fact a little later).

The Wilson loop tagged by the thin vortex has almost the same string tension as the full Wilson loop. This shows that the thin vortices are indeed irrelevant for confinement.

The unexpected result is the fact that the Wilson loop tagged by thick vortices shows an area law behavior. We expected to lose the string tension when we removed the thick degrees of freedom. The only available mechanism left to disorder the Wilson loop is the thin vortices which we believe to generate, at best, an area law. However, since our counters are defined only on minimal area the hybrid vortices that happen to be thin when they intersect the minimal are can provide an area law. We believe that this string tension is due to these thin patches that form the hybrid vortices. We also see that the thick vortices are relevant for confinement since by tagging them we lost some of the string tension. The area law behavior for the Wilson loop tagged by thick vortices is our first indication that although the thick and hybrid vortices have almost the same densities their dynamics is different.

To understand better the behavior of different vortex counters we looked at the potentials generated by them.

Vortex Potentials

To extract the vortex potentials we measured the Wilson loops and vortex counters at $\beta = 2.3, 2.4, 2.5$ on a 22×14^3 lattice. The number of configuration used are 3000, 1000 and 1228 for β 2.3, 2.4 and 2.5 respectively. The configurations are thermalized using 1000 updates and the measurements are separated by 40 updates. The acceptance was calibrated to be around 50%.

The potential is extracted from the average values of the Wilson loop and vortex counters:

$$V_{counter}(R) = -\lim_{T\to\infty} \frac{1}{T} \ln\langle N_{counter}(W(R,T))\rangle$$

where $N_{counter}(W(R,T))$ is the counter signal for that particular Wilson loop (it can only assume values of ± 1). We use this potentials because we believe that the remaining part of the Wilson loop is not going to affect the long distance physics. To determine the potential for a particular R we use Wilson loops $W(R,T)$ and an array of T's that are large enough for the exponential behavior to set in and do a fit with an exponential in T's. In Fig. 5.3 we show the various potentials for different values of β.

The first thing we notice is that, as we mentioned before, the hybrid counter produces the same potential as the full potential. This is due to the fact that the sign function, as mentioned in a previous chapter, has a character expansion that

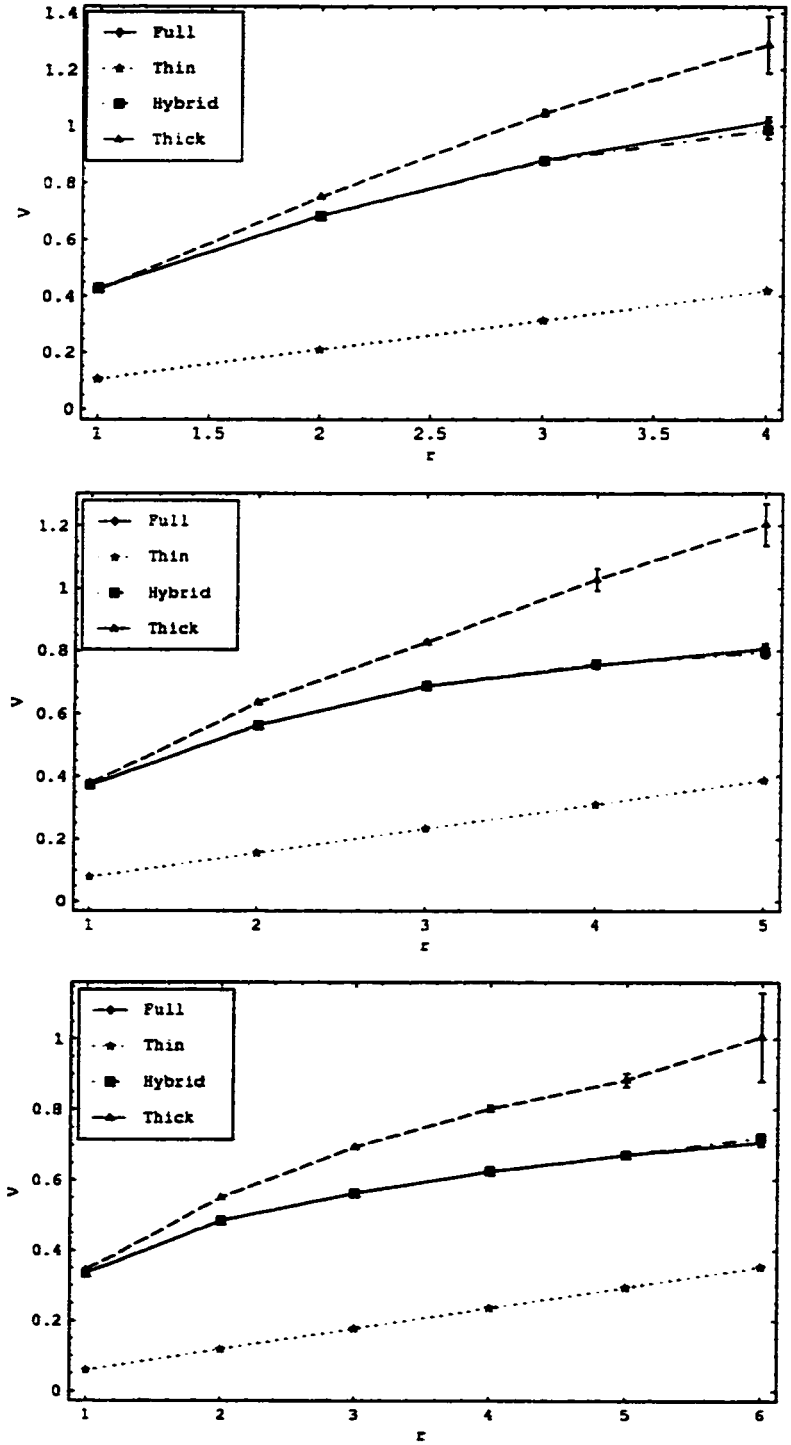

Figure 5.3: Vortex potentials in lattice units at β 2.3 (top), 2.4 (middle), 2.5 (bottom).

has only semi-integer components:

$$\text{sign}(\text{Tr}(U)) = \sum_{j=1/2,3/2,\ldots} c_j \chi_j(U)$$

Since $\chi_j(W(A))$ for $j \geq 3/2$ decays faster with area A that $\text{Tr}(W(A))$, for big enough Wilson loops we have $\text{Tr}(W) \simeq c_{1/2} \,\text{sign}\,\text{Tr}(W)$. Thus the potentials generated by the full Wilson loop and the hybrid counter are the same. This was first noticed by Kovacs and Tomboulis [13].

We also see that the potential generated by the thick counter differs substantially from the full potential. This is contrary to our expectations since we expected that the thick counter will behave approximatively as the hybrid counter. We will show that this is a consequence of the existence of thin patches in the hybrid vortices.

We first notice that the thin counter produces a very clear string tension. This agrees with our observation of the string tension in the Wilson loop tagged by thick vortices (the string tension there was roughly 1.1 where the string tension at $\beta = 2.3$ extracted from thin potential is 1.043(1)). The important question is whether this string tension goes away as we approach the continuum limit.

To determine the behavior in the continuum limit we need to see if these potentials scale. The first thing we need to do is to calibrate the lattice using the string tension of the Wilson loop. The string tension is determined using by fitting the data with the function:

$$V(r) = \sigma r - \frac{e}{r} + V_0$$

where σ is the string tension, e/r represents the Coulomb part of the potential at short distances and V_0 is a self-energy. σ and e are expected to scale whereas V_0 which depends strongly on the cut-off is not expected to scale. Using the physical value of the string tension $\sigma = (440MeV)^2$ we determine the lattice spacing. The results are in the Table 5.1. It is obvious that e scales and V_0 doesn't.

Table 5.1: String tension and lattice spacing.

β	σ [lattice units]	lattice spacing [fm]	e [natural units]	V_0 [GeV]
2.3	0.157(14)	0.177(8)	0.193(25)	0.51(11)
2.4	0.083(10)	0.129(8)	0.217(24)	0.78(20)
2.5	0.043(1)	0.093(2)	0.211(3)	1.07(6)

To get an idea of the scaling characteristics we show the scaled plot of the full potential. In Fig. 5.4 we plot $\frac{V(r/a)-V_0}{a}$ with a the lattice spacing for different values of β. We see that the full potential scales as expected.

In Fig. 5.5 we present the scaling graphs for the potentials extracted using the vortex counters. We see that the hybrid potential scales since it follows exactly the full potential.

On the other hand the thin and thick potentials do not scale. Moreover, we see from these plots that the thin potential increases in physical unit rather that vanishing. Thus the potential produced by thin patches, although not relevant for confinement, cannot be disregarded. The fact that the string tension due to the thin patches doesn't vanish as we approach continuum limit is also producing a non-scaling behavior for our thick potential. To see this we write down the hybrid

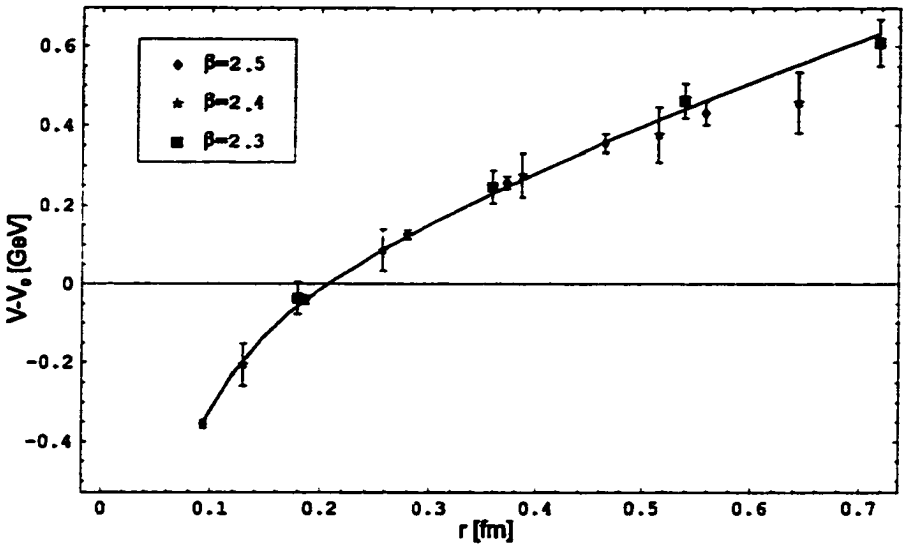

Figure 5.4: Adjusted potential $V-V_0$ extracted from the full Wilson loop for different values of β. The solid line represents a fit with a potential of the form $V(r) = \sigma r - \frac{e}{r}$.

counter:

$$N_{hybrid} = N_{thin} \times N_{thick}$$

If the thin and thick counters were completely uncorrelated then we would expect that:

$$\langle N_{hybrid} \rangle = \langle N_{thin} \rangle \times \langle N_{thick} \rangle$$

Since we know now that $\langle N_{thin} \rangle \sim e^{-\sigma A}$ with increasing σ (in physical units) as we approach the continuum limit the hybrid vortex will also have a non-physical string tension. However, we know that the hybrid potential scales properly (since it behaves exactly like the full potential) and thus the thin and thick counters cannot be uncorrelated. The correlation comes from the hybrid vortices since our counters measure the signal only on the minimal surface. A hybrid vortex will then

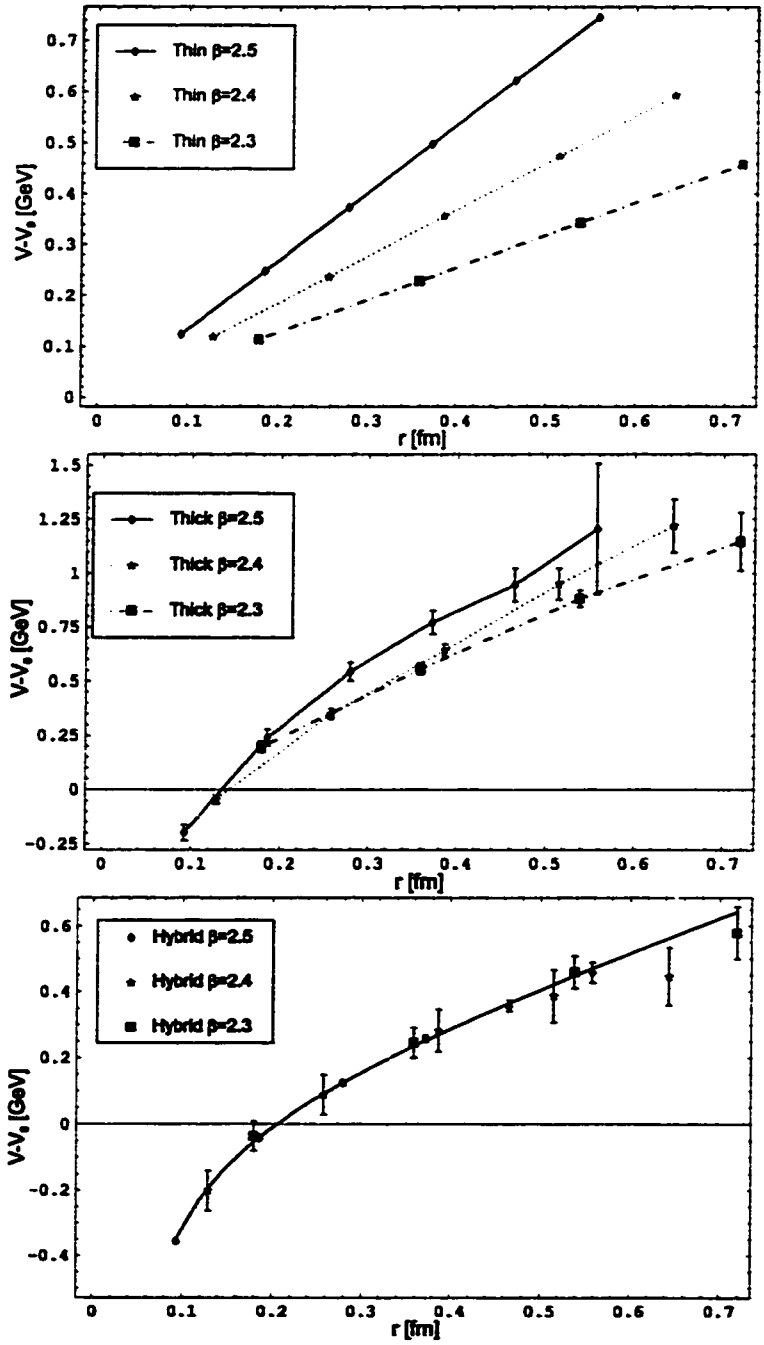

Figure 5.5: Vortex potentials in physical units: thin (top), thick (middle), hybrid (bottom). The line in the hybrid plot represents a fit.

produce a thin or thick signal depending on how it pierces the minimal surface. Thus both our thin counter and the thick counter will include extraneous signals due to hybrid vortices. Since we believe that the pure thin vortices cannot produce any string tension as we approach the continuum limit we are led to believe that the string tension that we see in the thin counters is due to these hybrid vortices (more precisely the thin patches in the hybrid vortices). These vortices are the reason for the correlation of our thin and thick counters and they also introduce an extraneous string tension in our thick potential.

In order to see the properties of the pure thick vortices we will need then to remove the contribution due to the hybrid vortices. One way to do it, if the above reasoning is true, is by subtracting the thin potential out of the thick potential. In Fig. 5.6 we plot the potentials difference. We see that apart from a constant the full potential and difference of the thick and thin potentials are the same. The string tension recovered from the scaling graph is the same within the error bars with the full string tension.

To sum up we have seen that the potential generated by the hybrid vortex matches the full potential. We've also seen that the thick and thin potentials don't scale. The surprising part was that the string tension in the thin potential doesn't vanish. On the contrary it increases as we approach the continuum limit. We've argued that this is due to thin patches detected by our simplified thin counter and this induces an non-scaling behavior in our thick potential. If we eliminate the extra thick patches from our thick counter by subtracting the thin potential out of the thick potential we get a potential that scales properly and mathces the full potential.

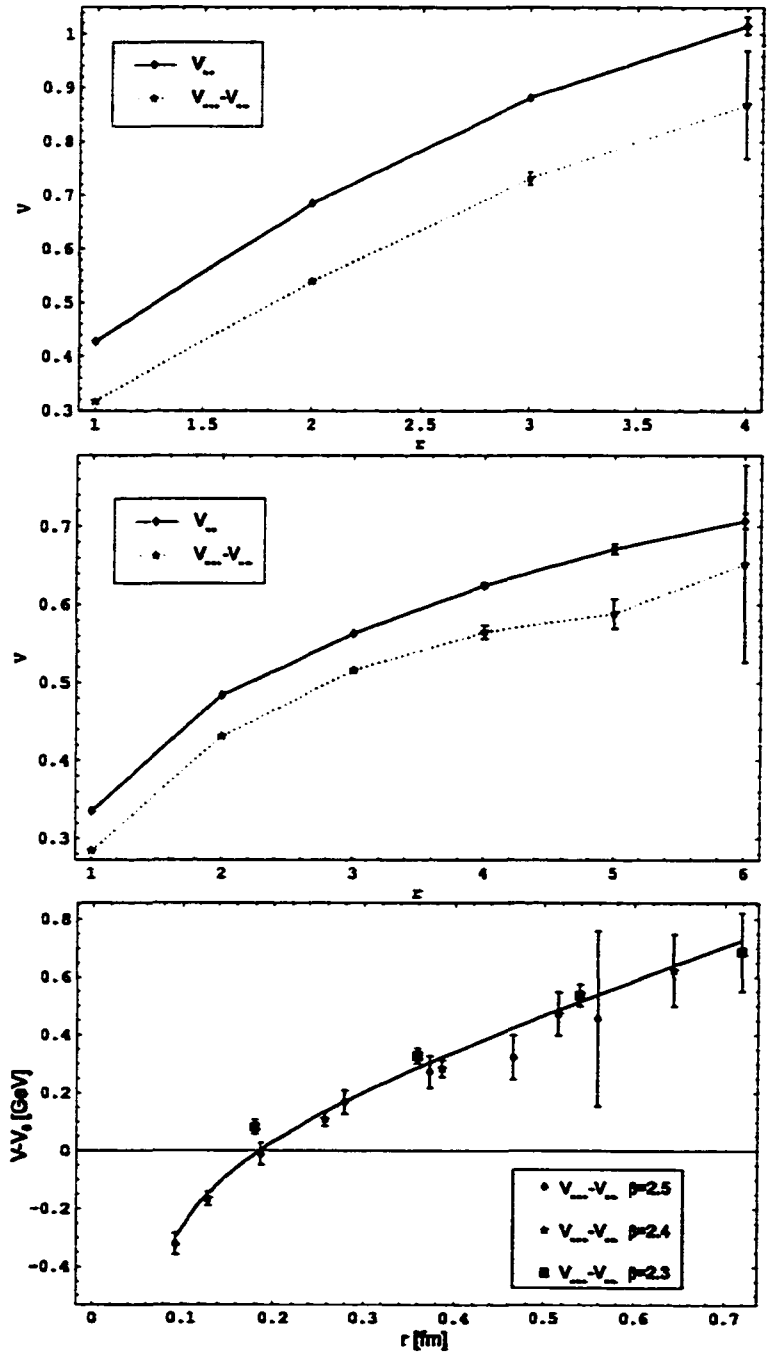

Figure 5.6: The difference between the thick and the thin potential plotted against the full potential. The graph on top is at $\beta = 2.3$, the one in the middle is at $\beta = 2.5$ and the one at the bottom represents the scaled graph.

To see that this is indeed the potential due to pure thick vortices a more careful analysis is required. We need to find first a definition for pure thick vortices that works in a general configuration (even in one that includes monopoles). Using this vortex counter is then possible to decide if the thick vortices are indeed generating the full potential (or at least the string tension). A different approach is to use the definition that we have now but generate configurations that have no monopoles. In such configurations we have only pure thin and thick vortices. It is very likely that in such an approach that the thick potential will be identical with the full potential (at least at large distances) since we expect that the pure thin vortices produce at best a perimeter law. The problem with this approach is that we are changing the dynamics of the system by forbidding the monopoles.

Vortex Comparison

The Tomboulis definition for vortices is appealing since it is a gauge invariant definition. These vortices seem to produce the right physics but they are hard to localize on a lattice. Projection vortices, on the other hand, are easy to localize but are not gauge invariant.

It is interesting to see if these two definitions agree. To see if there is an agreement we can look at the dynamical features like string tension etc. However, we don't see too much of a difference at this level. The basic reason is that these theories were designed to produce the string tension of the full theory. A more meaningful way to compare these definitions will be to compare the response of these vortex counters on the same configurations. We will try to do this in this section.

A first method will be to take a thermalized $SU(2)$ gauge configuration and project it. We will measure then the Tomboulis counters on the original gauge configuration and the P-vortex counter on the projected configuration. We will count only the fraction of loops of a certain size that produce negative signal:

$$f_{counter} = \langle \frac{1}{2}(1 - N_{counter}) \rangle$$

where the counter can be thin, thick, hybrid or projection. We will then measure the coincidence between the projection counter and one of the Tomboulis counter. This will measure the fraction of Wilson loops of a certain size that bas both the projection counter and that particular Tomboulis counter negative:

$$p_{counter} = \langle \frac{1}{2}(1 - N_{projection}) \times \frac{1}{2}(1 - N_{counter}) \rangle$$

where the counter can be thin, thick or hybrid. If the vortices are completely uncorrelated then:

$$p_{counter} = \langle \frac{1}{2}(1 - N_{projection}) \rangle \times \langle \frac{1}{2}(1 - N_{counter}) \rangle = f_{projection} \times f_{counter}$$

If they are completely correlated then:

$$p_{counter} = \min\{f_{projection}, f_{counter}\}$$

These are the bounds that on the coincidence counter. If the $p_{counter}$ approaches

the lower bound $f_{proj} \times f_{counter}$ then the vortex counters are uncorrelated and we conclude that the physics that generates the counters is different. If the coincidence counter is closer to the upper bound then we conclude that the counters detect the same structures.

The results are presented in Fig. 5.7. We see that the counters show no correlation. We are led to believe that the P-vortices and Tomboulis vortices are different objects. However, there is another possibility. The P-vortices are defined using a projection. As we mentioned before, the projection procedure can produce different results for gauge equivalent configurations. The argument is that when we have a thick vortex the projection produces a P-vortex somewhere inside the core of the thick vortex. However, this P-vortex can be anywhere inside the thick core depending on the gauge copy we used. Thus the P-vortices may oscillate and the correlation signal might be lost due to vortices very close to the perimeter.

In order to take into account this oscillation we took a $SU(2)$ gauge configuration, created 100 gauge copies of it and then we projected each copy. We used these 100 projected configurations to define an average P-vortex counter. For a particular Wilson loop, at a certain position in the lattice we take the sum of the P-vortex signals in all 100 configurations. We then say that we have a negative P-vortex trapped if this sum is negative. This counter is going to pick up those loops that are negative in most of the projected configurations. If there is a perimeter effect we expect this procedure to cancel it.

In Fig. 5.8 we present the results. We showed both the upper and the lower bound for $p_{counter}$. Although the correlation is now a little farther from the lower

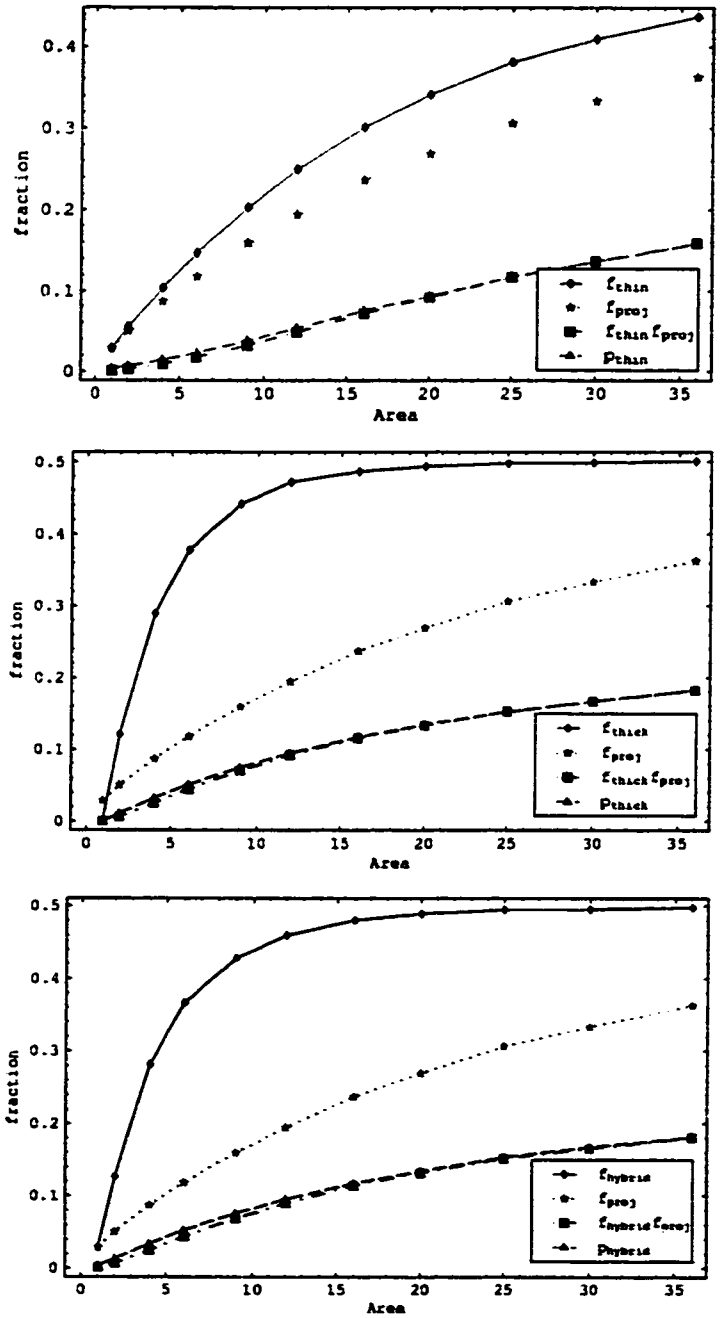

Figure 5.7: Tomboulis counters and their coincidence with the projection vortices. The $p_{counter}$ is very close to the lower bound $f_{proj} \times f_{counter}$ which indicates no correlation.

bound there is still no convincing evidence that even these modified P-vortices are correlated with the Tomboulis vortices. Moreover, the density of these P-vortices is even lower than the density of the real P-vortices which was already a lot smaller that the density of Tomboulis vortices. It is then difficult to see how it is possible that both P-vortices and the Tomboulis vortices are generated by the same structure. The only conclusion that we can draw is that these are fundamentally different objects.

We expected the P-vortices to show a correlation at least with the hybrid counter. The hybrid counter is nothing more than the sign of the Wilson loop. The P-vortex counter is the sign of the Wilson loop in the projected configuration. If we are to believe that by projection we only loose perimeter related information then we expect to see some correlation between the P-vortices and hybrid counter. Our simulations show that they are almost uncorrelated.

It is still possible that the perimeter effect is producing this uncorrelation. However it is rather difficult to find a way to get rid of it especially since we are interested in comparing the response of the vortex counters on a particular configurations rather that on an ansamble of such configurations. This issue remains to be settled.

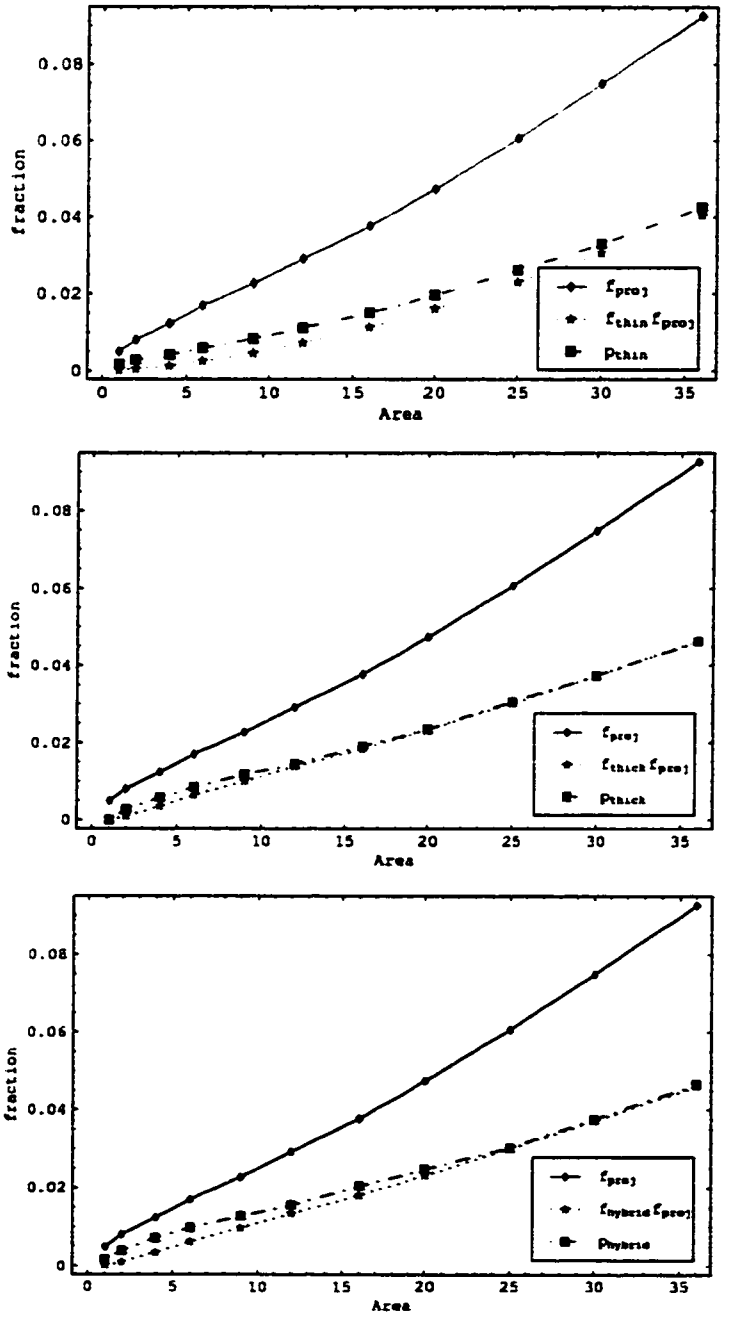

Figure 5.8: Tomboulis counters and their coincidence with the modified projection vortices.

Conclusions

In this dissertation we have shown how to implement numerically the Tomboulis formulation. We have presented an algorithm that generates $SU(2)/Z(2) \times Z(2)$ configurations and we described how the boundary conditions restrict the configuration space. Using this method we verified numerically the ideas behind the Tomboulis formulation.

We presented evidence that the thick vortices are connected with the confinement. We have seen that by removing the thick vortices the only string tension left is that due to thin patches. The thin patches seem to be irrelevant for confinement. Using tagging we removed the thin patches and we've seen that the string tension remains the same. However, the thin patches are producing a string tension that cannot be completely disregarded. We have shown how these patches can affect both the thin and thick vortex counters. To completely settle the issue we need a definition for pure vortices that will work even in the presence of monopoles.

A different method was also presented that enabled us to measure the vortex counters defined by Tomboulis directly on regular $SU(2)$ configurations. We used this method to compare the signal generated by Tomboulis vortex counters with the

ones generated by P-vortices. Although the results are not definitive refinements of the coincidence method can be used to see if the P-vortices and Tomboulis vortices are describing the same physics. We have presented evidence that support the idea that they are not correlated. Moreover, this method can be used to investigate the properties of Tomboulis formulation using the simpler $SU(2)$ algorithms.

The duality of the Z_2 theory is well known. However, we were able to use the idea of vortices to put some limits on the critical point of the theory. We have shown there how to use the vortex mechanism to get the behavior of the 't Hooft loop in the weak coupling limit. We have checked that the string tension of the 't Hooft computed in the first order using the vortex mechanism corresponds to the string tension deduced using the strong coupling expansion for the Wilson loop and the duality transformations.

All the numerical work presented here was done for $SU(2)$. The generalization of this work to $SU(3)$ is straightforward. However, we do not expect qualitatively new results to come out of a study of Tomboulis vortices in $SU(3)$. A study into finding a proper definition of pure thick and thin vortices on a configuration containing monopoles seems more interesting. Also, a study of thin vortices on configurations where monopoles are forbidden seems worthwhile. We believe that they will vanish in the continuum limit but this needs to be proved.

The vortex mechanism of confinement was presented in the text. However, no attempt was made to exhibit the vortices directly. All the evidence we presented supports the idea of vortices, but only indirectly. Whether the vortices have a physical existence or are mere mathematical devices is still an open question. The

P-vortices cannot be used to address this question since they create these vortex structures by fiat. The Tomboulis definition of vortices is more suitable since it doesn't start with any bias toward a vortex topology. Unfortunately, all the tests that we have performed [54] using Tomboulis definition of vortex counters do not exhibit any vortex structure embedded in gauge field.

Bibliography

[1] C. N. Yang, R. L. Mills, Phys. Rev. **96**, 191 (1954).

[2] M. Creutz, *Quarks, Gluons and Lattices*, Cambridge University Press (1983).

[3] H.G. Rothe, *Lattice Gauge Theories - An Introduction*, World Scientific, Singapore (1992).

[4] I. Montvay, G. Munster, it Quantum Fields on a Lattice, Cambridge University Press (1997).

[5] M. Creutz, Phys. Rev. **D21**, 2308 (1980).

[6] P. F. Smith, Ann. Rev. Nucl. and Part. Sci. **39**, 73 (1989).

[7] L. B. Okun, *Leptons and Quarks*, North Holland (1982).

[8] D. J. Gross, F. Wilczek, Phys. Rev. **D8**, 3633 (1973).

[9] G. 't Hooft, Nucl. Phys. **B138**, 1 (1978).

[10] L. Del Debbio, M. Faber, J. Giedt, J. Greensite, S. Olejnik, hep-lat/9801027.

[11] P. de Forcrand, M. Pepe, hep-lat/0008016.

[12] E. Tomboulis, Phys. Rev. **D23**, 2371 (1980).

[13] T. Kovacs, E. Tomboulis, hep-lat/9711009.

[14] F. J. Dyson, Phys. Rev. **75**, 1736 (1949).

[15] K. G. Wilson, Phys. Rev. **B4**, 3174, 3184 (1971).

[16] J. D. Jackson, *Classical Electrodynamics*, John Wiley & Sons, Inc (1975).

[17] W. Pauli, F. Villars, Rev. Mod. Phys. **21**, 434 (1949).

[18] G. 't Hooft, M. Veltman, Nucl. Phys. **B44**, 189 (1972).

[19] S. Aoki, Nucl. Phys. **B** (Proc. Suppl.) **94**, 3 (2001).

[20] S. Ejiri, Nucl. Phys. **B** (Proc. Suppl.) **94**, 19 (2001).

[21] M. G. Perez, Nucl. Phys. **B** (Proc. Suppl.) **94**, 27 (2001).

[22] T. Bhattacharya et all, Nucl. Phys. **B** (Proc. Suppl.) **94**, 1 (2001).

[23] K. Symanzik, Nucl. Phys. **B226**, 2445 (1983).

[24] K. G. Wilson, *New Phenomena in Subnuclear Physics*, Erice (1975).

[25] K. G. Wilson, Phys. Rev. **D10**, 2445 (1974).

[26] G. Bali, K. Schilling, C. Schlichter, Phys. Rev. **D51**, 5165 (1995).

[27] G. Bali, K. Schilling, A. Wachter, hep-lat/9506017.

[28] E. Eichten, F. Feinberg, Phys. Rev. **D23**, 2724 (1981).

[29] E.T. Tomboulis, L. G. Yaffe, Commun. Math. Phys. **100**, 313 (1985).

[30] K. Osterwalder, E. Seiler, Ann. Phys. (New York) **110**, 440 (1978).

[31] L. Yaffe, Phys. Rev. **D21**, 1574 (1980).

[32] G. Mack, V. Petkova, Ann. Phys. (N.Y.) **123**, 442 (1979).

[33] C. Hoelbling, C. Rebbi, V. Rubakov, hep-lat/0003010.

[34] G. 't Hooft, Nucl. Phys. **B153**, 141 (1979).

[35] T. Kovacs, E. Tomboulis, Phys. Rev. Lett. **85**, 704 (2000).

[36] M. Engelhardt, K. Langfeld, H. Reinhardt, O. Tennert, hep-lat/9904004.

[37] R. Balian, J. M. Drouffe, C. Itzykson, Phys. Rev. **D11**, 2098 (1975).

[38] M. Faber, J. Greensite, S. Olejnik, J. High Energy Phys. **06**, 041 (2000).

[39] J. Ambjorn, J. Greensite, hep-lat/9804022.

[40] M. Faber, J. Greensite, S. Olejnik, hep-lat/0103030.

[41] L. Del Debbio, M. Faber, J. Greensite, S. Olejnik, hep-lat/9708023.

[42] V. N. Gribov, Nucl. Phys. **B139**, 1 (1978).

[43] V. Bornyakov, D. Komarov, M. Polykarpov, Phys. Lett. **B497**, 151 (2001).

[44] T. Kovacs, E. Tomboulis, hep-lat/9905029.

[45] J. Stack, W. Tucker, A. Hart, hep-lat/0011057.

[46] M. Faber, J. Greensite, S. Olejnik, D. Yamada, hep-lat/9910033.

[47] J.C. Wink, U.J. Wiese, Phys. Let. **B289**, 122 (1992).

[48] C. Alexandrou, P. de Forcrand, M. D'Elia, hep-lat/9909005.

[49] K. Lanfeld, H. Reinhardt, A. Schafke, hep-lat/0101010.

[50] A. Alexandru, R.W. Haymaker, Phys. Rev. **D62** 074509 (2000).

[51] A. Alexandru, R.W. Haymaker, Nucl.Phys.Proc.Suppl. **94** 543 (2001).

[52] A. Alexandru, R.W Haymaker, Nucl.Phys.Proc.Suppl. **94** 475 (2001).

[53] A. Alexandru, R.W. Haymaker, hep-lat/0009011, hep-lat/0009010.

[54] A. Alexandru, R.W. Haymaker, work in progress.

[55] C. Nash, S. Sen, *Topology and Geometry for Physicists*, Academic Press (1983).

Appendix

A.1 Notation

We will denote with Λ the lattice in four dimensions:

$$\Lambda = \{(n_1, n_2, n_3, n_4) | n_i \in Z_{N_i}\}$$

where Z_{N_i} is the set of integers modulo N_i. The elements of the lattice will be denoted with s for site, b for bonds or links, p for plaquettes, c for cubes and h for hypercubes. Sometimes we will use a more general notation c^r to denote a cell of rank r in the lattice: c^0 for s, c^1 for b, c^2 for p, c^3 for c and c^4 for h. A cell of rank r is denoted by its position in the lattice (n_1, n_2, n_3, n_4) and its direction $(i_1, i_2, ..., i_r)$ where $i_k \in \{1, 2, 3, 4\}$. When necessary we will indicate a cell by its direction and position: $(c^r)^{i_1,...,i_r}_{n_1,n_2,n_3,n_4}$. We will require that in indicating a direction we order the indices $i_k < i_{k+1}$ so that we have a unique way of referring to an element in the lattice. We will sometimes denote with Λ^r the set of all c^r cells in the lattice. The volume of the lattice will be denoted by N_s or $|\Lambda|$. We will always use $|A|$ to denote the number of elements in the set A.

A.2 Dual Lattice

For every lattice:

$$\Lambda = \{(n_1, n_2, n_3, n_4) | n_i \in Z_{N_i}\}$$

we can define a dual lattice:

$$\Lambda^* = \{(n_1, n_2, n_3, n_4) | n_i \in Z_{N_i}\}$$

The dual lattice has the same size as the original lattice and we will define an one to one mapping between the r-cells in the original lattice and the $4-r$-cells in the dual lattice. Let $(c^r)^{i_1,\ldots,i_r}_{n_1,\ldots,n_4}$ be an r-cell in the original lattice; define the mapping:

$$* \ : \Lambda^r \to \Lambda^{*r}$$

$$* \ (c^r)^{i_1,\ldots,i_r}_{(n_1,n_2,n_3,n_4)} = (c^{4-r})^{j_1,\ldots,j_{4-r}}_{(n_1,n_2,n_3,n_4)+\vec{i_1}+\ldots+\vec{i_r}}$$

where $j_1, \ldots, j_{4-r} \in \{1,2,3,4\}$ with $j_1, \ldots, j_{4-r}$ being the complement to $i_1, \ldots, i_r$ in the set $\{1,2,3,4\}$ (i.e. for $i_1, i_2 = 1,3$ we have $j_1, j_2 = 2,4$). Also $\vec{j_i}$ denotes the unit vector in the direction j_i. To understand the mapping better we will give a couple of examples:

$$*(p^{12}_{0000}) = p^{*34}_{1100}$$

$$*(b^1_{0000}) = c^{*234}_{1000}$$

$$*(b^2_{0000}) = c^{*134}_{0100}$$

$$*(b^1_{-1000}) = c^{*234}_{1000}$$

$$*(b^2_{0-100}) = c^{*134}_{0100}$$

This mapping is one-to-one so it has an inverse. It is easy to write down the inverse $*^{-1}$.

It is interesting to note that this mapping preserves the idea of neighborhood: cells that are neighbors on the original lattice are mapped into neighbors on the dual lattice. For example the cells $\{b^1_{0000}, b^2_{0000}, b^1_{-1000}, b^2_{0-1000}\}$ are surrounding the plaquette p^{12}_{0000}. On the dual lattice the plaquette p^{*34}_{1100} which is the image of p^{12}_{0000} is the common face of the cubes $\{c^{*234}_{1000}, c^{*134}_{0100}, c^{*234}_{1000}, c^{*134}_{0100}\}$ which are the images of the links surrounding the plaquette.

In the text we will denote with c^* the cells in the dual lattice Λ^*. To get a pictorial idea of this dual mapping we can imagine the dual lattice superimposed on the direct lattice but shifted with $\frac{1}{2}$ in all four directions. Then the mapping will associate to a c^r cell in a direct lattice the c^{*4-r} cell in the dual lattice that intersects the original c^r cell.

In order to implement the ideas of orientation and boundary we will have to use the $Z(N)$ groups. We will take now a quick look at the $Z(N)$ groups.

A.3 The $Z(N)$ Groups

We will use two equivalent notations for the $Z(N)$ group: the additive notation where the elements of the group are seen as members of the Z_N, the additive group of integers modulo N. For $a, b \in Z_N$ their sum will be understood modulo N.

The other notation will be multiplicative where the elements of $Z(N)$ are seen as the roots of the equation $z^N = 1$. They will be $z_n = e^{i\frac{2\pi}{N}n}$ where $n \in \{0, 1, ..., N-1\}$. The connection between the two notations is given by $n \leftrightarrow e^{i\frac{2\pi}{N}n}$. We will use the multiplicative notation most of the time.

The group $Z(N)$ has N irreducible representations. Since the group is Abelian all its irreducible representations are one dimensional. Using the multiplicative notation we write the characters in the irreducible representations as:

$$\chi_k(U) = U^k$$

for $U \in Z(N)$ and $k \in \{0, 1, ..., N-1\}$. k will be called the n-ality of the representation. All class functions have a character expansion:

$$f(U) = \sum_k c_k \chi_k(U) = \sum_k c_k U^k$$

We see that for the $Z(N)$ group this is nothing more than a Fourier transformation.

A.4 The Homology Groups for the Lattice

To define the $Z(N)$ homology groups [55] for the lattice we will first define the simplexes. Let's take a particular $Z(N)$ and define for every cell c_0^r the function:

$$\begin{aligned} s_{c_0^r} &: \Lambda^r \to Z(N) \\ s_{c_0^r}(c^r) &= \begin{cases} 1 & c^r \neq c_0^r \\ e^{i\frac{2\pi}{N}} & c^r = c_0^r \end{cases} \end{aligned}$$

These functions will be called *simplexes*. The set of all simplexes of rank r generate the group $C^r(\Lambda)$ of all functions defined on Λ^r with value in $Z(N)$:

$$C^r(\Lambda) = \{f | f : \Lambda \to Z(N)\}$$

This group has the following multiplicative law. Let $f, g \in C^r(\Lambda)$ and define:

$$(f \cdot g)(c^r) = f(c^r) \cdot g(c^r)$$

for all cells $c^r \in \Lambda^r$. It is easy to see that the rank r simplexes generate all the elements of this group since we can write for any $f \in C^r(\Lambda)$:

$$f = \prod_{c^r \in \Lambda^r} s_{c_r}^{n(f(c_r))} \tag{A.4}$$

where $n(f(c^r))$ is the additive notation for $f(c^r) \in Z(N)$.

We will identify the r-cells c^r with the simplexes s_{c^r} throughout the text. We will denote the simplex s_{c^r} for $(c^r)_{\vec{n}}^{i_1,\ldots,i_r}$ with $(s^r)_{\vec{n}}^{i_1,\ldots,i_r}$.

Now we define the action of the boundary operator on a simplex:

$$\partial(s^r)_{\vec{n}}^{i_1,\ldots,i_r} = \prod_{k=1}^{r} [(s^{r-1})_{\vec{n}}^{i_1,\ldots,\hat{i_k},\ldots,i_r}]^{(-1)^k} \prod_{k=1}^{r} [(s^{r-1})_{\vec{n}+\vec{i_k}}^{i_1,\ldots,\hat{i_k},\ldots,i_r}]^{(-1)^{k+1}}$$

where the hat denotes a missing index and $\vec{i_k}$ is the unit vector in the i_k direction. It is not very clear why the boundary operator is defined this way but if we look at

the equivalent definition in the additive notation things will become clearer:

$$\partial(s^r)^{i_1,\ldots,i_r}_{\vec{n}} = \sum_{k=1}^{r}(-1)^k(s^{r-1})^{i_1,\ldots,\hat{i_k},\ldots,i_r}_{\vec{n}} - \sum_{k=1}^{r}(-1)^k(s^{r-1})^{i_1,\ldots,\hat{i_k},\ldots,i_r}_{\vec{n}+\vec{i_k}}$$

To clarify things even further we will show a couple of examples:

$$\partial(s^1)^i_{\vec{n}} = -s^0_{\vec{n}} + s^0_{\vec{n}+\vec{i}} \quad \Leftrightarrow \quad \partial b^i_{\vec{n}} = -s_{\vec{n}} + s_{\vec{n}+\vec{i}}$$

$$\partial(s^2)^{ij}_{\vec{n}} = -(s^1)^j_{\vec{n}} + (s^1)^i_{\vec{n}} + (s^1)^j_{\vec{n}+\vec{i}} - (s^1)^i_{\vec{n}+\vec{j}} \quad \Leftrightarrow \quad \partial p^{ij}_{\vec{n}} = -b^j_{\vec{n}} + b^i_{\vec{n}} + b^j_{\vec{n}+\vec{i}} - b^i_{\vec{n}+\vec{j}}$$

Returning to the multiplicative notation we see that the boundary of $s^r \in C^r(\Lambda)$ is a product of simplexes in $C^{r-1}(\Lambda)$. We can extend now the boundary operator to act on all elements of $C^r(\Lambda)$ by requiring it to be an homomorphism. Let $f \in C^r(\Lambda)$ where f is written as a product of simplexes as in (A.4). Then we define:

$$\partial f = \prod_{c^r \in \Lambda^r} (\partial s_{c^r})^{n(f(c^r))}$$

Then the boundary operator defined above is a homomorphism from the group $C^r(\Lambda)$ to the group $C^{r-1}(\Lambda)$. A very important property of this homomorphism is that:

$$\partial(\partial f) = \phi_{r-2}$$

for all $f \in C^r(\Lambda)$. ϕ_r is the identity element in the group $C^r(\Lambda)$ (it has the value 1 (0) on all cells c^r in the multiplicative (additive) notation). Using this boundary operator and the dual lattice we can define the co-boundary operator. To see this

take a simplex s^r in the direct lattice. Take the $4-r$-simplex s^{*4-r} on the dual lattice associated with s^r. (The dual of a simplex is the function that is different from identity only on the dual cell. On that cell it has the same value as the simplex on original cell.) Take the boundary on the dual lattice of this cell ∂s^{*4-r} and then map back this boundary on the original lattice. This will be our co-boundary operator. More specifically:

$$\hat{\partial} f = *^{-1} \partial * f$$

for all $f \in C^r(\Lambda)$. The $*$ operator maps an element of $C^r(\Lambda)$ in an element $C^{4-r}(\Lambda^*)$:

$$(*f)(c^{*4-r}) = f(*^{-1} c^{*4-r})$$

We see now that the co-boundary operator is a homeomorphism from $C^r(\Lambda)$ to $C^{r-1}(\Lambda)$. It has a very important property:

$$\hat{\partial}(\hat{\partial} f) = \phi_{r+2}$$

for all $f \in C^r(\Lambda)$.

Now that we have defined the boundary operators and the configuration groups $C^r(\Lambda)$ we can define the homology groups. We say that an configuration $f \in C^r(\Lambda)$ is *closed* if its boundary is zero:

$$\partial f = \phi_{r-1}$$

The set of all such configurations form a subgroup of $C^r(\Lambda)$ since the boundary

operator is an homeomorphism. We will denote this subgroup with $Z^r(\Lambda)$. We will call a configuration $f \in C^r(\Lambda)$ an *boundary* configuration if there is a configuration $F \in C^{r+1}(\Lambda)$ such that $\partial F = f$. The set of all such configurations form a subgroup of $C^r(\Lambda)$ that we will denote with $B^r(\Lambda)$. Since $\partial^2 F = \phi_{r-1}$ we see that all boundary configuration are also closed configurations and thus $B^r(\Lambda)$ is a subgroup of $Z^r(\Lambda)$.

We define the homology groups to be the factor group of $Z^r(\Lambda)$ and $B^r(\Lambda)$:

$$H^r(\Lambda) = Z^r(\Lambda)/B^r(\Lambda)$$

To understand the significance of the homology groups we see that if $B^r(\Lambda) = Z^r(\Lambda)$ all closed configurations are also the boundary of a configuration $F \in C^{r+1}(\Lambda)$. In this case $H^r(\Lambda) = \{\bar{\phi}_r\}$ the trivial group. ($\bar{\phi}_r$ is the equivalence class of the identity configuration ϕ_r). Now, if $H^r(\Lambda)$ is not the trivial group then there are configurations that are closed but are not the boundary of any other configuration (such configurations are usually wrapped around holes in the space). Thus the $H^r(\Lambda)$ carries information regarding the topology of the lattice.

We will write down the homology groups for the four dimensional lattice (in our definition the lattice is equivalent with a four dimensional torus):

$$\begin{aligned} H^0(\Lambda) &= Z(N) \\ H^1(\Lambda) &= Z(N)^4 \\ H^2(\Lambda) &= Z(N)^6 \\ H^3(\Lambda) &= Z(N)^4 \end{aligned}$$

$$H^4(\Lambda) \;=\; Z(N)$$

where $Z(N)$ is the group used to define the configuration groups.

We can see why, for example, $H^1(\Lambda) = Z(N)^4$. Let's take a line that wraps around the lattice in a given direction (we put 1 everywhere except on this line where we put the generator of the group $Z(N)$). This is a closed configuration but it is not the boundary of any surface. Therefore the equivalence class of this element will be in the homology group together with all different powers of this configuration. This will generate us a subgroup $Z(N)$ in $H^1(\Lambda)$. The power four is due to the fact that there are four possible directions that we can choose to wrap the line around.

The idea of orientation is introduced by the inverse element in $Z(N)$. For every simplex s^r we have a configuration that is oriented oppositely namely $\bar{s^r} = (s^r)^{-1}$. We see that $s^r \cdot \bar{s^r} = \phi_r$ or in the additive notation we have $s^r + \bar{s^r} = 0$ which emulates our intuitive idea about orientation.

In the text we sometimes refer to the elements of $C^r(\Lambda)$ as configurations. We do that since there are a number of physical systems defined on the lattice that have the configuration space given by $C^r(\Lambda)$ for a certain r (for example $Z(N)$ gauge theory has the configuration space $C^1(\Lambda)$ whereas the action is defines in terms of $\hat{\partial}C^1(\Lambda) \subset C^2(\Lambda)$).

A.5 Further Definitions and Notations

In this section we will define the bracket $\{\alpha, \beta\}$ of two configurations. We note first that for $Z(N)$ we have a very interesting property. Using the multiplicative

notation we write:

$$\chi_{U_n}(U_m) = U_m^n = e^{i\frac{2\pi}{N}mn} = U_n^m = \chi_{U_m}(U_n)$$

where $U_m = e^{i\frac{2\pi}{N}m} \in Z(N)$ and χ_{U_n} is the n-ality irreducible representation of $Z(N)$.

We introduce now a definition that will be very useful through the text. Let us take two configurations $f, g \in C^r(\Lambda)$. We define the bracket:

$$\{f, g\} = \prod_{c^r \in \Lambda^r} \chi_{f(c_r)}(g(c_r))$$

We have the following properties for the bracket:

$$\begin{aligned} \{f, g\} &= \{g, f\} \\ \{f, gh\} &= \{f, g\}\{f, h\} \\ \{f, f^{-1}\} &= 1 \\ \{f, \phi_r\} &= 1 \end{aligned}$$

for all $f, g, h \in C^r(\Lambda)$. Moreover:

$$\{\partial f, g\} = \{f, \hat{\partial} g\} \tag{A.5}$$

for $f \in C^{r+1}(\Lambda)$ and $g \in C^r(\Lambda)$.

For any subgroup $\mathcal{K} \in C^r(\Lambda)$ we can define [50]:

$$K[f] = \sum_{g \in \mathcal{K}} \{f, g\} \tag{A.6}$$

Using this definition we have:

$$K[f] = \sum_{g \in \mathcal{K}} \{f, g\} = \sum_{g \in \mathcal{K}} \{f, gh\} = \sum_{g \in \mathcal{K}} \{f, g\}\{f, h\} = \{f, h\} \sum_{g \in \mathcal{K}} \{f, g\} = \{f, h\} K[f]$$

where we used the summation invariance for the group $\mathcal{K}$ ($h \in \mathcal{K}$) and the distributivity of the bracket. We see that if there is at least one element $h \in \mathcal{K}$ such that $\{f, h\} \neq 1$ then $K[f] = 0$. Then we have:

$$K[f] = \begin{cases} 0 & f \notin \bar{\mathcal{K}} \\ |\mathcal{K}| & f \in \bar{\mathcal{K}} \end{cases}$$

where

$$\bar{\mathcal{K}} = \{f \in C^r(\Lambda) | \{f, g\} = 1 \ \forall g \in \mathcal{K}\}$$

The bar set has the following properties:

$$\begin{aligned} \bar{\bar{\mathcal{K}}} &= \mathcal{K} \\ |\bar{\mathcal{K}}||\mathcal{K}| &= |C^r(\Lambda)| \\ \bar{C^r(\Lambda)} &= \{\phi_r\} \end{aligned} \tag{A.7}$$

Vita

Andrei Alexandru was born in Vaslui, România, on the 24th day of September, 1974. He graduated from the Mathematics and Physics High School "Mihail Kogălniceanu", Vaslui, in 1993. He entered the University of Bucharest in 1993, where he received "Diploma de Licenţă" in physics, theory section, in 1997.

In August 1997 he entered the graduate program in physics at Louisiana State University, Baton Rouge, Louisiana. In the Summer he will earn the degree of Doctor of Philosophy.

DOCTORAL EXAMINATION AND DISSERTATION REPORT

Candidate: Viorel - Andrei Alexandru

Major Field: Physics

Title of Dissertation: Center Vortices in Confinement

Approved:

Major Professor and Chairman

Dean of the Graduate School

EXAMINING COMMITTEE:

Date of Examination:

June 28, 2001